

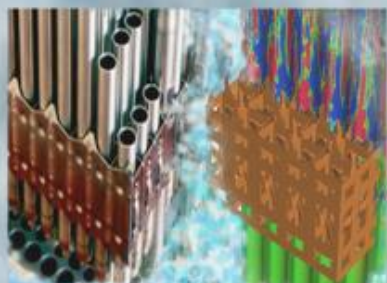
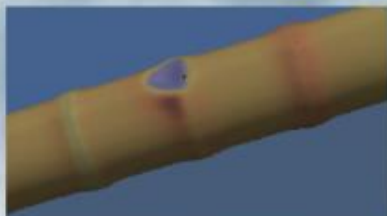
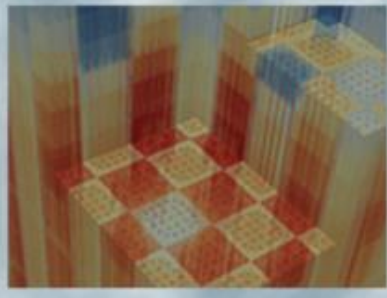
Neutron Capture Energies for Flux Normalization and Approximate Model for Gamma-Smeared Power

Revision 0

Kang Seog Kim
Kevin T. Clarno
Benjamin S. Collins
Oak Ridge National Laboratory

Yuxuan Liu
Xinyan Wang
William R. Martin
University of Michigan

September 28, 2017



DOCUMENT AVAILABILITY

Reports produced after January 1, 1996, are generally available free via US Department of Energy (DOE) SciTech Connect.

Website <http://www.osti.gov/scitech/>

Reports produced before January 1, 1996, may be purchased by members of the public from the following source:

National Technical Information Service
5285 Port Royal Road
Springfield, VA 22161

Telephone 703-605-6000 (1-800-553-6847)

TDD 703-487-4639

Fax 703-605-6900

E-mail info@ntis.gov

Website <http://www.ntis.gov/help/ordermethods.aspx>

Reports are available to DOE employees, DOE contractors, Energy Technology Data Exchange representatives, and International Nuclear Information System representatives from the following source:

Office of Scientific and Technical Information
PO Box 62
Oak Ridge, TN 37831

Telephone 865-576-8401

Fax 865-576-5728

E-mail reports@osti.gov

Website <http://www.osti.gov/contact.html>

This report was prepared as an account of work sponsored by an agency of the United States Government. Neither the United States Government nor any agency thereof, nor any of their employees, makes any warranty, express or implied, or assumes any legal liability or responsibility for the accuracy, completeness, or usefulness of any information, apparatus, product, or process disclosed, or represents that its use would not infringe privately owned rights. Reference herein to any specific commercial product, process, or service by trade name, trademark, manufacturer, or otherwise, does not necessarily constitute or imply its endorsement, recommendation, or favoring by the United States Government or any agency thereof. The views and opinions of authors expressed herein do not necessarily state or reflect those of the United States Government or any agency thereof.



REVISION LOG

Revision	Date	Affected Pages	Revision Description
0	9/28/2017	All	Initial version

Export Controlled None

IP/Proprietary/NDA Controlled None

Sensitive Controlled None

Unlimited All Pages

Requested Distribution:

To: N/A

Copy: N/A

Reviewed by:

Date:

Reviewer:

EXECUTIVE SUMMARY

The Consortium for Advanced Simulation of Light Water Reactors (CASL) Virtual Environment for Reactor Applications (VERA) neutronics simulator MPACT has used a single recoverable fission energy for each fissionable nuclide assuming that all recoverable energies come only from fission reaction, for which capture energy is merged with fission energy. This approach includes approximations and requires improvement by separating capture energy from the merged effective recoverable energy. This report documents the procedure to generate recoverable neutron capture energies and the development of a program called *CapKappa* to generate capture energies. Recoverable neutron capture energies have been generated by using *CapKappa* with the evaluated nuclear data file (ENDF)/B-7.0 and 7.1 cross section and decay libraries. The new capture kappas were compared to the current SCALE-6.2 and the CASMO-5 capture kappas. These new capture kappas have been incorporated into the Simplified AMPX 51- and 252-group libraries, and they can be used for the AMPX multigroup (MG) libraries and the SCALE code package.

The CASL VERA neutronics simulator MPACT does not include a gamma transport capability, which limits it to explicitly estimating local energy deposition from fission, neutron, and gamma slowing down and capture. Since the mean free path of gamma rays is typically much longer than that for the neutron, and the total gamma energy is about 10% to the total energy, the gamma-smeared power distribution is different from the fission power distribution. Explicit local energy deposition through neutron and gamma transport calculation is significantly important in multi-physics whole core simulation with thermal-hydraulic feedback. Therefore, the gamma transport capability should be incorporated into the CASL neutronics simulator MPACT. However, this task will be time-consuming in developing the neutron induced gamma production and gamma cross section libraries. This study is to investigate an approximate model to estimate gamma-smeared power distribution without performing any gamma transport calculation. A simple approximate gamma smearing model has been investigated based on the facts that pin-wise gamma energy depositions are almost flat over a fuel assembly, and assembly-wise gamma energy deposition is proportional to kappa-fission energy deposition. The approximate gamma smearing model works well for single assembly cases, and can partly improve the gamma smeared power distribution for the whole core model.

Although the power distributions can be improved by the approximate gamma smearing model, still there is an issue to explicitly obtain local energy deposition. A new simple approach or gamma transport/diffusion capability may need to be incorporated into MPACT to estimate local energy deposition for more robust multi-physics simulation.



TABLE OF CONTENTS

REVISION LOG	iii
EXECUTIVE SUMMARY.....	iv
TABLE OF CONTENTS	v
FIGURES	vi
TABLES	viii
ACRONYMS	ix
1. INTRODUCTION.....	1
2. NEUTRON CAPTURE ENERGY IN FLUX NORMALIZATION	2
2.1 RECOVERABLE ENERGY AND NUCLEAR DATA	2
2.2 EFFECTIVE RECOVERABLE ENERGY PER FISSION.....	3
2.3 EXPLICIT NEUTRON FLUX NORMALIZATION	6
2.4 FRACTIONS OF CAPTURE REACTIONS	8
2.5 DEVELOPMENT OF THE CAPKAPPA PROGRAM	10
2.6 CALCULATION OF CAPTURE KAPPAS	12
2.7 BENCHMARK CALCULATION USING CAPTURE KAPPAS.....	21
3. DEVELOPMENT OF APPROXIMATE GAMMA SMEARING MODEL	24
3.1 RECOVERABLE ENERGY AND ENERGY DEPOSITION	24
3.2 BENCHMARK PROBLEMS.....	24
3.3 CONTRIBUTION OF GAMMA ENERGY DEPOSITION.....	28
3.4 OPTIMIZATION OF GAMMA SMEARING FACTOR.....	29
3.5 RESULTS FOR 1D CORE PROBLEMS.....	43
3.6 RESULTS FOR 2D CORE PROBLEMS.....	49
4. MODEL EFFECT OF DELAYED ENERGY ON POWER NORMALIZATION IN DEPLETION CALCULATIONS.....	52
4.1 OVERVIEW.....	52
4.2 THEORY	52
4.3 BENCHMARK RESULTS.....	54
5. CONCLUSIONS AND FUTURE WORK.....	59
REFERENCES	60
APPENDIX A. Program source of CapKappa	62
APPENDIX B. Result of CapKappa with ENDF/B-7.0	69
APPENDIX C. Result of CapKappa with ENDF/B-7.1.....	75
APPENDIX D. PROOF OF EQUATION (4.8)	82

FIGURES

Figure 2.1. Capture Energy Production.....	8
Figure 2.2. Typical PWR Neutron Spectrum.	8
Figure 2.3. Sample input for CapKappa.	11
Figure 2.4. Comparison of Effective Kappa and Eigenvalue in Depletion for 2B.....	22
Figure 2.5. Comparison of Effective Kappa and Eigenvalue in Depletion for 2P.....	23
Figure 3.1. VERA Progression Problems for Fuel Assemblies.....	26
Figure 3.2. 1D Core Problems with Various Numbers of Assemblies.	27
Figure 3.3. Fractions of Gamma Energy Deposition as a Function of Burnup by a Deterministic Code.....	29
Figure 3.4. Comparison of the Gamma-Smeared Power Distribution (Case 2B).	37
Figure 3.5. Comparison of the Gamma-Smeared Power Distribution (Case 2F).....	38
Figure 3.6. Comparison of the Gamma-Smeared Power Distribution (Case 2G).	39
Figure 3.7. Comparison of the Gamma-Smeared Power Distribution (Case 2H).	40
Figure 3.8. Comparison of the Gamma-Smeared Power Distribution (Case 2M).....	41
Figure 3.9. Comparison of the Gamma-Smeared Power Distribution (Case 2P).	42
Figure 3.10. Comparison of the Fission and Gamma Power Distribution (Case 1D-a).....	46
Figure 3.11. Comparison of the Fission and Gamma Power Distribution (Case 1D-b).....	46
Figure 3.12. Comparison of the Fission and Gamma Power Distribution (Case 1D-c).....	47
Figure 3.13. Comparison of the Adjusted and Unadjusted Power Distribution (Case 1D-a).	47
Figure 3.14. Comparison of the Adjusted and Unadjusted Power Distribution (Case 1D-b).	48
Figure 3.15. Comparison of the Adjusted and Unadjusted Power Distribution (Case 1D-c).	48



Figure 3.16. Comparison of the Fission Powers (MCNP vs. MPACT).....	50
Figure 3.17. Comparison between Fission and Gamma Smeared Powers (MCNP & MPACT).....	50
Figure 3.18. Comparison between the MCNP Gamma Smeared and MPACT Fission Powers.....	51
Figure 3.19. Comparison of the Gamma Smeared Powers (MCNP vs. MPACT).....	51
Figure 4.1. Energy per Fission of 10,000 h at Constant Full Power.	55
Figure 4.2. Energy per Fission in the First 150 h at Constant Full Power.....	55
Figure 4.3. Normalized Flux in the First 1,000 h at Constant Full Power.....	56
Figure 4.4. The Effect of Time-Dependent Delayed Energy on k_{eff}	58

TABLES

Table 2.1. Components of energy release from fission and capture reaction.....	2
Table 2.2. Data resource	3
Table 2.3. Effective recoverable energy per fission.....	5
Table 2.4. Fractions of capture reaction rates	9
Table 2.5. Description of subroutines	10
Table 2.6. Comparison of the capture kappas with ENDF/B-7.0	13
Table 2.7. Comparison of the capture kappas with ENDF/B-7.1	17
Table 2.8. Comparison of Effective Kappas	21
Table 3.1. Benchmark problems	25
Table 3.2. Fraction of gamma energy deposition by a Monte Carlo code	28
Table 3.3. Fraction of gamma energy deposition (Case 2C)	31
Table 3.4. Fraction of gamma energy deposition (Case 2F)	32
Table 3.5. Fraction of gamma energy deposition (Case 2G).....	33
Table 3.6. Fraction of gamma energy deposition (Case 2H)	34
Table 3.7. Fraction of gamma energy deposition (Case 2M).....	35
Table 3.8. Fraction of gamma energy deposition (Case 2P)	36
Table 3.9. Sensitivity of the gamma smearing factors (Case 1D-a)	44
Table 3.10. Sensitivity of the gamma smearing factors (Case 1D-b)	44
Table 3.11. Sensitivity of the gamma smearing factors (Case 1D-c).....	45
Table 3.12. Comparison of power distributions (5B-2D).....	49
Table 4.1. Data of delayed heat group	54
Table 4.2. Results verification with 2005 ANS standard.....	57



ACRONYMS

AMPX	resonance processing code; the name is no longer an acronym
ANS	American Nuclear Society
CASL	Consortium for Advanced Simulation of Light Water Reactors
CE	continuous energy (as in cross sections)
CENTRM	PW transport code in SCALE
CMFD	coarse-mesh finite difference
ENDF	evaluated nuclear data file
KERMA	kinetic energy released per unit mass
LWR	light-water reactor
MCNP	Monte Carlo N-Particle
MG	multigroup (as in cross sections)
MPIACT	radiation transport code in VERA; the name is no longer an acronym
NJOY	nuclear data code
ORIGEN	Oak Ridge Isotopic Generation code in SCALE
ORNL	Oak Ridge National Laboratory
PW	pointwise
PWR	pressurized water reactor
RIA	Reactivity insertion accident
SAMPX	Simplified AMPX
SCALE	Standardized Computer Analyses for Licensing Evaluations code
VERA	Virtual Environment for Reactor Applications
VERA-CS	VERA Core Simulator
XS	cross section



1. INTRODUCTION

The MPACT [MPA15] neutronics code, within the Virtual Environment for Reactor Analysis (VERA) [Tur16] code suite, is being developed by the Consortium for Advanced Simulation of LWRs (CASL) [CAS15]. MPACT provides a three-dimensional, full-core neutron transport solution with isotopic depletion/decay by coupling with the SCALE/ORIGEN [Section 5.1 in Rea16] code. MPACT primarily uses the subgroup method for resonance self-shielding [Gol62, Sta98]. The cross section library is based on evaluated nuclear data file (ENDF)/B-VII data [Cha11], which has been processed using the AMPX [Wia16] and SCALE [Rea16] code packages, along with a few other CASL utility programs.

The CASL VERA neutronics simulator MPACT has used single recoverable fission energy for each fissionable nuclide, assuming that all recoverable energies come only from fission reaction, for which capture energy is merged with fission energy. The MPACT multigroup (MG) library [Kim17] includes effective recoverable fission energies which are called *effective fission kappas*. This approach includes approximation and must be improved by separating capture energy from the merged effective recoverable energy. Normalized neutron flux levels are estimated from a given thermal power and energy production through neutron fission and capture reactions. Estimation of neutron flux level impacts the prediction of isotopic inventories and thus multiplication factors at different burnups. A more accurate approach is to obtain recoverable energies from fission and capture reactions, which requires recoverable capture energy for each nuclide. ENDF/B provides recoverable fission energy for each fissionable nuclide. The AMPX MG library includes recoverable fission and capture energies which were evaluated a long time ago based on ENDF/B-IV. Therefore, this study focuses on establishing a procedure to obtain and estimate recoverable capture energies.

The MPACT code does not include a gamma transport capability, and it assumes local energy deposition from fission, neutron, and gamma slowing down and capture. Since the mean free path of gamma rays is much longer than the neutron path and the total gamma energy is about 10% of the total energy, the gamma-smeared power distribution is different from the fission power distribution. Non-local energy deposition computed from neutron and gamma transport calculations may be significantly important in multiphysics whole core simulations with thermal-hydraulic feedback. Therefore, the ideal gamma transport capability should be incorporated into the CASL neutronics simulator MPACT. However, this task will be time-consuming, requiring coupled MG libraries with neutron-induced gamma production and gamma interaction cross section libraries, as well as the usual neutron interaction data. This study investigated an approximate model to estimate gamma-smeared power distribution without performing any gamma transport calculation.

Chapter 2 addresses the investigation of neutron capture energy in flux normalization. Chapter 3 describes development of an approximate method for gamma-smeared power distributions, and Chapter 4 presents the investigation of the impact of a delayed heat source on the neutron flux normalization and eigenvalues.

2. NEUTRON CAPTURE ENERGY IN FLUX NORMALIZATION

2.1 RECOVERABLE ENERGY AND NUCLEAR DATA

Estimation of the neutron flux level will impact the prediction of isotopic inventories, as well as multiplication factors throughout depletion. When evaluating the neutron flux level based on thermal power, the following recoverable energies must be considered.

- Fission reactions
 - Fission fragments (instant)
 - Fission neutrons (instant)
 - Beta decay of fission products (delayed)
 - Prompt gammas (instant)
 - Delayed gammas of fission products (delayed)
- Capture reactions
 - Alpha, gamma and other elementary particles (instant)
 - Beta decay of production isotopes produced by neutron capture (delayed)

Some recoverable energies are instant, while others are time dependent. This study assumes that all of the recoverable energies are instantly deposited somewhere in the system without any loss.

Table 2.1 provides various energy release modes from neutron fission and capture reactions for ^{235}U and ^{238}U . Table 2.2 shows where the data for various energy release modes can be obtained.

Given thermal power, neutron flux levels can be evaluated by considering all of recoverable energies from fission and capture reactions.

Table 2.1. Components of energy release from fission and capture reaction

Reaction	Energy modes	Fraction (%)	Energy (MeV)		Range	Time
			^{235}U	^{238}U		
Fission	Fission fragments	80	169.13	169.80	Local	Instant
	Fission neutrons	2–3	4.85	4.57	Global	Instant
	Beta decay of FPs	3–4	6.50	8.48	Local	Delayed
	Gammas	Prompt	3–4	6.60	Global	Instant
		Delayed	3–4	6.33	Global	Delayed
	Neutrinos	4–5	8.75	11.39	-	-
	Total	100	202.16	209.18	-	-
Capture	Total minus neutrinos		193.41	197.79	-	-
	Gammas		6.55	4.81	Global	Instant
	Alpha and other particles		-	-	Local	Instant
	Beta decay of product		-	0.46*	Global	Delayed

* ^{239}U beta decay $T_{1/2} = 1.407\text{E}+03$ sec

**Table 2.2. Data resource**

Reaction	Energy modes	Resource
Fission	Total	ENDF/B XS data MF=1 MT=458
	Total – neutrinos	ENDF/B XS data MF=1 MT=458
Capture	Gammas	ENDF/B XS data MF=3 MT=102
	Alpha and other particles	ENDF/B XS data MF=3 MT=107 & others
	Beta decay of product	ENDF/B Decay data

2.2 EFFECTIVE RECOVERABLE ENERGY PER FISSION

Most transport lattice codes, including WIMS [Les07] and HELIOS [Sta98], use a single value of recoverable energy release per fission for each fissionable nuclide, which includes recoverable fission and capture energies and incident neutron energy.

The energy release per fission is required for burnup calculations and is usually defined without the kinetic energy of the incident neutrons or the energy carried away by neutrinos. However, the energy release per fission should include the contributions from the kinetic energy of incident neutrons and from the decay of the capture products [Les07]:

$$W_{\text{fiss}}^i = E_r^i + Q_c^i + W_n^i, \quad (2.1)$$

where W_{fiss} is the effective energy release in fission, E_r^i is the energy release in fission excluding the energy carried away by neutrinos and the kinetic energy of the incident neutrons, Q_c^i is the contribution from the decay of the capture products, and W_n^i is the kinetic energy of the incident neutrons. Index i refers to a fissionable nuclide in all cases.

E_r^i values are extracted from the MF=1/MT=458 section of an evaluated nuclear data file, while the kinetic energy of the incident neutron is obtained by approximately averaging the energy with the fission reaction rate. The averaging process involved the multigroup approximation and the cross sections obtained from the Monte Carlo N-Particle (MCNP) calculations based on ENDF/B cross section data:

$$W_n^i = \frac{\sum_g \bar{E}_g \sigma_{f,g}^i \phi_g}{\sum_g \sigma_{f,g}^i \phi_g}, \quad (2.2)$$

where $\sigma_{f,g}$ is the microscopic fission cross section of the fissionable nuclide i in the energy group g , ϕ_g is the neutron spectrum, and \bar{E}_g is the average group energy. A typical pressurized water reactor (PWR) fuel pin was used in this calculation.

The average group energy was a simple mean of the group boundary values, except for the highest energy groups for which more accurate values were adopted to give the average energy in a Maxwellian fission spectrum at a temperature corresponding to 1.4 MeV:

$$E_g = \frac{\int_g^s E \sqrt{E} \cdot \exp(-E/T) dE}{\int_g^s \sqrt{E} \cdot \exp(-E/T) dE}. \quad (2.3)$$

It should be noted that W_n is not for direct energy deposition but for E_r because the recoverable fission energy depends upon the incident neutron energy.

The additional energy released due to gamma activation is calculated from

$$Q_c = (\bar{\nu} - 1) Q, \quad (2.4)$$

where $(\bar{\nu} - 1)$ represents the average number of neutrons that are captured, and $Q=6.1$ MeV [Jam99].

Table 2.3 provides the effective recoverable energies per fission with ENDF/B-7.0 and 7.1 which are included in all of the MPACT and Simplified AMPX MG libraries [Kim17].

The following equation will be used for the neutron flux normalization:

$$P_{thermal} = f \sum_j \left(\sum_i K'_{f,i} n_{i,j} \sum_g \sigma_{f,g,i,j} \phi_{g,j} \right) V_j, \quad (2.5)$$

where

- $P_{thermal}$ = thermal power,
- f = flux normalization factor,
- $K'_{f,i}$ = effective fission energy of fissionable isotope i ,
- $n_{i,j}$ = atomic number density for isotope i at material zone j ,
- $\phi_{g,j}$ = neutron flux of group g at material zone j ,
- $\sigma_{f,g,i,j}$ = fission cross section of group g for isotope i at material zone j , and
- V_j = volume of material zone j .

**Table 2.3. Effective recoverable energy per fission**

Nuclide	Recoverable energy (w-s)		Recoverable energy (MeV)	
	ENDF/B-7.0	ENDF/B-7.1	ENDF/B-7.0	ENDF/B-7.1
90230	3.24352E-11	3.08011E-11	202.44	192.24
90232	3.22079E-11	3.22079E-11	201.02	201.02
91231	3.22345E-11	3.13618E-11	201.19	195.74
91233	3.27020E-11	3.18390E-11	204.11	198.72
92232	3.22345E-11	3.12001E-11	201.19	194.73
92233	3.20712E-11	3.20712E-11	200.17	200.17
92234	3.26107E-11	3.26107E-11	203.54	203.54
92235	3.24142E-11	3.24017E-11	202.31	202.23
92236	3.29604E-11	3.29604E-11	205.72	205.72
92237	3.30896E-11	3.17375E-11	206.53	198.09
92238	3.39762E-11	3.39368E-11	212.06	211.82
92240	3.33592E-11	3.33592E-11	208.21	208.21
93237	3.36975E-11	3.36975E-11	210.32	210.32
93238	3.34842E-11	3.35984E-11	208.99	209.70
93239	3.40989E-11	3.26536E-11	212.83	203.81
94236	3.26352E-11	3.34433E-11	203.69	208.73
94237	3.30131E-11	3.38885E-11	206.05	211.51
94238	3.36489E-11	3.41258E-11	210.02	212.99
94239	3.36876E-11	3.36970E-11	210.26	210.32
94240	3.42944E-11	3.42944E-11	214.05	214.05
94241	3.42699E-11	3.42699E-11	213.89	213.89
94242	3.47382E-11	3.49302E-11	216.82	218.02
94244	3.41266E-11	3.35567E-11	213.00	209.44
95241	3.48153E-11	3.48153E-11	217.30	217.30
95242	3.45085E-11	3.51714E-11	215.38	219.52
95243	3.56147E-11	3.56147E-11	222.29	222.29
95342	3.56147E-11	3.56147E-11	222.29	222.29
96241	3.40465E-11	3.51880E-11	212.50	219.62
96242	3.42433E-11	3.43892E-11	213.73	214.64
96243	3.41026E-11	3.43147E-11	212.85	214.17
96244	3.42189E-11	3.51043E-11	213.58	219.10
96245	3.43622E-11	3.45060E-11	214.47	215.37
96246	3.47142E-11	3.54721E-11	216.67	221.40
96247	3.48348E-11	3.51698E-11	217.42	219.51
96248	3.50703E-11	3.55936E-11	218.89	222.16
97249	3.50703E-11	3.60559E-11	218.89	225.04
98249	3.50703E-11	3.55494E-11	218.89	221.88
98250	3.50703E-11	3.68134E-11	218.89	229.77
98251	3.50703E-11	3.58147E-11	218.89	223.54
98252	3.50703E-11	3.68984E-11	218.89	230.30

2.3 EXPLICIT NEUTRON FLUX NORMALIZATION

Total thermal power should include recoverable energies from both neutron fission and capture reactions. An explicit neutron flux normalization formula can be as follows:

$$P_{\text{thermal}} = f \sum_j \left(\sum_i \kappa_{f,i} n_{i,j} \sum_g \sigma_{f,g,i,j} \phi_{g,j} + \sum_i \kappa_{c,i} n_{i,j} \sum_g \sigma_{c,g,i,j} \phi_{g,j} \right) V_j , \quad (2.6)$$

where

- $\kappa_{f,i}$ = recoverable fission energy of isotope i ,
- $\kappa_{c,i}$ = capture energy of isotope i ,
- $\sigma_{c,g,i,j}$ = capture cross section of group g for isotope i at fuel zone j , and
- f = flux normalization factor.

The recoverable fission energy is provided by the ENDF/B MF=1 MT=458 and is dependent upon incident neutron energy as follows [Trk12]:

$$\kappa_{f,i}(E_{\text{inc}}) = \kappa_{f,i}(0) + 1.157 \cdot E_{\text{inc}} - 8.07 \cdot [\bar{v}_i(E_{\text{inc}}) - \bar{v}_i(0)] , \quad (2.7)$$

where

- E_{inc} = incident neutron energy, and
- \bar{v}_i = average number of neutrons released per fission for isotope i .

Since the AMPX MG master library includes $\kappa_{f,i}(0)$, the effective \bar{E}_{inc} and \bar{v}_i should be estimated in a transport code by using the following equations.

$$\bar{E}_{\text{inc}} = \frac{\sum_g \bar{E}_g \sigma_{f,g}^i \phi_g}{\sum_g \sigma_{f,g}^i \phi_g} , \quad (2.8)$$

where the group average energy can be obtained by Eq. (2.3).

Recoverable capture energy can be obtained from mass difference between before-and-after reactions. Sometimes the capture energy would be obtained by kinetic energy released per unit mass (KERMA) ($K_{c,g,i}$) [Mac94], which is defined as

$$K_{c,g,i} = (E_g + Q_{c,i} - \bar{E}_{c,i,n} - \bar{E}_{c,i,\gamma}) \sigma_{c,g,i} \quad (2.9)$$

where

- E_g : incident neutron energy,
- $Q_{c,i}$: mass difference Q-value for capture reaction,
- $\bar{E}_{c,i,n}$: total energy of secondary neutrons including multiplicity,
- $\bar{E}_{c,i,\gamma}$: total energy of secondary photons including photon yield, and



$\sigma_{c,g,i}$: microscopic capture cross section.

Total energies of secondary neutrons and photons are negligible compared to the mass difference Q-value. Most secondary particles from decay will stay inside the core, but the emission rate is time-dependent. When estimating total core power, secondary particles should be considered in normalizing neutron flux. Theoretically, using mass difference Q-value is more reasonable than using KERMA. Therefore, the capture energy can be identical to the mass difference Q-value for capture reaction, as follows:

$$\kappa_{c,i} = q_{c,i}. \quad (2.10)$$

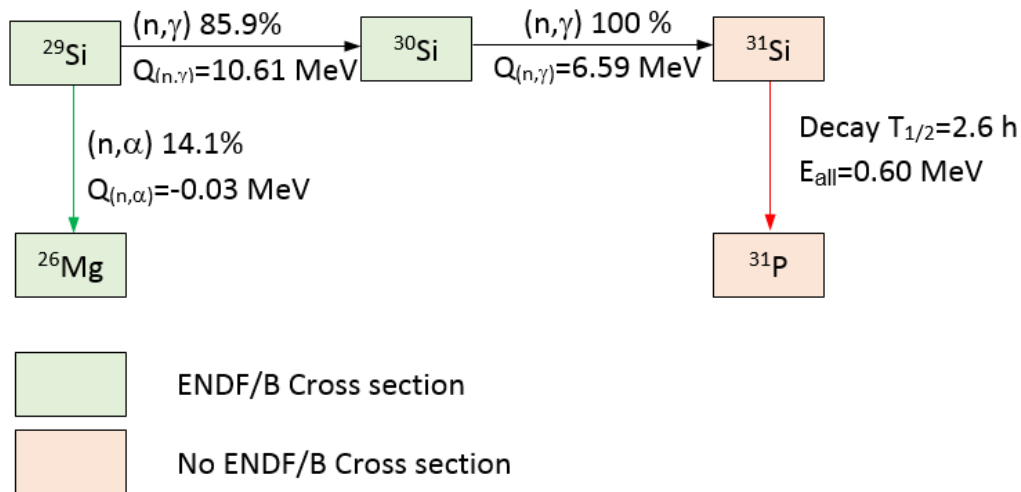
As described in Section 2.1, the capture energies are produced from various neutron capture reactions such as (n,γ) and (n,α) which can be obtained from the mass difference Q-values. To slightly simplify the procedure to obtain capture energy, only (n,γ) and (n,α) reactions are considered. In addition, decay energy from activation products created by the capture reaction needs to be considered. The capture energy can be obtained by following the procedure below.

- Obtain reaction rate fractions of (n,γ) and (n,α) reactions ($f_{c,i}^\gamma$ and $f_{c,i}^\alpha$) for each nuclide by using typical PWR neutron spectra and infinite dilution cross sections.
- Read Q-values of (n,γ) and (n,α) reactions from ENDF/B, and obtain the effective Q-values by the following weighting:

$$Q_{c,i} = Q_{(n,\gamma),i} \cdot f_{c,i}^\gamma + Q_{(n,\alpha),i} \cdot f_{c,i}^\alpha. \quad (2.11)$$

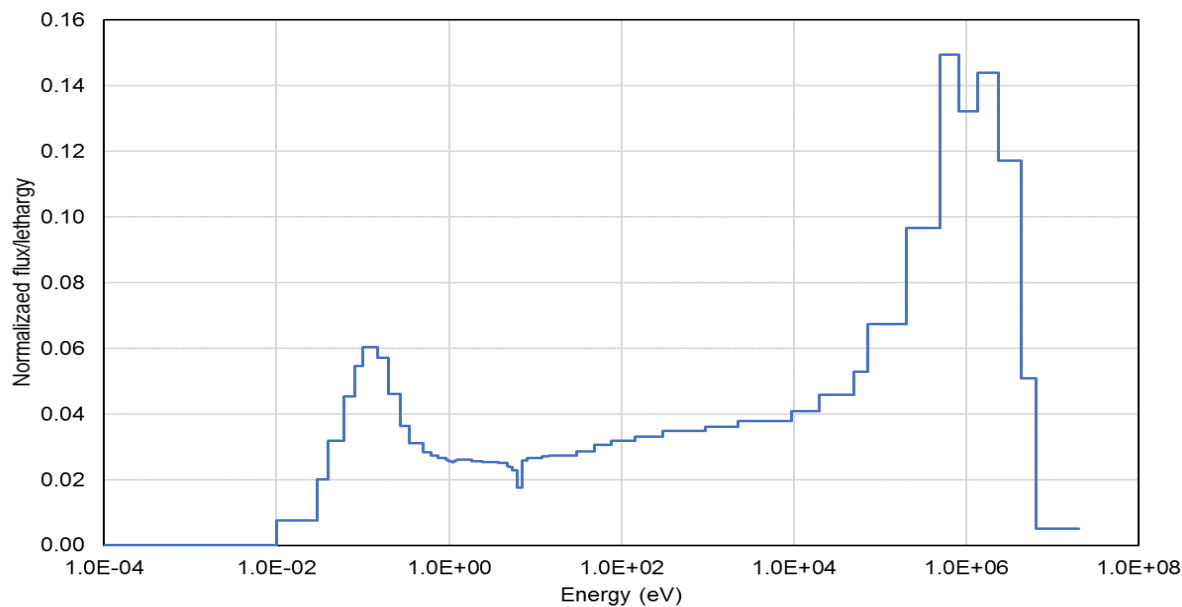
$Q_{(n,\gamma)}$ is always positive, but $Q_{(n,\alpha)}$ can be negative. Negative $Q_{(n,\alpha)}$ is neglected to simplify the procedure. Figure 2.1 provides a sample of capture energy production of Si isotopes. ^{29}Si includes both (n,γ) and (n,α) reactions with 85.9% and 14.1%, respectively. The weight capture energy will be $Q_{c,i}=9.11$ MeV, where $Q_{(n,\alpha)}$ can be neglected.

- ^{30}Si includes only (n,γ) reaction, of which $Q_{(n,\gamma)}$ is 6.59 MeV. The product isotope ^{31}Si decays to ^{31}P by beta(-) of which recoverable energy (0.60 MeV) can be obtained by the difference between effective Q-value (1.49 MeV) and neutrino energy (0.80 MeV). Add this recoverable decay energy to the capture energy. Since the decay energy is time dependent, only $T_{1/2} < 5.0\text{E+5}$ sec decay is considered. And secondary decay is also considered when obtaining total decay energy.

**Figure 2.1. Capture Energy Production.**

2.4 FRACTIONS OF CAPTURE REACTIONS

Fractions of (n,γ) and (n,α) reaction rates have been obtained for all the ENDF/B nuclides by using the 51-g MT=102 and MT=107 infinite dilution cross sections and typical PWR neutron spectrum as shown in Figure 2.2. Table 2.4 provides fractions of (n,γ) and (n,α) reaction rates for nuclides of which $f_{c,i}^\alpha$ is larger than 0.5%. These were obtained by slightly modifying the program Ampxm2s to convert the AMPX MG library into the Simplified AMPX MG library.

**Figure 2.2. Typical PWR Neutron Spectrum.**

**Table 2.4. Fractions of capture reaction rates**

No	Nuclide	Nuclide ID	Fraction of reaction rate (%)	
			MT=102[a]	MT=107[b]
1	⁷ Be	4007	0	100
2	⁹ Be	4009	6.4	93.6
3	¹⁰ B	5010	0	100
4	¹¹ B	5011	96.5	3.5
5	C	6000	45.7	54.3
6	¹⁴ N	7014	18.8	81.2
7	¹⁵ N	7015	35.5	64.5
8	¹⁶ O	8016	0.6	99.4
9	¹⁷ O	8017	0.7	99.3
10	¹⁹ F	9019	24.1	75.9
11	²⁴ Mg	12024	74.5	25.5
12	²⁵ Mg	12025	77	23
13	²⁶ Mg	12026	98.3	1.7
14	²⁷ Al	13027	98.9	1.1
15	²⁸ Si	14028	93.8	6.2
16	²⁹ Si	14029	85.9	14.1
17	³¹ P	15031	96.9	3.1
18	³² S	16032	60.5	39.5
19	³³ S	16033	14.1	85.9
20	³⁴ S	16034	94.9	5.1
21	³⁶ Ar	18036	94.1	5.9
22	³⁸ Ar	18038	97.3	2.7
23	³⁹ K	19039	93.5	6.5
24	⁴⁰ K	19040	96	4
25	⁴⁰ Ca	20040	74.9	25.1
26	⁴² Ca	20042	98.8	1.2
27	⁴⁶ Ti	22046	99.5	0.5
28	⁴⁷ Ti	22047	99.4	0.6
29	⁵⁸ Ni	28058	99.3	0.7
30	⁵⁹ Ni	28059	85.7	14.3
31	⁹⁶ Ru	44096	99.1	0.9

[a] (n,γ) ($n,\gamma\gamma\gamma\gamma$)[b] (n,γ) reaction

2.5 DEVELOPMENT OF THE CAPKAPPA PROGRAM

A program called *CapKappa* has been developed to calculate the effective capture energy based on the methodology described in Section 2.1.3. The program includes six subroutines, as shown in Table 2.5. Program sources are provided in Appendix A and located at the XSTools repository.

Table 2.5. Description of subroutines

Subroutine	Function
CapKappa.F90	Main program to generate capture kappas
param.M.F90	All the variables and parameters
rdendfdecay.F90	Read decay constants & Q-values from the ENDF decay library
rdendfxs.F90	Read MT=102 & 107 Q-values from the ENDF XS library
readin.F90	Read input file 'CapKappa.in'
writeout.F90	Write output file 'CapKappa.out'

The program requires a user input file, CapKappa.in, ENDF/B cross section, and decay data libraries. Figure 2.3 provides sample input for CapKappa. User input is as follows:

```
[XS      endflib]
[DECAY  decaylib]
[ALPHA  nuclidalpha(i),weightalpha(i)]i=1,numalpha
[%END]

Variables      Format      Description
-----  -----
endflib        a100       ENDF/B cross section library file name
decaylib       a100       ENDF/B decay library file name
nuclidalpha(i) integer    Nuclide ID
weightalpha(i) real       % fraction
numalpha       integer    # of nuclides
```

The program prints out two output files, including CapKappa.out and CapKappa.dat. The CapKappa.out includes detailed output, and the CapKappa.dat includes the following data. A sample can be seen in Appendix B.

```
[numnuc]
[i, mat(i), nuclid(i), nuclaid(i), capkappa0(i), capkappa1(i)]i=1,numnuc
[%END]

Variables      Format      Description
-----  -----
numnuc         integer    # of nuclides in ENDF/B
i               integer    ENDF/B cross section library file name
mat(i)         integer    ENDF/B nuclide ID
nuclid(i)     integer    Nuclide ID
capkappa0(i)   real       Capture kappa without product decay energy
capkappa1(i)   real       product isotope decay energy
```



```
XS      \PROJECTS\13_Endf\endfb7.1\n-endfb7.1
DECAY  \PROJECTS\13_Endf\dec-endfb7.1
ALPHA   40070    100.0
ALPHA   40090    93.6
ALPHA   50100    100.0
ALPHA   50110    3.5
ALPHA   60000    54.3
ALPHA   70140    81.2
ALPHA   70150    64.5
ALPHA   80160    99.4
ALPHA   80170    99.3
ALPHA   90190    75.9
ALPHA   120240   25.5
ALPHA   120250   23.0
ALPHA   120260   1.7
ALPHA   130270   1.1
ALPHA   140280   6.2
ALPHA   140290   14.1
ALPHA   150310   3.1
ALPHA   160320   39.5
ALPHA   160330   85.9
ALPHA   160340   5.1
ALPHA   180360   5.9
ALPHA   180380   2.7
ALPHA   190390   6.5
ALPHA   190400   4.0
ALPHA   200400   25.1
ALPHA   200420   1.2
ALPHA   220460   0.5
ALPHA   220470   0.6
ALPHA   280580   0.7
ALPHA   280590   14.3
ALPHA   440960   0.9
%END
```

Figure 2.3. Sample input for CapKappa.

2.6 CALCULATION OF CAPTURE KAPPAS

The capture kappas have been calculated by using the CapKappa program with the ENDF/B-7.0 and 7.1 data. Appendices B and C provide output files of CapKappa.dat with ENDF/B-7.0 and 7.1, respectively. Tables 2.6 and 2.7 compares new capture kappas with the old ones used in AMPX and SCALE. In addition, new capture kappas are compared to the CASMO-5 capture kappas [Rho08]. The following is a summary of the comparison.

- a. Old SCALE capture kappas were generated only for important nuclides, and constant 5.0 MeV was assigned to other nuclides.
- b. ^{16}O includes 99.4 % of (n,α) reaction out of neutron capture reaction of which Q-value is negative. Therefore the new capture kappa of ^{16}O is $4.1434 \times 0.006 = 0.0249$ MeV, which is very different from the old SCALE and CASMO-5 capture kappa.
- c. New capture kappas of ^{155}Gd and ^{157}Gd are 8.536 and 7.937 MeV, respectively, which are very consistent with the CASMO-5 capture kappas but very different from the old SCALE values.
- d. New capture kappa of ^{235}U is very consistent with the CASMO-5 and the old SCALE capture kappas.
- e. New capture kappa of ^{238}U (5.716 MeV in ENDF/B-7.1) is very consistent with the CASMO-5 capture kappa (5.68 MeV), but not the old SCALE capture kappa (4.804 MeV). It seems that the old SCALE capture kappa does not include decay energies of ^{239}U and ^{239}Np followed by ^{238}U (n,γ) reaction.

**Table 2.6. Comparison of the capture kappas with ENDF/B-7.0**

No	Nuclide	Capture kappa (MeV)			No	Nuclide	Capture kappa (MeV)		
		SCALE 6.2	New	CASMO-5			SCALE 6.2	New	CASMO-5
1	1001	2.2246	2.2246	2.22	51	22050	5.0000	7.6094	
2	1002	5.0000	6.2574	6.26	52	23000	5.0000	7.3113	
3	1003	0.0000	0.0000		53	24050	5.0000	9.2617	
4	2003	5.0000	20.5778		54	24052	5.0000	7.9392	
5	2004	0.0000	0.0000		55	24053	5.0000	9.7191	
6	3006	5.0000	7.2506		56	24054	5.0000	7.3480	
7	3007	5.0000	2.0328		57	25055	5.0000	9.7908	
8	4007	0.0000	0.0000		58	26054	5.0000	9.2980	
9	4009	5.0000	0.4360		59	26056	7.6000	7.6461	
10	5010	2.7900	2.7895	2.79	60	26057	5.0000	10.0445	
11	5011	5.0000	9.5496		61	26058	5.0000	6.5810	
12	6000	5.0000	2.2608		62	27058	5.0000	10.4500	
13	7014	5.0000	2.0367		63	27059	5.0000	7.4900	
14	7015	5.0000	3.4555		64	27601	5.0000	10.4500	
15	8016	4.1430	0.0249	4.14	65	28058	9.0200	8.9568	
16	8017	5.0000	1.8630		66	28059	5.0000	10.3302	
17	9019	5.0000	2.5827		67	28060	5.0000	7.8201	
18			12.4200		68	28061	5.0000	10.5973	
19	11023	5.0000	11.6368		69	28062	5.0000	6.8379	
20	12024	5.0000	5.4623		70	28064	5.0000	7.2838	
21	12025	5.0000	8.6523		71	29063	5.0000	8.2262	
22	12026	5.0000	7.9023		72	29065	5.0000	8.2304	
23	13027	5.0000	10.6332		73	30000	5.0000	10.1981	
24	14028	5.0000	7.9485		74	31069	5.0000	8.3061	
25	14029	5.0000	9.1140		75	31071	5.0000	9.7261	
26	14030	5.0000	7.1881		76	32070	5.0000	7.4159	
27	15031	5.0000	7.6842		77	32072	5.0000	6.7829	
28	16032	5.0000	5.8317		78	32073	5.0000	10.1962	
29	16033	5.0000	4.6095		79	32074	5.0000	6.9607	
30	16034	5.0000	6.6307		80	32076	5.0000	8.0271	
31	16036	5.0000	8.0463		81	33074	5.0000	10.2430	
32	17035	5.0000	8.5798		82	33075	5.0000	8.8165	
33	17037	5.0000	9.1014		83	34074	5.0000	8.0277	
34	18036	5.0000	8.2695		84	34076	5.0000	7.4184	
35	18038	5.0000	6.4215		85	34077	5.0000	10.4970	
36	18040	5.0000	7.8471		86	34078	5.0000	6.9606	
37	19039	5.0000	7.3825		87	34079	5.0000	9.9121	
38	19040	5.0000	9.8471		88	34080	5.0000	7.3202	
39	19041	5.0000	9.2443		89	34082	5.0000	6.2284	
40	20040	5.0000	6.7025		90	35079	5.0000	8.6934	
41	20042	5.0000	7.8419		91	35081	5.0000	10.3698	
42	20043	5.0000	11.1320		92	36078	5.0000	10.8142	
43	20044	5.0000	7.4148		93	36080	5.0000	7.8814	
44	20046	5.0000	8.9491		94	36082	5.0000	7.4651	
45	20048	5.0000	9.9994		95	36083	5.0000	10.5200	
46	21045	5.0000	8.7607		96	36084	5.0000	7.1114	
47	22046	5.0000	8.8330		97	36085	5.0000	9.8560	
48	22047	5.0000	11.5707		98	36086	5.0000	7.6194	
49	22048	5.0000	8.1424		99	37085	5.0000	8.6503	
50	22049	5.0000	10.9394		100	37086	5.0000	9.9190	

(continued)

No	Nuclide	Capture kappa (MeV)			No	Nuclide	Capture kappa (MeV)		
		SCALE 6.2	New	CASMO-5			SCALE 6.2	New	CASMO-5
101	37087	5.0000	8.8061		151	47111	5.0000	8.4753	
102	38084	5.0000	8.5300		152	47601	5.0000	9.2376	
103	38086	5.0000	8.4282		153	48106	5.0000	9.8414	
104	38087	5.0000	11.1130		154	48108	5.0000	7.3300	
105	38088	5.0000	6.3670		155	48110	5.0000	6.9768	
106	38089	5.0000	7.8024		156	48111	5.0000	9.3953	
107	38090	5.0000	7.1923		157	48112	5.0000	6.5398	
108	39089	5.0000	7.7908		158	48113	5.0000	9.0427	
109	39090	5.0000	7.9290		159	48114	5.0000	6.6592	
110	39091	5.0000	8.2441		160	48116	5.0000	8.2869	
111	40090	7.2026	7.1940		161	48601	5.0000	11.6944	
112	40091	8.6351	8.6351		162	49113	5.0000	8.0518	
113	40092	6.7580	6.7320		163	49115	5.0000	8.1681	
114	40093	5.0000	8.2186		164	50112	5.0000	7.7454	
115	40094	5.0000	6.4709		165	50113	5.0000	10.2990	
116	40095	5.0000	7.8527		166	50114	5.0000	7.5466	
117	40096	5.5710	6.7136		167	50115	5.0000	9.5624	
118	41093	5.0000	7.2140		168	50116	5.0000	6.9442	
119	41094	5.0000	8.4908		169	50117	5.0000	9.3262	
120	41095	5.0000	9.5843		170	50118	5.0000	6.4845	
121	42092	5.0000	8.0674		171	50119	5.0000	9.1066	
122	42094	5.0000	7.3712		172	50120	5.0000	6.2870	
123	42095	9.1542	9.1540	9.15	173	50122	5.0000	5.9464	
124	42096	5.0000	6.8211		174	50123	5.0000	8.4904	
125	42097	5.0000	8.6423		175	50124	5.0000	5.7334	
126	42098	5.0000	6.4646		176	50125	5.0000	8.1930	
127	42099	5.0000	8.2909		177	50126	5.0000	6.6301	
128	42100	5.0000	8.1823		178	51121	5.0000	7.8137	
129	43099	5.0000	8.1606	8.16	179	51123	5.0000	6.4672	
130	44096	5.0000	10.1595		180	51124	5.0000	8.7101	
131	44098	5.0000	7.4652		181	51125	5.0000	6.2214	
132	44099	5.0000	9.6732		182	51126	5.0000	9.5942	
133	44100	5.0000	6.8014		183	52120	5.0000	7.1754	
134	44101	9.2161	9.2190		184	52122	5.0000	6.9334	
135	44102	5.0000	6.2324		185	52123	5.0000	9.4254	
136	44103	5.0000	8.9039		186	52124	5.0000	6.5714	
137	44104	5.0000	7.2941		187	52125	5.0000	9.1184	
138	44105	5.0000	8.4652		188	52126	5.0000	6.5198	
139	44106	5.0000	7.6357		189	52128	5.0000	6.6893	
140	45103	6.9993	7.9962	8.00	190	52130	5.0000	7.0600	
141	45105	7.0941	8.2065	8.20	191	52132	5.0000	8.7130	
142	46102	5.0000	7.6244		192	52601	5.0000	8.8670	
143	46104	5.0000	7.0944		193	52611	5.0000	8.5179	
144	46105	5.0000	9.5620		194	53127	5.0000	7.6402	
145	46106	5.0000	6.5384		195	53129	5.0000	8.8782	
146	46107	5.0000	9.2234		196	53130	5.0000	8.5830	
147	46108	5.0000	6.5148		197	53131	5.0000	9.0709	
148	46110	5.0000	6.6368		198	53135	5.0000	8.1203	
149	47107	5.0000	7.8950		199	54123	5.0000	10.4720	
150	47109	6.8250	8.0260		200	54124	5.0000	8.9274	



(continued)

No	Nuclide	Capture kappa (MeV)			No	Nuclide	Capture kappa (MeV)		
		SCALE 6.2	New	CASMO-5			SCALE 6.2	New	CASMO-5
201	54126	5.0000	7.2254		251	61601	5.0000	7.4080	
202	54128	5.0000	6.9077		252	62144	5.0000	6.7570	
203	54129	5.0000	9.2551		253	62147	8.1402	8.1420	
204	54130	5.0000	6.6056		254	62148	5.0000	5.8710	
205	54131	8.9363	8.9350	8.94	255	62149	7.9824	7.9850	
206	54132	5.0000	6.6207		256	62150	5.5960	5.5960	5.60
207	54133	5.0000	8.5344		257	62151	8.2580	8.2580	8.26
208	54134	5.0000	7.0162		258	62152	5.8670	6.1985	
209	54135	7.8800	7.9904	7.99	259	62153	5.0000	7.9670	
210	54136	5.0000	5.9085		260	62154	5.0000	6.4740	
211	55133	6.7044	6.8910		261	63151	5.0000	6.3079	
212	55134	6.5500	8.8274		262	63152	5.0000	8.5504	
213	55135	5.0000	6.7644		263	63153	6.4440	6.4422	
214	55136	5.0000	8.2734		264	63154	8.1670	8.1522	
215	55137	5.0000	7.8820		265	63155	6.4900	6.3386	
216	56130	5.0000	7.4944		266	63156	5.0000	8.1108	
217	56132	5.0000	7.1874		267	63157	5.0000	5.8150	
218	56133	5.0000	9.4680		268	64152	5.0000	6.2470	
219	56134	5.0000	6.9734		269	64153	5.0000	8.8940	
220	56135	5.0000	9.1074		270	64154	5.0000	6.4350	
221	56136	5.0000	6.8984		271	64155	5.0000	8.5360	8.54
222	56137	5.0000	8.6114		272	64156	5.0000	6.3600	
223	56138	5.0000	5.6700		273	64157	5.0000	7.9370	7.94
224	56140	5.0000	7.6406		274	64158	5.0000	6.3088	
225	57138	5.0000	8.7784		275	64160	5.0000	6.6165	
226	57139	5.0000	8.0375		276	65159	5.0000	6.3754	
227	57140	5.0000	7.6769		277	65160	5.0000	7.6970	
228	58136	5.0000	8.0972		278	66156	5.0000	7.3344	
229	58138	5.0000	7.4550		279	66158	5.0000	6.8310	
230	58139	5.0000	9.2010		280	66160	5.0000	6.4540	
231	58140	5.0000	5.4284		281	66161	5.0000	8.1960	
232	58141	5.0000	7.1686		282	66162	5.0000	6.2710	
233	58142	5.0000	5.8679		283	66163	5.0000	7.6580	
234	58143	5.0000	6.8960		284	66164	5.0000	6.1886	
235	58144	5.0000	5.4842		285	67165	5.0000	6.9664	
236	59141	5.0000	6.7092		286	67601	5.0000	7.4978	
237	59142	5.0000	7.3520		287	68162	5.0000	6.9531	
238	59143	5.0000	6.9953		288	68164	5.0000	7.2981	
239	60142	5.0000	6.1230		289	68166	5.0000	6.4367	
240	60143	7.8174	7.8160	7.82	290	68167	5.0000	7.7707	
241	60144	5.0000	5.7560		291	68168	5.0000	6.0037	
242	60145	7.5654	7.5650	7.57	292	68170	5.0000	6.4736	
243	60146	5.0000	5.2910		293	71175	5.0000	6.1914	
244	60147	5.0000	7.3330		294	71176	5.0000	7.0720	
245	60148	5.0000	5.0380		295	72174	5.0000	6.8242	
246	60150	5.0000	5.9607		296	72176	5.0000	6.4046	
247	61147	5.9000	7.2032		297	72177	5.0000	7.6699	
248	61148	7.2660	7.2644		298	72178	5.0000	6.1157	
249	61149	5.0000	7.7456		299	72179	5.0000	7.1800	
250	61151	5.0000	5.9400		300	72180	5.0000	5.6540	

(continued)

No	Nuclide	Capture kappa (MeV)			No	Nuclide	Capture kappa (MeV)		
		SCALE 6.2	New	CASMO-5			SCALE 6.2	New	CASMO-5
301	73181	5.0000	6.0700		351	93235	5.0000	5.7394	
302	73182	5.0000	7.5628		352	93236	5.0000	6.5734	
303	74182	5.0000	6.1907		353	93237	5.4900	6.3215	
304	74183	5.0000	7.4118		354	93238	5.0000	6.6597	
305	74184	5.0000	5.7538		355	93239	4.9700	5.1681	
306	74186	5.0000	6.2227		356	94236	5.0000	5.8770	
307	75185	5.0000	6.5347		357	94237	5.0000	6.9980	
308	75187	5.0000	6.7156		358	94238	5.5500	4.8060	
309	77191	5.0000	6.1980		359	94239	6.5330	6.5337	6.53
310	77193	5.0000	6.9683		360	94240	5.2410	5.2410	5.24
311	79197	5.0000	7.2431		361	94241	6.3010	6.3008	6.30
312	80196	5.0000	7.4627		362	94242	5.0710	5.2642	5.27
313	80198	5.0000	6.6490		363	94243	6.0200	6.0200	
314	80199	5.0000	8.0290		364	94244	5.0000	5.7754	
315	80200	5.0000	6.2250		365	94246	5.0000	6.6812	
316	80201	5.0000	7.7560		366	95241	5.5290	5.5391	
317	80202	5.0000	5.9930		367	95242	6.4260	6.3671	
318	80204	5.0000	6.2114		368	95243	5.3630	6.5129	6.47
319	82204	5.0000	6.7315		369	95244	5.0000	6.3768	
320	82206	5.0000	6.7378		370	95601	5.0000	6.3700	
321	82207	5.0000	7.3678		371	95611	5.0000	6.1410	
322	82208	5.0000	4.1349		372	96241	5.0000	6.9680	
323	83209	5.0000	4.9890		373	96242	5.0000	5.7030	
324	88223	5.0000	13.1325		374	96243	5.0000	6.7995	
325	88224	5.0000	4.8887		375	96244	6.4510	5.5224	
326	88225	5.0000	6.3887		376	96245	6.1100	6.4500	
327	88226	5.0000	5.0895		377	96246	5.0000	5.1600	
328	89225	5.0000	11.8352		378	96247	5.0000	6.2114	
329	89226	5.0000	6.5277		379	96248	5.0000	5.0136	
330	89227	5.0000	5.0357		380	96249	5.0000	5.8324	
331	90227	5.0000	7.1287		381	96250	5.0000	4.9697	
332	90228	5.0000	5.2488		382	97249	5.0000	6.1653	
333	90229	5.0000	6.7897		383	97250	5.0000	0.8650	
334	90230	5.0100	5.1205		384	98249	5.0000	6.6230	
335	90232	4.7860	5.2124		385	98250	5.0000	5.1100	
336	90233	6.0800	6.1920		386	98251	5.0000	6.1700	
337	90234	5.0000	5.0227		387	98252	5.0000	4.7900	
338	91231	5.6600	6.6482		388	98253	5.0000	5.9800	
339	91232	5.0000	6.5167		389	98254	5.0000	4.4500	
340	91233	5.1970	5.2190		390	99253	5.0000	5.0920	
341	92232	5.9300	5.7434		391	99254	5.0000	5.9827	
342	92233	6.8410	6.8442		392	99255	5.0000	4.9017	
343	92234	5.2970	5.2978	5.30	393	100255	5.0000	6.3867	
344	92235	6.5451	6.5452	6.55					
345	92236	5.1240	5.1259						
346	92237	5.0000	6.1538						
347	92238	4.8040	5.7090	5.68					
348	92239	5.0000	6.0217						
349	92240	5.0000	5.0291						
350	92241	5.0000	6.8315						

**Table 2.7. Comparison of the capture kappas with ENDF/B-7.1**

No	Nuclide	Capture kappa (MeV)			No	Nuclide	Capture kappa (MeV)		
		SCALE 6.2	New	CASMO-5			SCALE 6.2	New	CASMO-5
1	1001	2.2246	2.2246	2.22	51	22050	5.0000	7.6114	
2	1002	5.0000	6.2574	6.26	52	23050	5.0000	11.0512	
3	1003	0.0000	0.0000		53	23051	5.0000	9.8253	
4	2003	5.0000	20.5778		54	24050	5.0000	9.2617	
5	2004	0.0000	0.0000		55	24052	5.0000	7.9392	
6	3006	5.0000	7.2506		56	24053	5.0000	9.7191	
7	3007	5.0000	2.0328		57	24054	5.0000	7.3484	
8	4007	0.0000	0.0000		58	25055	5.0000	9.7920	
9	4009	5.0000	0.4360		59	26054	5.0000	9.2980	
10	5010	2.7900	2.7895	2.79	60	26056	7.6000	7.6461	
11	5011	5.0000	9.5505		61	26057	5.0000	10.0445	
12	6000	5.0000	2.2605		62	26058	5.0000	6.5810	
13	7014	5.0000	2.0367		63	27058	5.0000	10.4540	
14	7015	5.0000	3.4559		64	27059	5.0000	7.4900	
15	8016	4.1430	0.0249	4.14	65	27601	5.0000	10.4500	
16	8017	5.0000	1.8630		66	28058	9.0200	8.9568	
17	9019	5.0000	2.5829		67	28059	5.0000	10.3302	
18		12.4200			68	28060	5.0000	7.8201	
19	11023	5.0000	11.6365		69	28061	5.0000	10.5973	
20	12024	5.0000	5.4623		70	28062	5.0000	6.8379	
21	12025	5.0000	8.6523		71	28064	5.0000	7.2840	
22	12026	5.0000	7.9026		72	29063	5.0000	8.2293	
23	13027	5.0000	10.6280		73	29065	5.0000	8.2300	
24	14028	5.0000	7.9485		74	30064	5.0000	7.9793	
25	14029	5.0000	9.1140		75	30065	5.0000	11.0592	
26	14030	5.0000	7.1889		76	30066	5.0000	7.0523	
27	15031	5.0000	7.6842		77	30067	5.0000	10.1981	
28	16032	5.0000	5.8317		78	30068	5.0000	6.8037	
29	16033	5.0000	4.6095		79	30070	5.0000	7.1906	
30	16034	5.0000	6.6307		80	31069	5.0000	8.3061	
31	16036	5.0000	8.0460		81	31071	5.0000	9.7601	
32	17035	5.0000	8.5798		82	32070	5.0000	7.4159	
33	17037	5.0000	9.1338		83	32072	5.0000	6.7829	
34	18036	5.0000	8.2695		84	32073	5.0000	10.1962	
35	18038	5.0000	6.4215		85	32074	5.0000	6.9604	
36	18040	5.0000	7.8475		86	32076	5.0000	8.0268	
37	19039	5.0000	7.3825		87	33074	5.0000	10.2430	
38	19040	5.0000	9.8471		88	33075	5.0000	8.8176	
39	19041	5.0000	9.2440		89	34074	5.0000	8.0277	
40	20040	5.0000	6.7025		90	34076	5.0000	7.4184	
41	20042	5.0000	7.8419		91	34077	5.0000	10.4970	
42	20043	5.0000	11.1320		92	34078	5.0000	6.9606	
43	20044	5.0000	7.4148		93	34079	5.0000	9.9121	
44	20046	5.0000	8.8916		94	34080	5.0000	7.3200	
45	20048	5.0000	10.0126		95	34082	5.0000	9.1301	
46	21045	5.0000	8.7607		96	35079	5.0000	8.6934	
47	22046	5.0000	8.8330		97	35081	5.0000	10.3702	
48	22047	5.0000	11.5707		98	36078	5.0000	10.8353	
49	22048	5.0000	8.1424		99	36080	5.0000	7.8814	
50	22049	5.0000	10.9394		100	36082	5.0000	7.4651	

(continued)

No	Nuclide	Capture kappa (MeV)			No	Nuclide	Capture kappa (MeV)		
		SCALE 6.2	New	CASMO-5			SCALE 6.2	New	CASMO-5
101	36083	5.0000	10.5200		151	46106	5.0000	6.5384	
102	36084	5.0000	7.1114		152	46107	5.0000	9.2234	
103	36085	5.0000	9.8560		153	46108	5.0000	6.5149	
104	36086	5.0000	7.6194		154	46110	5.0000	6.6364	
105	37085	5.0000	8.6503		155	47107	5.0000	7.8950	
106	37086	5.0000	9.9190		156	47109	6.8250	8.0260	
107	37087	5.0000	8.8067		157	47111	5.0000	8.4750	
108	38084	5.0000	8.5300		158	47601	5.0000	9.3016	
109	38086	5.0000	8.4282		159	48106	5.0000	9.8304	
110	38087	5.0000	11.1130		160	48108	5.0000	7.3300	
111	38088	5.0000	6.3670		161	48110	5.0000	6.9768	
112	38089	5.0000	7.8024		162	48111	5.0000	9.3953	
113	38090	5.0000	7.1770		163	48112	5.0000	6.5398	
114	39089	5.0000	7.7900		164	48113	5.0000	9.0427	
115	39090	5.0000	7.9290		165	48114	5.0000	6.6577	
116	39091	5.0000	8.2459		166	48116	5.0000	8.2404	
117	40090	7.2026	7.1940		167	48601	5.0000	11.6899	
118	40091	8.6351	8.6350		168	49113	5.0000	8.0518	
119	40092	6.7580	6.7330		169	49115	5.0000	8.1704	
120	40093	5.0000	8.2200		170	50112	5.0000	7.7454	
121	40094	5.0000	6.4630		171	50113	5.0000	10.2990	
122	40095	5.0000	7.8540		172	50114	5.0000	7.5466	
123	40096	5.5710	7.5743		173	50115	5.0000	9.5624	
124	41093	5.0000	7.2140		174	50116	5.0000	6.9442	
125	41094	5.0000	8.4908		175	50117	5.0000	9.3262	
126	41095	5.0000	9.5843		176	50118	5.0000	6.4845	
127	42092	5.0000	8.0674		177	50119	5.0000	9.1066	
128	42094	5.0000	7.3712		178	50120	5.0000	6.2872	
129	42095	9.1542	9.1540	9.15	179	50122	5.0000	5.9464	
130	42096	5.0000	6.8211		180	50123	5.0000	8.4904	
131	42097	5.0000	8.6423		181	50124	5.0000	5.7334	
132	42098	5.0000	6.4665		182	50125	5.0000	8.1930	
133	42099	5.0000	8.2909		183	50126	5.0000	8.9217	
134	42100	5.0000	8.1823		184	51121	5.0000	7.8160	
135	43099	5.0000	8.1580	8.16	185	51123	5.0000	6.4672	
136	44096	5.0000	10.1731		186	51124	5.0000	8.7101	
137	44098	5.0000	7.4652		187	51125	5.0000	6.2214	
138	44099	5.0000	9.6732		188	51126	5.0000	9.5839	
139	44100	5.0000	6.8014		189	52120	5.0000	7.1754	
140	44101	9.2161	9.2190		190	52122	5.0000	6.9334	
141	44102	5.0000	6.2324		191	52123	5.0000	9.4254	
142	44103	5.0000	8.9039		192	52124	5.0000	6.5714	
143	44104	5.0000	7.2940		193	52125	5.0000	9.1184	
144	44105	5.0000	8.4652		194	52126	5.0000	6.5198	
145	44106	5.0000	7.6178		195	52128	5.0000	6.6915	
146	45103	6.9993	7.9962	8.00	196	52130	5.0000	7.0607	
147	45105	7.0941	8.2093	8.20	197	52132	5.0000	8.6939	
148	46102	5.0000	7.6244		198	52601	5.0000	8.8670	
149	46104	5.0000	7.0944		199	52611	5.0000	8.8069	
150	46105	5.0000	9.5620		200	53127	5.0000	7.6402	



(continued)

No	Nuclide	Capture kappa (MeV)			No	Nuclide	Capture kappa (MeV)		
		SCALE 6.2	New	CASMO-5			SCALE 6.2	New	CASMO-5
201	53129	5.0000	8.8782		251	60148	5.0000	6.2458	
202	53130	5.0000	8.5830		252	60150	5.0000	7.4205	
203	53131	5.0000	9.0709		253	61147	5.9000	7.2044	
204	53135	5.0000	8.0863		254	61148	7.2660	7.6439	
205	54123	5.0000	10.4829		255	61149	5.0000	7.7884	
206	54124	5.0000	8.9453		256	61151	5.0000	7.5630	
207	54126	5.0000	7.2254		257	61601	5.0000	7.4080	
208	54128	5.0000	6.9077		258	62144	5.0000	6.7570	
209	54129	5.0000	9.2551		259	62147	8.1402	8.1420	
210	54130	5.0000	6.6056		260	62148	5.0000	5.8710	
211	54131	8.9363	8.9350	8.94	261	62149	7.9824	7.9850	
212	54132	5.0000	6.6207		262	62150	5.5960	5.5960	5.60
213	54133	5.0000	8.5344		263	62151	8.2580	8.2580	8.26
214	54134	5.0000	7.0214		264	62152	5.8670	6.1982	
215	54135	7.8800	7.9904	7.99	265	62153	5.0000	7.9670	
216	54136	5.0000	5.8908		266	62154	5.0000	6.4741	
217	55133	6.7044	6.8910		267	63151	5.0000	6.3079	
218	55134	6.5500	8.8274		268	63152	5.0000	8.5504	
219	55135	5.0000	6.7644		269	63153	6.4440	6.4422	
220	55136	5.0000	8.2734		270	63154	8.1670	8.1522	
221	55137	5.0000	7.8824		271	63155	6.4900	6.3386	
222	56130	5.0000	7.4944		272	63156	5.0000	8.1108	
223	56132	5.0000	7.1874		273	63157	5.0000	7.9750	
224	56133	5.0000	9.4680		274	64152	5.0000	6.2470	
225	56134	5.0000	6.9734		275	64153	5.0000	8.8940	
226	56135	5.0000	9.1074		276	64154	5.0000	6.4350	
227	56136	5.0000	6.8984		277	64155	5.0000	8.5360	8.54
228	56137	5.0000	8.6114		278	64156	5.0000	6.3600	
229	56138	5.0000	5.6704		279	64157	5.0000	7.9370	7.94
230	56140	5.0000	7.6322		280	64158	5.0000	6.3087	
231	57138	5.0000	8.7784		281	64160	5.0000	6.6173	
232	57139	5.0000	8.0130		282	65159	5.0000	6.3754	
233	57140	5.0000	7.6770		283	65160	5.0000	7.6970	
234	58136	5.0000	8.0860		284	66156	5.0000	8.0304	
235	58138	5.0000	7.4550		285	66158	5.0000	6.8310	
236	58139	5.0000	9.2010		286	66160	5.0000	6.4540	
237	58140	5.0000	5.4284		287	66161	5.0000	8.1960	
238	58141	5.0000	7.1686		288	66162	5.0000	6.2710	
239	58142	5.0000	5.8684		289	66163	5.0000	7.6580	
240	58143	5.0000	6.8960		290	66164	5.0000	6.1889	
241	58144	5.0000	6.9934		291	67165	5.0000	6.9674	
242	59141	5.0000	6.7092		292	67601	5.0000	7.4978	
243	59142	5.0000	7.3520		293	68162	5.0000	8.3617	
244	59143	5.0000	6.9954		294	68164	5.0000	7.9375	
245	60142	5.0000	6.1230		295	68166	5.0000	6.4367	
246	60143	7.8174	7.8160	7.82	296	68167	5.0000	7.7707	
247	60144	5.0000	5.7560		297	68168	5.0000	6.0037	
248	60145	7.5654	7.5650	7.57	298	68170	5.0000	6.4739	
249	60146	5.0000	5.2910		299	69168	5.0000	8.0324	
250	60147	5.0000	7.3330		300	69169	5.0000	6.5930	

(continued)

No	Nuclide	Capture kappa (MeV)			No	Nuclide	Capture kappa (MeV)		
		SCALE 6.2	New	CASMO-5			SCALE 6.2	New	CASMO-5
301	69170	5.0000	7.4860		351	90234	5.0000	5.1393	
302	71175	5.0000	6.1914		352	91229	5.0000	5.7948	
303	71176	5.0000	7.0720		353	91230	5.0000	6.8201	
304	72174	5.0000	6.7897		354	91231	5.6600	6.6467	
305	72176	5.0000	6.3837		355	91232	5.0000	6.5291	
306	72177	5.0000	7.6267		356	91233	5.1970	6.9044	
307	72178	5.0000	6.0997		357	92230	5.0000	6.0458	
308	72179	5.0000	7.3887		358	92231	5.0000	7.2680	
309	72180	5.0000	5.6957		359	92232	5.9300	5.7621	
310	73180	5.0000	7.5768		360	92233	6.8410	6.8442	
311	73181	5.0000	6.0629		361	92234	5.2970	5.2978	5.30
312	73182	5.0000	7.5625		362	92235	6.5451	6.5452	6.55
313	74180	5.0000	6.6810		363	92236	5.1240	5.1259	
314	74182	5.0000	6.1910		364	92237	5.0000	6.1538	
315	74183	5.0000	7.4110		365	92238	4.8040	5.7161	5.68
316	74184	5.0000	5.7530		366	92239	5.0000	7.5716	
317	74186	5.0000	6.2610		367	92240	5.0000	5.0329	
318	75185	5.0000	6.5360		368	92241	5.0000	7.2450	
319	75187	5.0000	6.7138		369	93234	5.0000	6.9831	
320	77191	5.0000	6.1980		370	93235	5.0000	5.7367	
321	77193	5.0000	6.9610		371	93236	5.0000	6.5774	
322	79197	5.0000	7.2427		372	93237	5.4900	6.3215	
323	80196	5.0000	7.6057		373	93238	5.0000	6.6651	
324	80198	5.0000	6.6490		374	93239	4.9700	6.5999	
325	80199	5.0000	8.0290		375	94236	5.0000	5.8807	
326	80200	5.0000	6.2250		376	94237	5.0000	6.9999	
327	80201	5.0000	7.7560		377	94238	5.5500	5.6466	
328	80202	5.0000	5.9930		378	94239	6.5330	6.5337	6.53
329	80204	5.0000	6.2125		379	94240	5.2410	5.2415	5.24
330	81203	5.0000	6.6560		380	94241	6.3010	6.3008	6.30
331	81205	5.0000	7.0424		381	94242	5.0710	5.2330	5.27
332	82204	5.0000	6.7315		382	94243	6.0200	6.0200	
333	82206	5.0000	6.7378		383	94244	5.0000	5.8350	
334	82207	5.0000	7.3678		384	94246	5.0000	5.1823	
335	82208	5.0000	4.1348		385	95240	5.0000	6.6471	
336	83209	5.0000	4.9891		386	95241	5.5290	5.7382	
337	88223	5.0000	13.1327		387	95242	6.4260	6.3671	
338	88224	5.0000	4.8887		388	95243	5.3630	6.5124	6.47
339	88225	5.0000	6.3887		389	95244	5.0000	6.3712	
340	88226	5.0000	5.0909		390	95601	5.0000	6.3700	
341	89225	5.0000	12.2736		391	95611	5.0000	6.1410	
342	89226	5.0000	6.5306		392	96240	5.0000	6.0933	
343	89227	5.0000	6.4382		393	96241	5.0000	6.9695	
344	90227	5.0000	7.1053		394	96242	5.0000	5.6929	
345	90228	5.0000	5.2570		395	96243	5.0000	6.8013	
346	90229	5.0000	6.7939		396	96244	6.4510	5.5203	
347	90230	5.0100	5.3014		397	96245	6.1100	6.4576	
348	90231	5.0000	6.4403		398	96246	5.0000	5.1559	
349	90232	4.7860	5.2121		399	96247	5.0000	6.2130	
350	90233	6.0800	6.1903		400	96248	5.0000	5.0137	



(continued)

No	Nuclide	Capture kappa (MeV)			No	Nuclide	Capture kappa (MeV)		
		SCALE 6.2	New	CASMO-5			SCALE 6.2	New	CASMO-5
401	96249	5.0000	5.8324						
402	96250	5.0000	5.4355						
403	97245	5.0000	13.6473						
404	97246	5.0000	6.5491						
405	97247	5.0000	5.4819						
406	97248	5.0000	6.3017						
407	97249	5.0000	6.1648						
408	97250	5.0000	6.2549						
409	98246	5.0000	6.1856						
410	98248	5.0000	5.5855						
411	98249	5.0000	6.6252						
412	98250	5.0000	5.1085						
413	98251	5.0000	6.1720						
414	98252	5.0000	4.8043						
415	98253	5.0000	6.0316						
416	98254	5.0000	4.6031						
417	99251	5.0000	5.2895						
418	99252	5.0000	6.3516						
419	99253	5.0000	5.0930						
420	99254	5.0000	5.9744						
421	99255	5.0000	4.9742						
422	99601	5.0000	6.0586						
423	100255	5.0000	6.3845						

2.7 BENCHMARK CALCULATION USING CAPTURE KAPPAS

To verify the effect of using explicit capture energy in depletion calculation, VERA Problem 2B (regular UO₂ fuel) and 2P (24 gadolinia fuels) are run for a comparison between single kappa and on-the-fly capture kappa. These calculations use the latest simplified AMPX library that includes the new method to generate capture kappa, as discussed in the previous sections. Table 2.8 shows the comparison of the overall effective kappa between single and OTF kappa approaches, and the kappa tallied from MCNP [Wan17]. The MPACT OTF kappas are essentially consistent with MCNP for both cases. The MPACT single kappas are 2-3MeV off for 2B, and is certainly not able to model the Gd capture effect, so 2B and 2P have almost the same value for the single kappa approach.

Table 2.8. Comparison of Effective Kappas

	MCNP	MPACT single kappa	MPACT OTF kappa
2B	199.46	202.84	200.22
2P	202.17	202.96	202.74

Figures 2.4 and 2.5 compare the effective kappa between single and OTF kappa approaches with burnup. In general, the OTF kappa increases faster with burnup due to

the explicit model of capture energy for absorbers formed from depletion. The small dip of OTF kappa around 10 GWd/tU in 2P is due to the burn-out of Gd isotopes. The maximum differences of eigenvalues are around 100 pcm for both cases.

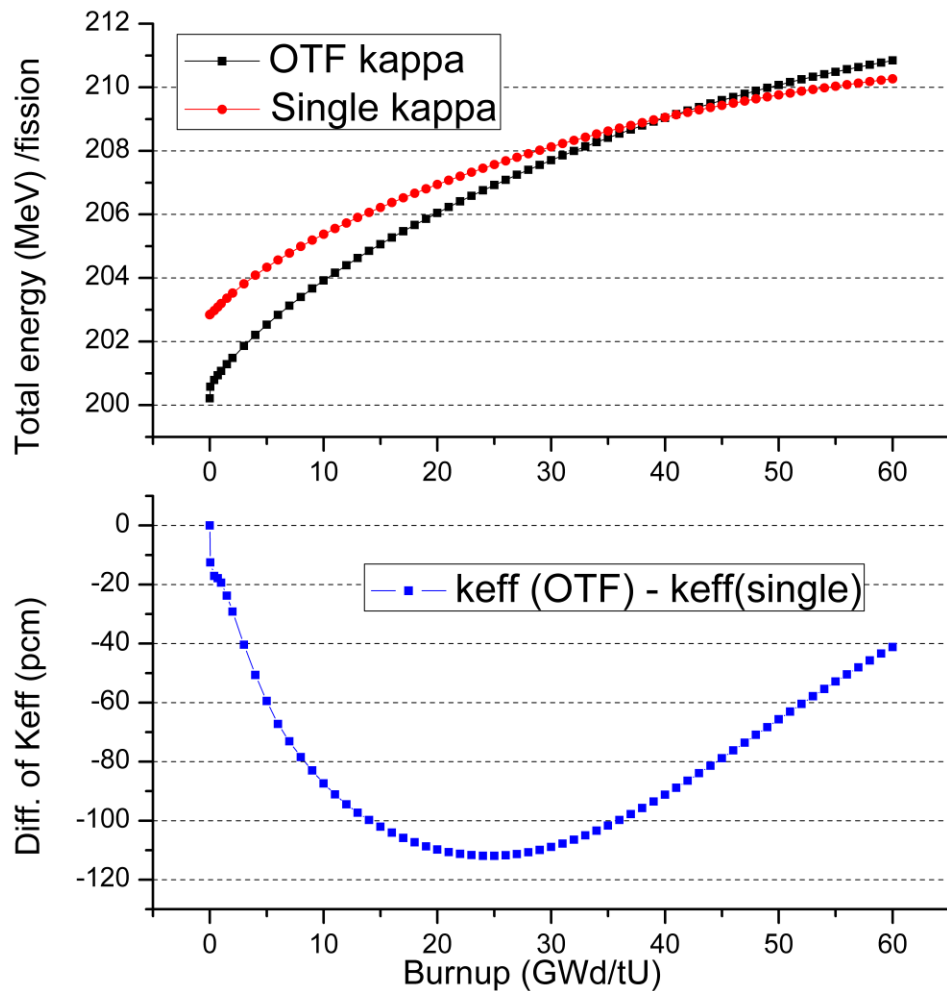


Figure 2.4. Comparison of Effective Kappa and Eigenvalue in Depletion for 2B.

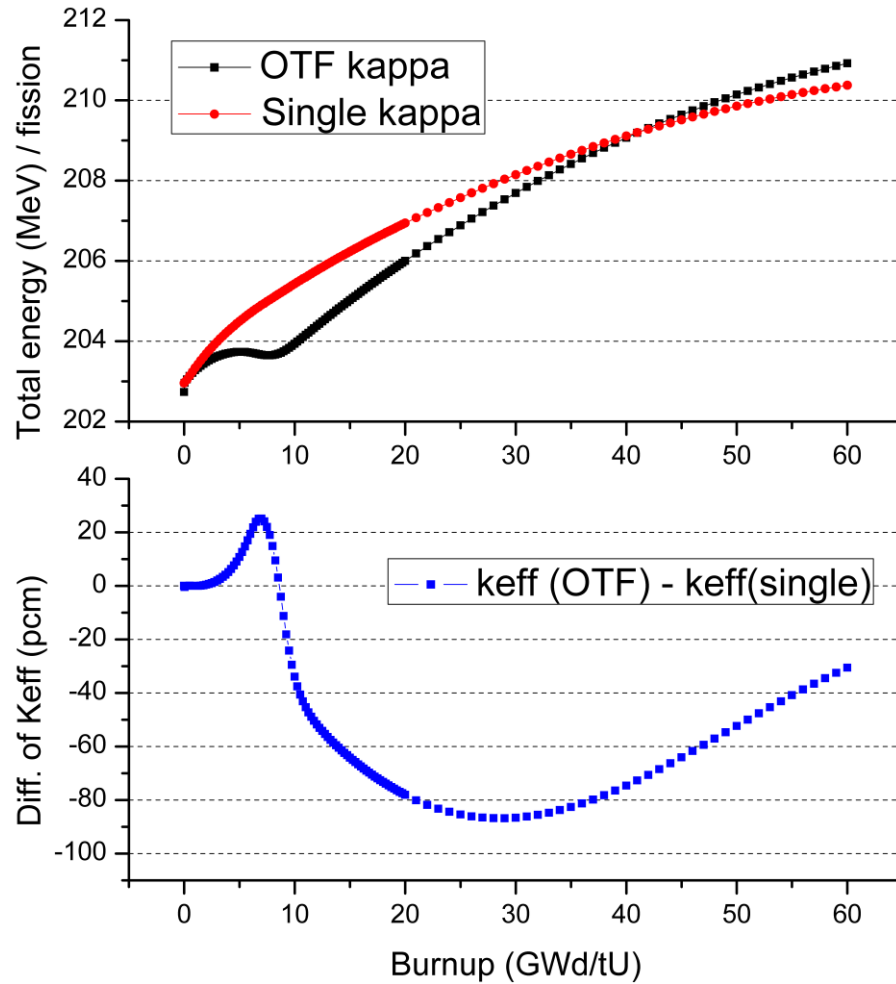


Figure 2.5. Comparison of Effective Kappa and Eigenvalue in Depletion for 2P.

3. DEVELOPMENT OF APPROXIMATE GAMMA SMEARING MODEL

3.1 RECOVERABLE ENERGY AND ENERGY DEPOSITION

Various recoverable energies from neutron reactions are deposited in the reactor core locally or globally. Below are the sources of recoverable energies and details on how they are assumed to be deposited.

- Fission reactions
 - Fission fragments (local)
 - Fission neutrons (global)
 - Beta decay of fission products (local)
 - Prompt gammas (global)
 - Delayed gammas of fission products (global)
- Capture reactions
 - Gamma (global)
 - Alpha and other elementary particles (local)
 - Beta decay of production isotope followed by neutron capture (local)

Energies of fission neutrons and various gammas are to be deposited globally, so neutron and gamma transport calculations are required to explicitly estimate their energy depositions. Table 2.1 provides various energy release modes from neutron fission and capture reactions for ^{235}U and ^{238}U .

Currently, since the CASL neutronic simulator MPACT is solving the Neutron Boltzmann equation for eigenvalue problems, spatial neutron energy deposition can be explicitly estimated. As shown in Table 2.1, the fraction of total gamma energy is about 10% of the total recoverable energy. However, since the MPACT code does not have the gamma transport capability or a gamma cross section library, spatial gamma energy deposition has been neglected. The mean free paths of photons are much longer than those of neutrons, which would make the power distribution flatter.

The objective of this study is to develop an approximate model for spatial energy deposition with a consideration of gamma energy deposition without solving gamma transport equation.

3.2 BENCHMARK PROBLEMS

Since the mean-free path of gamma rays is long, pin-wise gamma energy depositions are flat inside the fuel assembly [Kim13]. Therefore, the typically single gamma smearing factor can be obtained to make the best estimate of gamma-smeared power distribution without performing gamma transport calculation.

Table 3.1 provides various benchmark problems to obtain and verify the best gamma smearing factor which includes single fuel pin, fuel assemblies, 1D-like whole cores, and



2D whole core problems. The problems are based on CASL VERA progression problems [God14] except for the 1D core problems. Figure 3.1 provides pin configurations for the VERA progression problems of fuel assemblies. As shown in Figure 3.2, three 1D-like whole core problems with various core sizes have been devised to develop a procedure to apply the obtained gamma smearing factor to the whole core problem and to verify the procedure. Case 5A-2D is a 2D quarter core problem which also comes from the VERA progression problems.

Both MCNP and deterministic program KARMA [Kim13] with gamma transport capability have been used in the benchmark calculations.

Table 3.1. Benchmark problems

Case	ID	Description	Simulation Code	
			MCNP	KARMA
Pin	1C	VERA Progression 1C :: UO_2 $T_{\text{fuel}}=900 \text{ K}$, $T_{\text{mod}}=600 \text{ K}$	o	-
Fuel assembly	2B	VERA Progression 2B :: UO_2 $T_{\text{fuel}}=600 \text{ K}$, $T_{\text{mod}}=600 \text{ K}$	o	-
	2C	VERA Progression 2C :: UO_2 $T_{\text{fuel}}=600 \text{ K}$, $T_{\text{mod}}=900 \text{ K}$	-	o
	2F	VERA Progression 2F :: Pyrex $T_{\text{fuel}}=900 \text{ K}$, $T_{\text{mod}}=600 \text{ K}$	o	o
	2G	VERA Progression 2G :: AIC-CR $T_{\text{fuel}}=900 \text{ K}$, $T_{\text{mod}}=600 \text{ K}$	o	o
	2H	VERA Progression 2H :: B ₄ C-CR $T_{\text{fuel}}=900 \text{ K}$, $T_{\text{mod}}=600 \text{ K}$	o	o
	2M	VERA Progression 2M :: IFBA $T_{\text{fuel}}=900 \text{ K}$, $T_{\text{mod}}=600 \text{ K}$	o	o
	2P	VERA Progression 2P :: Gd ₂ O ₃ $T_{\text{fuel}}=900 \text{ K}$, $T_{\text{mod}}=600 \text{ K}$	o	o
1D core	1D-a	1D array of 153 fuel pins and 34 reflector cells	-	o
	1D-b	1D array of 187 fuel pins and 34 reflector cells	-	o
	1D-c	1D array of 272 fuel pins and 34 reflector cells	-	o
2D core	5A	VERA Progression 5A :: WBN-1	o	-

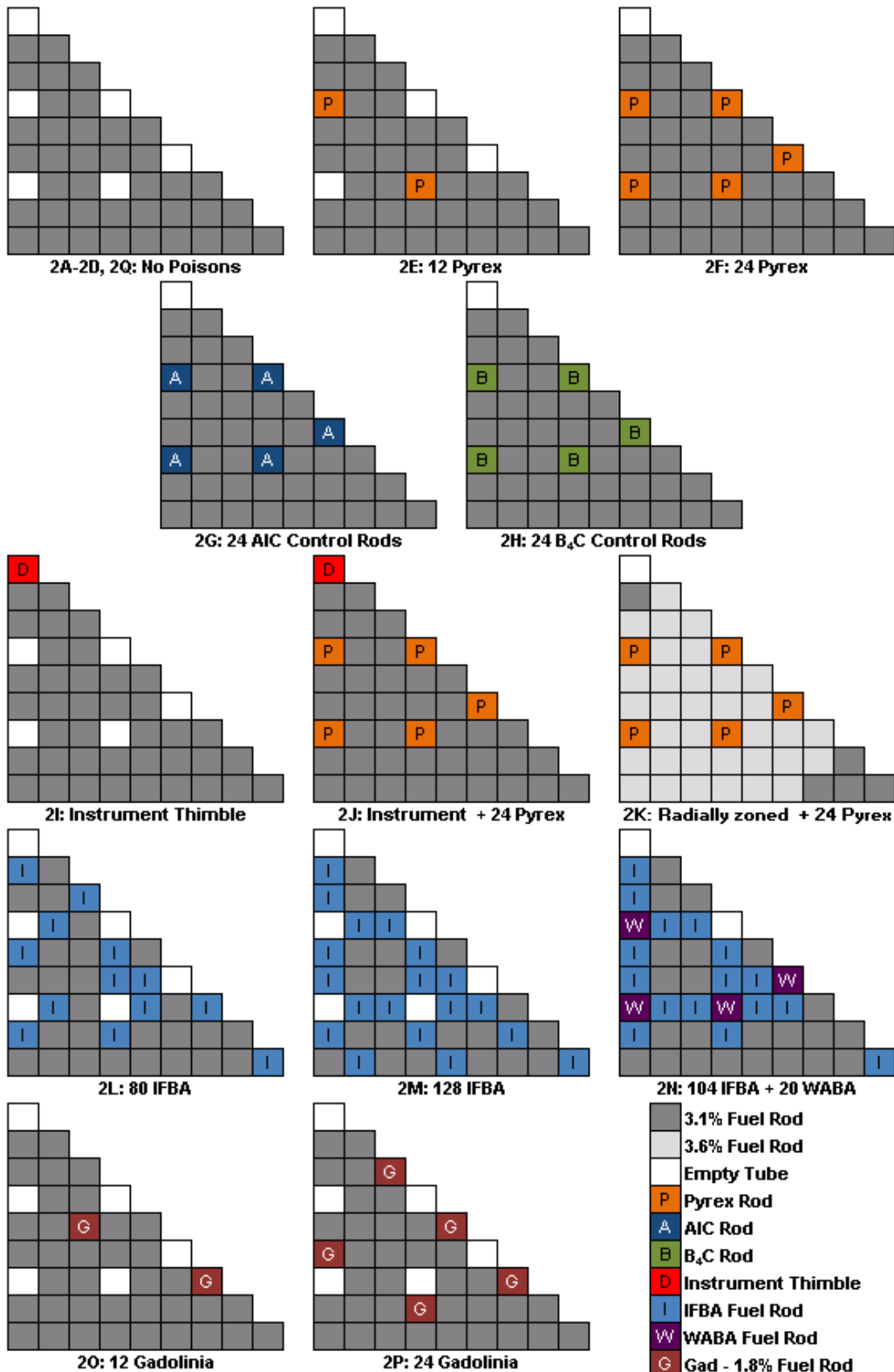


Figure 3.1. VERA Progression Problems for Fuel Assemblies.

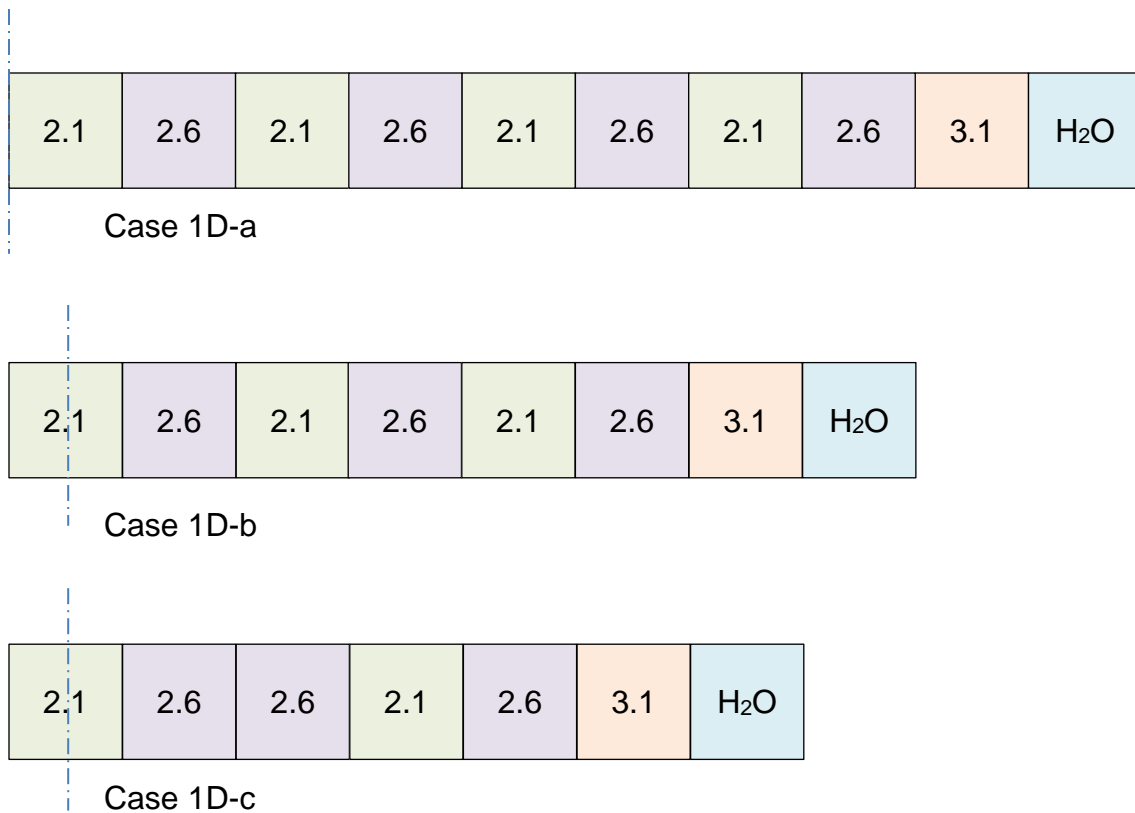


Figure 3.2. 1D Core Problems with Various Numbers of Assemblies.

3.3 CONTRIBUTION OF GAMMA ENERGY DEPOSITION

Benchmark calculations for the 2D fuel assembly problems have been performed to estimate fractions of total gamma energy deposition to total energy deposition by using MCNP and the deterministic code KARMA. The fractions of total gamma energy depositions as a function of burnup have been obtained only by the deterministic code.

Table 3.2 provides fractions of gamma energy deposition for the fresh fuels. Gamma energy deposition is at about 10% and is partly dependent upon burnable poison and absorber type. There are very good consistencies between the Monte Carlo and deterministic results except for the case with the Ag-In-Cd control rod inserted.

The fractions of gamma energy depositions as a function of burnup have been estimated by using the deterministic transport lattice code KARMA for six fuel assembly cases, as shown in Figure 3.3. The fraction of gamma energy depositions increases as burnup increases. Since gamma absorption cross sections of the gadolinium isotopes are very large, the fractions of gamma energy deposition for the case 2P with 24 gadolinia burnable poisons decrease until the gadolinium isotopes burn out.

Table 3.2. Fraction of gamma energy deposition by a Monte Carlo code

Case	Gamma (MeV), MCNP					Total (MeV)	KARMA
	Prompt	Delayed	Capture	Sum	%		
2B	6.575	6.423	5.329	18.327	9.27	197.7	8.99
2F	6.569	6.436	6.145	19.150	9.57	200.1	9.54
2G	6.568	6.452	8.408	21.428	10.43	205.5	12.07
2H	6.558	6.456	7.011	20.025	9.85	203.2	9.99
2M	6.570	6.440	6.065	19.075	9.51	200.5	9.48
2P	6.568	6.537	9.516	22.621	11.13	203.2	11.17

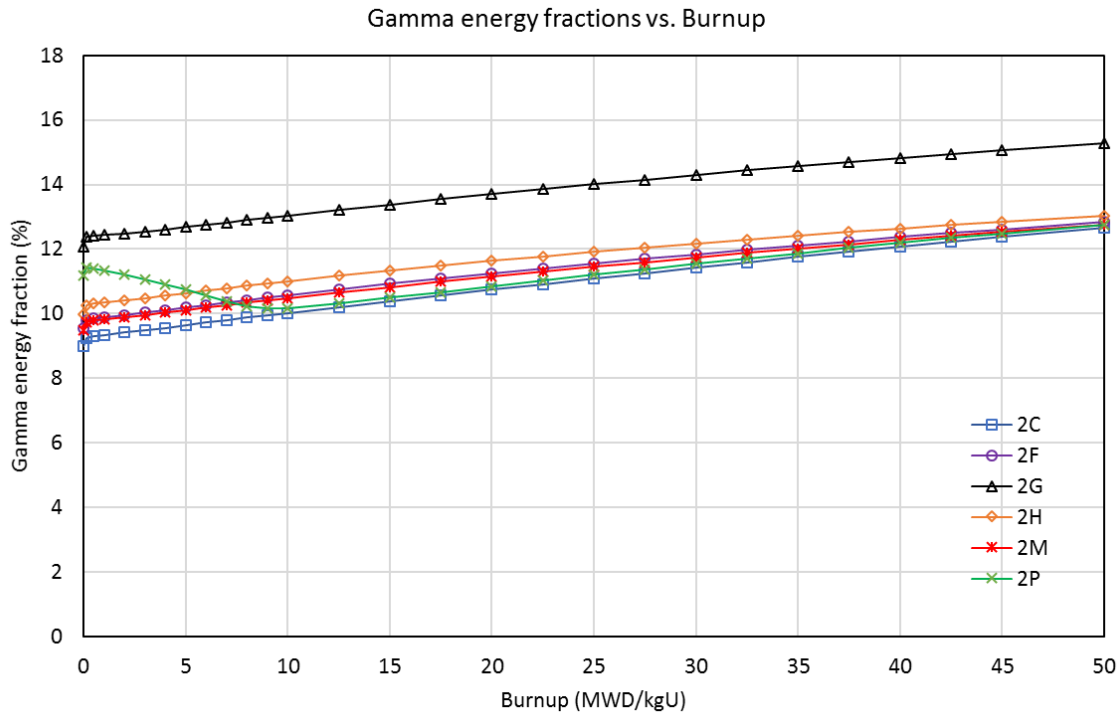


Figure 3.3. Fractions of Gamma Energy Deposition as a Function of Burnup by a Deterministic Code.

3.4 OPTIMIZATION OF GAMMA SMEARING FACTOR

Previously in some transport lattice codes such as CASMO-3, a constant gamma smearing factor was used to obtain more realistic pin power distribution by assuming that the gamma energy depositions for each fuel pin are constant. The constant gamma smearing factor (γ) was obtained to minimize the pin power differences between the actual adjusted gamma-smeared power distributions. The adjusted gamma power distributions can be obtained by using Eq. (3.1).

$$\tilde{P}_{i,j} = (1.0 - \gamma) \cdot P_{i,j} + \gamma , \quad (3.1)$$

where

γ = gamma smearing factor,

$P_{i,j}$ = normalized fission pin power for pin (i,j) , and

$\tilde{P}_{i,j}$ = normalized gamma-smeared pin power for pin (i,j) .

The burnup-dependent actual gamma-smeared power distributions and fission power distributions have been obtained for the six fuel assembly cases by using KARMA with neutron-photon coupled calculations.

Currently, in MPACT, the normalized pin power distribution is obtained from pin fission powers without considering local gamma energy deposition. Therefore, pin power distribution based on fission power must be adjusted by adopting a gamma smearing factor. Since the real gamma-smeared power distributions could be obtained by the neutron-photon coupled calculations, the gamma smearing factor can be optimized by trial and error to minimize the pin power differences between the real and adjusted gamma-smeared pin power distributions.

Eight different gamma smearing factors ranging from 6.5–10.0% in 0.5% intervals have been tried for the six 2D lattice problems. Tables 3.3–3.8 provide the standard deviations (SD) of the pin power differences and the maximum and minimum differences for assembly cases. In addition, the SDs of the differences between the real gamma-smeared and fission pin powers have been obtained. These can be understood as an error in power prediction in the current procedure. The optimal gamma smearing factor is case dependent. It can be concluded that the optimal gamma smearing factor is 8.5% based on the typical UO₂ fuel assembly case (2C).

Figures 3.4–3.9 provide comparisons of gamma-smeared power distributions obtained by using MCNP and 8.5% and 10% gamma smearing factors. The reference gamma-smeared power distributions were obtained by MCNP in Reference [Wan17]. The trend is different from comparisons with deterministic results. However, considering the gamma smearing factor significantly improves power distributions.

**Table 3.3. Fraction of gamma energy deposition (Case 2C)**

No	Burnup MWD/kgU	Gamma transport* (%)			SD with gamma smearing factor (%)							
		SD	Min	Max	6.5	7.0	7.5	8.0	8.5	9.0	9.5	10.0
1	0.0	0.20	-0.40	0.30	0.05	0.05	0.07	0.08	0.09	0.11	0.12	0.14
2	0.15	0.19	-0.30	0.30	0.05	0.06	0.07	0.09	0.10	0.12	0.13	0.15
3	0.5	0.19	-0.40	0.30	0.06	0.07	0.08	0.09	0.11	0.12	0.13	0.15
4	1.0	0.19	-0.40	0.40	0.05	0.06	0.07	0.09	0.10	0.12	0.13	0.15
5	2.0	0.18	-0.30	0.40	0.06	0.07	0.08	0.10	0.11	0.13	0.14	0.16
6	3.0	0.20	-0.40	0.30	0.05	0.06	0.07	0.08	0.10	0.11	0.13	0.14
7	4.0	0.19	-0.40	0.30	0.05	0.06	0.07	0.09	0.10	0.12	0.13	0.15
8	5.0	0.19	-0.30	0.40	0.06	0.07	0.08	0.09	0.11	0.12	0.13	0.15
9	6.0	0.20	-0.40	0.30	0.05	0.06	0.07	0.08	0.09	0.11	0.12	0.14
10	7.0	0.19	-0.30	0.40	0.06	0.06	0.07	0.09	0.10	0.11	0.13	0.14
11	8.0	0.19	-0.40	0.30	0.06	0.07	0.08	0.09	0.10	0.11	0.13	0.14
12	9.0	0.18	-0.30	0.30	0.05	0.06	0.07	0.08	0.10	0.11	0.12	0.14
13	10.0	0.19	-0.40	0.40	0.05	0.05	0.06	0.07	0.08	0.10	0.11	0.12
14	12.5	0.18	-0.30	0.30	0.05	0.05	0.06	0.07	0.09	0.10	0.11	0.13
15	15.0	0.18	-0.30	0.30	0.05	0.05	0.06	0.07	0.08	0.09	0.11	0.12
16	17.5	0.18	-0.30	0.30	0.05	0.05	0.06	0.07	0.07	0.09	0.10	0.11
17	20.0	0.17	-0.30	0.30	0.05	0.05	0.06	0.07	0.08	0.09	0.10	0.11
18	22.5	0.16	-0.30	0.30	0.05	0.06	0.06	0.07	0.08	0.09	0.10	0.11
19	25.0	0.15	-0.30	0.30	0.05	0.05	0.06	0.07	0.08	0.08	0.09	0.10
20	27.5	0.15	-0.30	0.30	0.05	0.05	0.05	0.06	0.07	0.07	0.08	0.09
21	30.0	0.14	-0.20	0.30	0.04	0.04	0.05	0.06	0.06	0.07	0.08	0.09
22	32.5	0.13	-0.30	0.20	0.04	0.05	0.05	0.06	0.06	0.07	0.08	0.09
23	35.0	0.13	-0.30	0.30	0.05	0.05	0.05	0.06	0.06	0.07	0.08	0.08
24	37.5	0.13	-0.30	0.20	0.05	0.05	0.05	0.06	0.06	0.07	0.07	0.08
25	40.0	0.12	-0.30	0.30	0.05	0.05	0.05	0.05	0.06	0.06	0.07	0.08
26	42.5	0.12	-0.20	0.20	0.04	0.05	0.05	0.05	0.06	0.06	0.07	0.07
27	45.0	0.13	-0.30	0.20	0.05	0.05	0.05	0.06	0.06	0.06	0.07	0.07
28	50.0	0.11	-0.20	0.20	0.05	0.05	0.05	0.05	0.06	0.06	0.07	0.07
Max. SD		0.20			0.06	0.07	0.08	0.1	0.11	0.13	0.14	0.16
Max. difference			-0.20		-0.16	-0.19	-0.22	-0.25	-0.28	-0.3	-0.33	-0.36
Min. difference				0.40	0.17	0.18	0.18	0.19	0.19	0.21	0.23	0.25

* Pin power differences between with and without considering gamma energy deposition

Table 3.4. Fraction of gamma energy deposition (Case 2F)

No	Burnup MWD/kgU	Gamma transport*(%)			SD with gamma smearing factor (%)						
		SD	Min	Max	6.5	7.0	7.5	8.0	8.5	9.0	10.0
1	0.0	0.36	-0.70	0.60	0.10	0.13	0.16	0.18	0.22	0.25	0.28
2	0.15	0.36	-0.70	0.60	0.11	0.13	0.16	0.18	0.21	0.24	0.27
3	0.5	0.36	-0.70	0.60	0.11	0.13	0.15	0.18	0.20	0.23	0.26
4	1.0	0.36	-0.70	0.60	0.10	0.12	0.14	0.17	0.19	0.22	0.25
5	2.0	0.34	-0.70	0.60	0.10	0.11	0.14	0.16	0.19	0.21	0.24
6	3.0	0.34	-0.70	0.60	0.10	0.11	0.13	0.15	0.18	0.20	0.23
7	4.0	0.32	-0.70	0.50	0.09	0.10	0.12	0.15	0.17	0.20	0.22
8	5.0	0.31	-0.70	0.50	0.09	0.10	0.12	0.14	0.16	0.19	0.21
9	6.0	0.30	-0.70	0.50	0.09	0.10	0.12	0.14	0.16	0.18	0.20
10	7.0	0.29	-0.70	0.50	0.10	0.11	0.13	0.14	0.16	0.19	0.21
11	8.0	0.28	-0.60	0.40	0.08	0.09	0.11	0.13	0.15	0.17	0.19
12	9.0	0.28	-0.60	0.40	0.08	0.09	0.10	0.12	0.13	0.15	0.17
13	10.0	0.27	-0.60	0.50	0.08	0.09	0.11	0.12	0.14	0.16	0.18
14	12.5	0.25	-0.60	0.40	0.08	0.09	0.10	0.11	0.13	0.14	0.16
15	15.0	0.22	-0.60	0.40	0.08	0.09	0.10	0.11	0.13	0.14	0.16
16	17.5	0.22	-0.60	0.30	0.07	0.08	0.09	0.10	0.11	0.12	0.14
17	20.0	0.20	-0.60	0.30	0.08	0.08	0.09	0.10	0.11	0.12	0.14
18	22.5	0.18	-0.60	0.20	0.07	0.08	0.09	0.10	0.11	0.12	0.13
19	25.0	0.16	-0.50	0.30	0.08	0.08	0.09	0.10	0.11	0.12	0.13
20	27.5	0.16	-0.50	0.30	0.07	0.07	0.08	0.09	0.10	0.11	0.12
21	30.0	0.15	-0.50	0.20	0.07	0.08	0.08	0.09	0.10	0.10	0.11
22	32.5	0.13	-0.40	0.20	0.07	0.08	0.08	0.09	0.10	0.11	0.12
23	35.0	0.11	-0.40	0.20	0.07	0.08	0.08	0.09	0.10	0.10	0.11
24	37.5	0.10	-0.40	0.10	0.07	0.07	0.08	0.09	0.09	0.10	0.11
25	40.0	0.11	-0.40	0.10	0.06	0.07	0.07	0.07	0.08	0.09	0.10
26	42.5	0.11	-0.40	0.20	0.06	0.07	0.07	0.07	0.08	0.08	0.09
27	45.0	0.09	-0.30	0.10	0.07	0.07	0.08	0.08	0.09	0.09	0.10
28	50.0	0.09	-0.40	0.10	0.08	0.08	0.09	0.09	0.10	0.10	0.11
Max. SD		0.36			0.11	0.13	0.16	0.18	0.22	0.25	0.28
Max. difference			-0.4		-0.26	-0.24	-0.24	-0.28	-0.33	-0.37	-0.41
Min. difference				0.6	0.28	0.35	0.43	0.5	0.58	0.65	0.73
											0.81

* Pin power differences between with and without considering gamma energy deposition

**Table 3.5. Fraction of gamma energy deposition (Case 2G)**

No	Burnup MWD/kgU	Gamma transport* (%)			SD with gamma smearing factor (%)							
		SD	Min	Max	6.5	7.0	7.5	8.0	8.5	9.0	9.5	10.0
1	0.0	1.16	-2.50	1.90	0.46	0.41	0.36	0.31	0.27	0.23	0.20	0.19
2	0.15	1.14	-2.50	1.90	0.46	0.41	0.36	0.32	0.27	0.24	0.21	0.19
3	0.5	1.12	-2.50	1.90	0.45	0.40	0.35	0.31	0.27	0.23	0.20	0.18
4	1.0	1.12	-2.40	1.90	0.46	0.41	0.36	0.31	0.27	0.23	0.20	0.18
5	2.0	1.09	-2.40	1.80	0.45	0.40	0.36	0.31	0.27	0.24	0.21	0.19
6	3.0	1.07	-2.30	1.80	0.45	0.41	0.36	0.32	0.28	0.24	0.21	0.18
7	4.0	1.04	-2.20	1.70	0.43	0.39	0.35	0.31	0.27	0.23	0.20	0.17
8	5.0	1.02	-2.20	1.80	0.44	0.40	0.36	0.32	0.28	0.25	0.21	0.19
9	6.0	1.00	-2.20	1.70	0.44	0.40	0.36	0.32	0.28	0.25	0.22	0.20
10	7.0	0.99	-2.10	1.70	0.44	0.40	0.36	0.32	0.28	0.25	0.22	0.19
11	8.0	0.98	-2.10	1.70	0.44	0.40	0.36	0.33	0.29	0.26	0.23	0.20
12	9.0	0.96	-2.00	1.70	0.44	0.40	0.37	0.33	0.30	0.26	0.23	0.20
13	10.0	0.93	-2.00	1.60	0.43	0.39	0.35	0.32	0.28	0.25	0.22	0.20
14	12.5	0.89	-1.90	1.60	0.42	0.38	0.35	0.32	0.28	0.25	0.23	0.20
15	15.0	0.87	-1.90	1.50	0.43	0.40	0.36	0.33	0.30	0.27	0.24	0.22
16	17.5	0.84	-1.80	1.40	0.42	0.39	0.36	0.33	0.30	0.27	0.24	0.22
17	20.0	0.81	-1.70	1.40	0.41	0.39	0.36	0.33	0.30	0.27	0.25	0.22
18	22.5	0.80	-1.70	1.40	0.43	0.40	0.37	0.35	0.32	0.30	0.27	0.25
19	25.0	0.76	-1.60	1.40	0.41	0.39	0.36	0.34	0.31	0.29	0.27	0.24
20	27.5	0.74	-1.60	1.30	0.41	0.39	0.36	0.34	0.31	0.29	0.27	0.25
21	30.0	0.71	-1.50	1.20	0.40	0.37	0.35	0.33	0.31	0.28	0.26	0.24
22	32.5	0.70	-1.40	1.30	0.40	0.38	0.36	0.34	0.32	0.30	0.28	0.26
23	35.0	0.68	-1.40	1.30	0.40	0.37	0.35	0.33	0.31	0.29	0.27	0.25
24	37.5	0.68	-1.40	1.20	0.41	0.39	0.37	0.35	0.33	0.31	0.29	0.27
25	40.0	0.65	-1.40	1.20	0.39	0.37	0.35	0.33	0.31	0.29	0.27	0.26
26	42.5	0.63	-1.30	1.10	0.38	0.36	0.35	0.33	0.31	0.29	0.28	0.26
27	45.0	0.62	-1.30	1.10	0.38	0.36	0.34	0.33	0.31	0.29	0.28	0.26
28	50.0	0.61	-1.20	1.10	0.38	0.37	0.35	0.33	0.32	0.30	0.28	0.27
Max. SD		1.16			0.46	0.41	0.37	0.35	0.33	0.31	0.29	0.27
Max. difference			-1.2		-0.87	-0.75	-0.67	-0.63	-0.59	-0.56	-0.53	-0.5
Min. difference				1.9	0.98	0.91	0.85	0.8	0.77	0.74	0.7	0.67

* Pin power differences between with and without considering gamma energy deposition

Table 3.6. Fraction of gamma energy deposition (Case 2H)

No	Burnup MWD/kgU	Gamma transport* (%)			SD with gamma smearing factor (%)							
		SD	Min	Max	6.5	7.0	7.5	8.0	8.5	9.0	9.5	10.0
1	0.0	0.76	-1.70	1.20	0.21	0.25	0.30	0.36	0.42	0.48	0.55	0.61
2	0.15	0.75	-1.60	1.20	0.19	0.23	0.28	0.34	0.40	0.46	0.52	0.58
3	0.5	0.75	-1.60	1.20	0.20	0.24	0.29	0.34	0.40	0.45	0.51	0.58
4	1.0	0.74	-1.60	1.20	0.19	0.23	0.28	0.33	0.38	0.44	0.50	0.56
5	2.0	0.71	-1.50	1.20	0.19	0.23	0.28	0.33	0.38	0.44	0.50	0.56
6	3.0	0.71	-1.50	1.10	0.18	0.21	0.26	0.31	0.36	0.42	0.47	0.53
7	4.0	0.70	-1.50	1.20	0.18	0.21	0.25	0.30	0.35	0.40	0.46	0.51
8	5.0	0.68	-1.40	1.20	0.18	0.20	0.24	0.29	0.34	0.39	0.44	0.49
9	6.0	0.68	-1.40	1.10	0.17	0.20	0.24	0.28	0.33	0.37	0.43	0.48
10	7.0	0.66	-1.30	1.10	0.18	0.20	0.24	0.28	0.32	0.37	0.42	0.47
11	8.0	0.64	-1.30	1.00	0.17	0.20	0.23	0.27	0.32	0.36	0.41	0.46
12	9.0	0.63	-1.30	1.10	0.16	0.19	0.22	0.26	0.31	0.35	0.40	0.45
13	10.0	0.62	-1.20	1.10	0.17	0.19	0.23	0.26	0.31	0.35	0.39	0.44
14	12.5	0.58	-1.20	1.10	0.16	0.18	0.21	0.25	0.29	0.33	0.37	0.42
15	15.0	0.58	-1.20	1.00	0.16	0.17	0.20	0.23	0.26	0.30	0.34	0.38
16	17.5	0.54	-1.00	0.90	0.15	0.16	0.19	0.22	0.26	0.29	0.33	0.37
17	20.0	0.53	-1.00	1.00	0.16	0.17	0.19	0.22	0.25	0.28	0.32	0.36
18	22.5	0.50	-1.00	0.90	0.15	0.16	0.18	0.21	0.24	0.27	0.31	0.34
19	25.0	0.48	-0.90	0.90	0.14	0.15	0.17	0.20	0.23	0.26	0.29	0.32
20	27.5	0.46	-0.80	0.90	0.14	0.16	0.18	0.20	0.23	0.26	0.29	0.32
21	30.0	0.44	-0.80	0.80	0.15	0.16	0.18	0.20	0.23	0.26	0.28	0.32
22	32.5	0.42	-0.80	0.80	0.15	0.16	0.18	0.20	0.22	0.25	0.28	0.31
23	35.0	0.42	-0.80	0.80	0.15	0.16	0.17	0.19	0.21	0.24	0.26	0.29
24	37.5	0.41	-0.80	0.80	0.14	0.15	0.17	0.18	0.21	0.23	0.26	0.28
25	40.0	0.39	-0.80	0.70	0.13	0.14	0.16	0.18	0.20	0.22	0.25	0.28
26	42.5	0.37	-0.70	0.70	0.14	0.15	0.17	0.19	0.21	0.23	0.25	0.28
27	45.0	0.36	-0.80	0.70	0.15	0.16	0.17	0.19	0.21	0.24	0.26	0.28
28	50.0	0.35	-0.70	0.60	0.14	0.15	0.17	0.18	0.20	0.23	0.25	0.27
Max. SD		0.76			0.21	0.25	0.3	0.36	0.42	0.48	0.55	0.61
Max. difference			-0.7		-0.55	-0.52	-0.49	-0.46	-0.52	-0.59	-0.67	-0.76
Min. difference				1.2	0.4	0.55	0.7	0.86	1.01	1.16	1.32	1.47

* Pin power differences between with and without considering gamma energy deposition

**Table 3.7. Fraction of gamma energy deposition (Case 2M)**

No	Burnup MWD/kgU	Gamma transport*(%)			SD with gamma smearing factor (%)							
		SD	Min	Max	6.5	7.0	7.5	8.0	8.5	9.0	9.5	10.0
1	0.0	0.27	-0.30	0.50	0.07	0.06	0.05	0.04	0.04	0.04	0.05	0.06
2	0.15	0.27	-0.40	0.50	0.08	0.07	0.06	0.05	0.05	0.05	0.06	0.06
3	0.5	0.28	-0.40	0.50	0.09	0.08	0.07	0.06	0.05	0.05	0.05	0.05
4	1.0	0.27	-0.30	0.50	0.09	0.08	0.07	0.06	0.05	0.05	0.05	0.06
5	2.0	0.26	-0.30	0.50	0.09	0.07	0.06	0.06	0.05	0.05	0.05	0.05
6	3.0	0.25	-0.30	0.50	0.09	0.08	0.06	0.06	0.05	0.05	0.05	0.05
7	4.0	0.22	-0.30	0.40	0.07	0.06	0.05	0.05	0.05	0.05	0.06	0.07
8	5.0	0.23	-0.30	0.50	0.08	0.07	0.07	0.06	0.06	0.05	0.06	0.06
9	6.0	0.21	-0.30	0.50	0.07	0.06	0.05	0.05	0.05	0.05	0.05	0.06
10	7.0	0.21	-0.30	0.50	0.08	0.07	0.06	0.06	0.06	0.06	0.06	0.06
11	8.0	0.21	-0.30	0.50	0.07	0.07	0.06	0.05	0.05	0.05	0.05	0.06
12	9.0	0.20	-0.30	0.40	0.07	0.06	0.06	0.06	0.05	0.05	0.06	0.06
13	10.0	0.20	-0.30	0.40	0.08	0.07	0.06	0.06	0.06	0.06	0.05	0.06
14	12.5	0.19	-0.30	0.40	0.08	0.07	0.06	0.06	0.05	0.05	0.05	0.05
15	15.0	0.19	-0.30	0.50	0.08	0.07	0.07	0.06	0.06	0.05	0.05	0.05
16	17.5	0.17	-0.20	0.40	0.08	0.07	0.07	0.06	0.06	0.06	0.06	0.06
17	20.0	0.16	-0.20	0.40	0.08	0.07	0.07	0.06	0.06	0.06	0.06	0.06
18	22.5	0.15	-0.30	0.40	0.07	0.06	0.06	0.06	0.05	0.05	0.05	0.05
19	25.0	0.15	-0.20	0.40	0.07	0.07	0.07	0.07	0.07	0.07	0.07	0.07
20	27.5	0.14	-0.20	0.30	0.07	0.06	0.06	0.06	0.06	0.06	0.06	0.06
21	30.0	0.14	-0.20	0.40	0.07	0.06	0.06	0.06	0.06	0.06	0.06	0.06
22	32.5	0.12	-0.20	0.30	0.06	0.05	0.05	0.05	0.05	0.05	0.05	0.05
23	35.0	0.11	-0.20	0.30	0.05	0.05	0.05	0.05	0.05	0.05	0.05	0.05
24	37.5	0.12	-0.20	0.30	0.06	0.06	0.06	0.05	0.05	0.05	0.05	0.06
25	40.0	0.10	-0.20	0.30	0.05	0.05	0.05	0.05	0.05	0.05	0.05	0.05
26	42.5	0.11	-0.20	0.30	0.06	0.05	0.05	0.05	0.05	0.05	0.05	0.05
27	45.0	0.11	-0.20	0.30	0.06	0.06	0.06	0.05	0.05	0.05	0.06	0.06
28	50.0	0.10	-0.20	0.30	0.06	0.06	0.06	0.06	0.06	0.06	0.07	0.07
Max. SD		0.28			0.09	0.08	0.07	0.07	0.07	0.07	0.07	0.07
Max. difference			-0.20		-0.16	-0.15	-0.15	-0.15	-0.15	-0.15	-0.16	-0.18
Min. difference				0.50	0.19	0.17	0.14	0.14	0.14	0.14	0.15	0.15

* Pin power differences between with and without considering gamma energy deposition

Table 3.8. Fraction of gamma energy deposition (Case 2P)

No	Burnup MWD/kgU	Gamma transport* (%)			SD with gamma smearing factor (%)							
		SD	Min	Max	6.5	7.0	7.5	8.0	8.5	9.0	9.5	10.0
1	0.0	2.97	-1.80	9.40	1.43	1.31	1.19	1.07	0.95	0.83	0.72	0.60
2	0.15	2.98	-1.80	9.50	1.46	1.34	1.22	1.11	0.99	0.87	0.76	0.65
3	0.5	2.91	-1.80	9.30	1.42	1.31	1.19	1.08	0.96	0.85	0.74	0.63
4	1.0	2.79	-1.80	8.90	1.34	1.23	1.12	1.01	0.90	0.79	0.68	0.58
5	2.0	2.56	-1.60	8.10	1.22	1.12	1.02	0.92	0.81	0.71	0.61	0.52
6	3.0	2.30	-1.30	7.30	1.08	0.99	0.89	0.80	0.71	0.62	0.53	0.44
7	4.0	2.03	-1.20	6.50	0.93	0.84	0.76	0.68	0.60	0.51	0.43	0.36
8	5.0	1.73	-1.00	5.60	0.76	0.68	0.61	0.54	0.46	0.39	0.33	0.26
9	6.0	1.44	-0.80	4.70	0.59	0.53	0.46	0.40	0.34	0.28	0.23	0.19
10	7.0	1.13	-0.60	3.90	0.41	0.36	0.31	0.26	0.21	0.17	0.15	0.14
11	8.0	0.87	-0.70	3.00	0.27	0.22	0.18	0.14	0.11	0.10	0.11	0.13
12	9.0	0.70	-0.60	2.40	0.17	0.13	0.10	0.08	0.08	0.10	0.13	0.17
13	10.0	0.61	-0.70	2.00	0.13	0.11	0.09	0.09	0.10	0.12	0.15	0.19
14	12.5	0.56	-0.60	1.70	0.12	0.09	0.07	0.07	0.08	0.10	0.13	0.16
15	15.0	0.52	-0.60	1.60	0.12	0.10	0.08	0.08	0.09	0.11	0.14	0.17
16	17.5	0.50	-0.60	1.60	0.12	0.09	0.08	0.07	0.08	0.10	0.12	0.15
17	20.0	0.48	-0.50	1.60	0.11	0.09	0.08	0.07	0.07	0.09	0.11	0.13
18	22.5	0.47	-0.50	1.50	0.12	0.09	0.07	0.06	0.06	0.07	0.08	0.11
19	25.0	0.44	-0.50	1.40	0.12	0.10	0.08	0.07	0.07	0.08	0.10	0.11
20	27.5	0.42	-0.50	1.30	0.11	0.09	0.08	0.07	0.06	0.07	0.08	0.10
21	30.0	0.41	-0.50	1.30	0.12	0.10	0.08	0.07	0.06	0.06	0.07	0.08
22	32.5	0.38	-0.40	1.30	0.11	0.10	0.08	0.07	0.07	0.07	0.08	0.09
23	35.0	0.35	-0.40	1.20	0.10	0.08	0.07	0.06	0.06	0.06	0.07	0.09
24	37.5	0.34	-0.30	1.10	0.11	0.09	0.08	0.07	0.07	0.07	0.07	0.08
25	40.0	0.32	-0.30	1.10	0.10	0.09	0.08	0.07	0.06	0.06	0.07	0.08
26	42.5	0.32	-0.40	1.10	0.11	0.10	0.09	0.08	0.07	0.07	0.07	0.07
27	45.0	0.30	-0.40	1.00	0.10	0.09	0.08	0.07	0.06	0.06	0.06	0.06
28	50.0	0.26	-0.30	0.90	0.09	0.08	0.07	0.06	0.06	0.06	0.06	0.07
Max. SD		2.98			1.46	1.34	1.22	1.11	0.99	0.87	0.76	0.65
Max. difference			-0.3		-0.92	-0.86	-0.79	-0.72	-0.65	-0.61	-0.57	-0.55
Min. difference				9.5	4.71	4.34	3.97	3.6	3.23	2.86	2.5	2.13

* Pin power differences between with and without considering gamma energy deposition

		Gamma smeared power			SD, %	Min, %	
		Fission power			0.23	-0.39	
		Adjusted gamma smeared power (10%)			0.10	-0.22	
		Adjusted gamma smeared power (8.5%)			0.06	-0.13	
0.000	1.035	1.013					
0.000	1.037	1.013					
0.000	1.033	1.012					
0.000	1.034	1.012	1.015				
	1.034	1.013	1.015				
	1.036	1.011	1.014				
	1.033	1.011	1.014				
	1.033	1.011	1.014				
0.000	1.033	1.037	0.000				
0.000	1.036	1.040	0.000				
0.000	1.032	1.036	0.000				
0.000	1.033	1.036	0.000				
1.031	1.010	1.012	1.039	1.028			
1.034	1.011	1.012	1.043	1.030			
1.030	1.010	1.011	1.038	1.027			
1.031	1.010	1.011	1.039	1.027			
1.028	1.006	1.008	1.040	1.043	0.000		
1.030	1.006	1.008	1.043	1.047	0.000		
1.027	1.006	1.007	1.039	1.043	0.000		
1.028	1.006	1.007	1.040	1.043	0.000		
0.000	1.022	1.026	0.000	1.030	1.011	0.977	
0.000	1.023	1.028	0.000	1.033	1.012	0.975	
0.000	1.021	1.026	0.000	1.030	1.011	0.977	
0.000	1.021	1.026	0.000	1.030	1.011	0.977	
1.008	0.990	0.989	1.008	0.985	0.968	0.954	0.945
1.009	0.989	0.988	1.009	0.984	0.966	0.951	0.941
1.008	0.991	0.989	1.008	0.986	0.969	0.956	0.947
1.008	0.990	0.989	1.009	0.986	0.969	0.955	0.946
0.981	0.976	0.975	0.977	0.969	0.960	0.950	0.947
0.979	0.975	0.973	0.975	0.967	0.957	0.947	0.943
0.981	0.977	0.975	0.977	0.970	0.961	0.952	0.949
0.981	0.977	0.975	0.977	0.969	0.961	0.951	0.948

Figure 3.4. Comparison of the Gamma-Smeared Power Distribution (Case 2B).

Gamma smeared power				SD, %	Min, %	Max, %		
Fission power				0.45	-0.89	0.75		
Adjusted gamma smeared power (10%)				0.26	-0.31	0.65		
Adjusted gamma smeared power (8.5%)				0.17	-0.21	0.42		
0.000	1.037							
1.070	1.042							
1.079	1.038							
1.071	1.039							
1.072	0.989	0.972						
0.972	0.990	0.972						
0.971	0.991	0.974						
0.974	0.990	0.974						
0.000	0.938	0.932	0.000					
0.000	0.934	0.928	0.000					
0.000	0.941	0.935	0.000					
0.000	0.940	0.934	0.000					
0.929	0.960	0.957	0.919	0.931				
0.924	0.959	0.955	0.914	0.926				
0.932	0.963	0.959	0.922	0.933				
0.931	0.962	0.959	0.921	0.932				
0.932	0.964	0.960	0.918	0.914	0.000			
0.927	0.962	0.957	0.912	0.907	0.000			
0.935	0.966	0.962	0.921	0.916	0.000			
0.934	0.966	0.961	0.919	0.915	0.000			
0.000	0.948	0.946	0.000	0.940	0.968	1.031		
0.000	0.944	0.941	0.000	0.934	0.964	1.032		
0.000	0.950	0.947	0.000	0.941	0.968	1.029		
0.000	0.949	0.946	0.000	0.940	0.967	1.029		
0.977	1.007	1.005	0.983	1.018	1.048	1.077	1.103	
0.975	1.008	1.005	0.981	1.019	1.051	1.081	1.109	
0.977	1.007	1.005	0.983	1.017	1.046	1.073	1.098	
0.977	1.007	1.005	0.983	1.017	1.047	1.074	1.100	
1.042	1.049	1.051	1.051	1.066	1.087	1.106	1.126	1.145
1.046	1.054	1.056	1.055	1.071	1.093	1.113	1.133	1.153
1.042	1.048	1.050	1.050	1.064	1.084	1.101	1.120	1.138
1.042	1.049	1.051	1.051	1.065	1.085	1.103	1.122	1.140

Figure 3.5. Comparison of the Gamma-Smeared Power Distribution (Case 2F).



		Gamma smeared power				
		Fission power				
		Adjusted gamma smeared power (10%)				
		Adjusted gamma smeared power (8.5%)				
0.000	1.064	0.944	0.941	0.947	0.946	0.942
0.000	1.075	0.941	0.966	0.970	0.969	0.939
0.000	1.067	0.947	0.967	0.970	0.969	0.945
0.000	1.068	0.946	0.968	0.970	0.969	0.944
0.000	0.894	0.890	0.886	0.887	0.897	0.885
0.000	0.894	0.890	0.886	0.887	0.896	0.885
0.000	0.894	0.890	0.886	0.887	0.896	0.885
0.000	0.894	0.890	0.886	0.887	0.896	0.885
0.882	0.925	0.918	0.921	0.912	0.929	0.918
0.873	0.921	0.912	0.921	0.912	0.928	0.912
0.885	0.929	0.921	0.927	0.921	0.934	0.921
0.883	0.928	0.920	0.927	0.920	0.934	0.920
0.887	0.932	0.925	0.927	0.925	0.932	0.925
0.878	0.927	0.920	0.935	0.928	0.934	0.920
0.890	0.935	0.928	0.934	0.928	0.934	0.928
0.888	0.934	0.927	0.934	0.927	0.934	0.927
0.000	0.916	0.914	0.908	0.915	0.916	0.914
0.000	0.916	0.914	0.908	0.915	0.916	0.914
0.000	0.917	0.915	0.916	0.915	0.917	0.915
0.000	0.916	0.913	0.916	0.913	0.916	0.913
0.969	1.005	1.008	0.965	1.009	0.977	1.008
0.965	1.006	1.009	0.965	1.009	0.977	1.009
0.969	1.005	1.008	0.968	1.008	0.979	1.008
0.968	1.005	1.008	0.968	1.008	0.979	1.008
1.061	1.074	1.079	1.069	1.087	1.090	1.082
1.069	1.082	1.087	1.062	1.074	1.081	1.078
1.062	1.074	1.078	1.063	1.075	1.083	1.080
1.063	1.075	1.080	1.063	1.075	1.083	1.080

Figure 3.6. Comparison of the Gamma-Smeared Power Distribution (Case 2G).

		Gamma smeared power						
		Fission power						
		Adjusted gamma smeared power (10%)						
		Adjusted gamma smeared power (8.5%)						
		SD,%	Min, %	Max, %				
0.000	1.013	0.95	-2.03	1.53				
0.000	1.020	0.46	-0.54	1.14				
0.000	1.018	0.29	-0.58	0.67				
0.000	1.018							
1.050	1.013							
1.061	1.020							
1.055	1.018							
1.056	1.018							
0.923	0.949	0.924						
0.919	0.948	0.921						
0.927	0.954	0.929						
0.926	0.953	0.928						
0.000	0.873	0.863	0.000					
0.000	0.865	0.854	0.000					
0.000	0.879	0.869	0.000					
0.000	0.877	0.867	0.000					
0.861	0.904	0.900	0.845	0.863				
0.851	0.898	0.894	0.833	0.851				
0.866	0.909	0.904	0.850	0.866				
0.864	0.907	0.903	0.847	0.863				
0.868	0.914	0.909	0.850	0.849	0.000			
0.858	0.909	0.903	0.837	0.834	0.000			
0.872	0.918	0.913	0.854	0.850	0.000			
0.870	0.916	0.911	0.851	0.848	0.000			
0.000	0.903	0.905	0.000	0.911	0.976	1.090		
0.000	0.895	0.897	0.000	0.901	0.971	1.094		
0.000	0.905	0.907	0.000	0.911	0.974	1.085		
0.000	0.904	0.905	0.000	0.909	0.973	1.086		
0.963	1.005	1.008	0.982	1.049	1.108	1.175	1.229	
0.960	1.006	1.009	0.978	1.051	1.115	1.187	1.244	
0.964	1.005	1.008	0.981	1.046	1.104	1.168	1.220	
0.963	1.005	1.008	0.980	1.047	1.105	1.171	1.223	
1.070	1.079	1.086	1.091	1.129	1.174	1.222	1.266	1.297
1.078	1.087	1.094	1.099	1.139	1.187	1.237	1.284	1.318
1.070	1.079	1.085	1.090	1.125	1.168	1.214	1.256	1.286
1.071	1.080	1.086	1.091	1.127	1.171	1.217	1.260	1.291

Figure 3.7. Comparison of the Gamma-Smeared Power Distribution (Case 2H).



Gamma smeared power				SD,%	Min, %	Max, %		
Fission power				0.85	-0.92	1.17		
Adjusted gamma smeared power (10%)				0.55	-0.58	0.61		
Adjusted gamma smeared power (8.5%)				0.59	-0.61	0.68		
0.990	1.029							
0.982	1.039							
0.984	1.035							
0.984	1.035							
0.992	1.029	1.029						
0.984	1.038	1.038						
0.986	1.034	1.034						
0.986	1.035	1.034						
0.000	0.990	0.988	0.000					
0.000	0.982	0.981	0.000					
0.000	0.984	0.982	0.000					
0.000	0.983	0.982	0.000					
0.989	1.027	1.024	0.984	1.012				
0.982	1.036	1.033	0.976	1.020				
0.984	1.033	1.030	0.979	1.018				
0.983	1.033	1.030	0.978	1.019				
0.989	1.025	1.024	0.981	0.978	0.000			
0.981	1.034	1.033	0.973	0.970	0.000			
0.983	1.030	1.029	0.975	0.973	0.000			
0.982	1.031	1.030	0.975	0.973	0.000			
0.000	0.985	0.985	0.000	0.980	0.975	0.998		
0.000	0.977	0.977	0.000	0.972	0.966	1.004		
0.000	0.979	0.980	0.000	0.975	0.969	1.003		
0.000	0.979	0.979	0.000	0.974	0.969	1.003		
0.981	1.012	1.022	0.987	1.012	1.008	0.956	1.008	
0.972	1.019	1.030	0.979	1.019	1.014	0.944	1.014	
0.975	1.017	1.027	0.981	1.017	1.013	0.950	1.013	
0.975	1.018	1.027	0.981	1.017	1.013	0.949	1.013	
1.003	0.956	1.025	1.023	0.957	1.026	1.031	1.022	0.954
1.009	0.945	1.034	1.032	0.947	1.035	1.040	1.031	0.943
1.008	0.950	1.030	1.028	0.952	1.031	1.036	1.027	0.948
1.009	0.950	1.031	1.029	0.951	1.032	1.037	1.028	0.948

Figure 3.8. Comparison of the Gamma-Smeared Power Distribution (Case 2M).

Gamma smeared power				SD,%	Min, %	Max, %		
Fission power				3.38	-2.04	10.71		
Adjusted gamma smeared power (10%)				0.96	-0.51	3.14		
Adjusted gamma smeared power (8.5%)				1.32	-0.69	4.27		
1.148	1.098							
1.168	1.111							
1.151	1.100							
1.154	1.102							
1.124	1.046	0.350						
1.142	1.052	0.243						
1.128	1.047	0.319						
1.130	1.048	0.307						
0.000	1.102	1.055	0.000					
0.000	1.117	1.062	0.000					
0.000	1.105	1.056	0.000					
0.000	1.107	1.057	0.000					
1.054	1.070	1.072	1.058	0.350				
1.062	1.081	1.084	1.066	0.243				
1.056	1.073	1.076	1.060	0.318				
1.057	1.074	1.077	1.061	0.307				
0.351	1.036	1.082	1.095	1.054	0.000			
0.244	1.042	1.096	1.109	1.062	0.000			
0.320	1.037	1.086	1.099	1.056	0.000			
0.309	1.038	1.087	1.100	1.057	0.000			
0.000	1.100	1.092	0.000	1.070	1.033	0.347		
0.000	1.115	1.106	0.000	1.082	1.039	0.242		
0.000	1.103	1.096	0.000	1.074	1.035	0.318		
0.000	1.105	1.097	0.000	1.075	1.036	0.306		
1.129	1.094	1.029	0.348	1.003	1.031	1.001	1.049	
1.149	1.109	1.035	0.243	1.006	1.039	1.004	1.059	
1.134	1.098	1.032	0.319	1.005	1.035	1.003	1.054	
1.136	1.099	1.032	0.307	1.005	1.036	1.003	1.054	
1.117	1.101	1.056	0.994	1.034	1.064	1.070	1.092	1.115
1.135	1.117	1.066	0.995	1.042	1.076	1.084	1.107	1.133
1.121	1.105	1.059	0.996	1.038	1.068	1.075	1.097	1.119
1.123	1.107	1.060	0.996	1.038	1.070	1.077	1.098	1.121

Figure 3.9. Comparison of the Gamma-Smeared Power Distribution (Case 2P).



3.5 RESULTS FOR 1D CORE PROBLEMS

Although photons mean free paths are longer than neutrons, it is not long enough for gamma fluxes to be almost flat over the reactor core. Figures 3.9–3.11 provide comparisons between pin/assembly fission powers and gamma energy depositions at various burnup points for the 1D-like core cases shown in Figure 3.2. Neutron-induced fission powers and gamma energy depositions have similar shapes over the core. Therefore, the adjusted gamma-smeared power distributions over the whole core can be obtained by using Eq. (3.2),

$$\tilde{P}_{i,j,k} = (1.0 - \gamma) \cdot P_{i,j,k} + \bar{P}_{i,j,k} \cdot \gamma, \quad (3.2)$$

where

- γ = Gamma smearing factor,
- $\bar{P}_{i,j,k}$ = Average fission pin power of the 7x7 pins surrounding pin (i,j,k) ,
- $P_{i,j,k}$ = Normalized fission pin power for pin (i,j) , and
- $\tilde{P}_{i,j,k}$ = Normalized gamma-smeared pin power for pin (i,j) of assembly (I,J,K) .

While discontinuities in the neutron-induced fission powers are observed at the assembly-assembly interfaces, gamma energy depositions are smooth even at the interfaces. In addition there are sharp increases of fission powers near the fuel-reflector interfaces. However, gamma energy depositions at the core boundary are monotonously decreasing. In other words there are some differences in the spatial neutron/gamma flux shape and leakage pattern. To resolve the assembly-assembly discontinuity issues, the approximate gamma smearing model has been developed such that average pin power for the 7x7 pins surrounding a pin is engaged in calculating gamma-smeared power.

Benchmark calculations have been performed for cases 1D-a, 1D-b and 1D-c by using various gamma smearing factors ranging between 6.5–10.0% at various burnup points, and then the gamma-smeared powers have been compared to the actual gamma-smeared powers obtained by the neutron-gamma coupled calculations. Tables 3.8–3.10 provide comparisons of the gamma-smeared powers by using various gamma smearing factors with the actual gamma-smeared powers at various burnup points. The approximate gamma smearing factors could make a slight improvement on the gamma-smeared power distributions.

Figures 3.13–3.15 demonstrate comparisons of the power distributions without and with considering 8.5% gamma smearing factor for various core sizes and burnup points. Using the gamma smearing factor could improve the peaked differences at the assembly-assembly interfaces. However, a significant improvement cannot be expected.

Table 3.9. Sensitivity of the gamma smearing factors (Case 1D-a)

No	Burnup MWD/kgU	No Gamma (%)			SD with gamma smearing factor (%)							
		SD	Min	Max	6.5	7.0	7.5	8.0	8.5	9.0	9.5	10.0
1	0.0	0.30	-1.20	0.90	0.27	0.27	0.27	0.28	0.28	0.28	0.29	0.29
2	2.5	0.34	-1.50	0.80	0.31	0.31	0.31	0.32	0.32	0.32	0.32	0.33
3	5.0	0.38	-1.80	0.70	0.36	0.36	0.36	0.36	0.36	0.37	0.37	0.37
4	7.5	0.43	-2.10	0.80	0.41	0.41	0.41	0.41	0.41	0.41	0.42	0.42
5	10.0	0.46	-2.30	0.70	0.44	0.44	0.44	0.44	0.44	0.44	0.45	0.45
6	15.0	0.51	-2.50	0.70	0.50	0.50	0.50	0.50	0.50	0.51	0.51	0.51
7	20.0	0.56	-2.70	0.70	0.55	0.55	0.55	0.55	0.55	0.55	0.55	0.55
8	25.0	0.58	-2.70	0.60	0.57	0.57	0.57	0.57	0.57	0.58	0.58	0.58
9	30.0	0.59	-2.60	0.60	0.59	0.59	0.59	0.59	0.59	0.59	0.59	0.59
10	35.0	0.59	-2.60	0.60	0.60	0.60	0.60	0.60	0.60	0.60	0.60	0.60
11	40.0	0.59	-2.40	0.60	0.59	0.59	0.59	0.59	0.59	0.59	0.60	0.60
12	45.0	0.58	-2.40	0.50	0.59	0.59	0.59	0.59	0.59	0.60	0.60	0.60
13	50.0	0.55	-2.10	0.50	0.56	0.56	0.56	0.57	0.57	0.57	0.57	0.57
Max. SD		0.59			0.60	0.60	0.60	0.60	0.60	0.60	0.60	0.60
Max. difference			-2.7		-2.43	-2.42	-2.41	-2.39	-2.38	-2.37	-2.36	-2.35
Min. difference				0.9	0.66	0.66	0.67	0.67	0.67	0.68	0.68	0.69

Table 3.10. Sensitivity of the gamma smearing factors (Case 1D-b)

No	Burnup MWD/kgU	No Gamma (%)			SD with gamma smearing factor (%)							
		SD	Min	Max	6.5	7.0	7.5	8.0	8.5	9.0	9.5	10.0
1	0.0	0.32	-1.10	0.80	0.29	0.30	0.30	0.30	0.31	0.31	0.31	0.32
2	2.5	0.35	-1.50	0.80	0.32	0.33	0.33	0.33	0.33	0.33	0.34	0.34
3	5.0	0.39	-1.90	0.70	0.37	0.37	0.37	0.37	0.37	0.37	0.37	0.38
4	7.5	0.42	-2.10	0.70	0.40	0.40	0.40	0.40	0.40	0.40	0.40	0.41
5	10.0	0.45	-2.30	0.70	0.44	0.44	0.44	0.44	0.44	0.44	0.44	0.44
6	15.0	0.49	-2.50	0.70	0.48	0.48	0.48	0.48	0.48	0.48	0.48	0.48
7	20.0	0.52	-2.70	0.60	0.52	0.52	0.52	0.52	0.52	0.52	0.52	0.52
8	25.0	0.54	-2.70	0.60	0.54	0.54	0.54	0.54	0.54	0.54	0.54	0.54
9	30.0	0.55	-2.70	0.50	0.55	0.55	0.55	0.55	0.55	0.55	0.55	0.55
10	35.0	0.55	-2.60	0.50	0.56	0.56	0.56	0.56	0.56	0.56	0.56	0.56
11	40.0	0.54	-2.50	0.50	0.54	0.54	0.54	0.54	0.54	0.54	0.55	0.55
12	45.0	0.52	-2.20	0.40	0.52	0.52	0.52	0.53	0.53	0.53	0.53	0.53
13	50.0	0.50	-2.10	0.40	0.51	0.51	0.51	0.51	0.51	0.51	0.51	0.51
Max. SD		0.55			0.56	0.56	0.56	0.56	0.56	0.56	0.56	0.56
Max. difference			-2.70		-2.47	-2.45	-2.43	-2.42	-2.4	-2.39	-2.37	-2.36
Min. difference				0.80	0.58	0.59	0.59	0.61	0.62	0.63	0.64	0.65

**Table 3.11. Sensitivity of the gamma smearing factors (Case 1D-c)**

No	Burnup MWD/kgU	No Gamma (%)			SD with gamma smearing factor (%)							
		SD	Min	Max	6.5	7.0	7.5	8.0	8.5	9.0	9.5	10.0
1	0.0	0.31	-0.90	0.80	0.27	0.28	0.28	0.28	0.29	0.29	0.29	0.30
2	2.5	0.31	-1.40	0.70	0.28	0.28	0.29	0.29	0.29	0.29	0.30	0.30
3	5.0	0.33	-1.70	0.70	0.31	0.31	0.31	0.31	0.32	0.32	0.32	0.32
4	7.5	0.36	-2.10	0.60	0.34	0.34	0.34	0.34	0.35	0.35	0.35	0.35
5	10.0	0.38	-2.20	0.60	0.37	0.37	0.37	0.37	0.37	0.37	0.37	0.37
6	15.0	0.41	-2.50	0.50	0.40	0.40	0.40	0.40	0.40	0.40	0.41	0.41
7	20.0	0.44	-2.60	0.50	0.43	0.43	0.43	0.43	0.43	0.43	0.43	0.43
8	25.0	0.46	-2.70	0.50	0.46	0.46	0.46	0.46	0.46	0.46	0.46	0.46
9	30.0	0.46	-2.70	0.40	0.46	0.46	0.46	0.46	0.46	0.46	0.46	0.46
10	35.0	0.46	-2.60	0.40	0.46	0.46	0.46	0.46	0.46	0.46	0.46	0.46
11	40.0	0.45	-2.40	0.40	0.46	0.46	0.46	0.46	0.46	0.46	0.46	0.46
12	45.0	0.44	-2.30	0.40	0.44	0.44	0.45	0.45	0.45	0.45	0.45	0.45
13	50.0	0.43	-2.20	0.40	0.43	0.43	0.43	0.43	0.43	0.43	0.44	0.44
Max. SD		0.46			0.46	0.46	0.46	0.46	0.46	0.46	0.46	0.46
Max. difference			-2.7		-2.46	-2.44	-2.42	-2.41	-2.39	-2.37	-2.36	-2.35
Min. difference				0.8	0.49	0.5	0.51	0.51	0.52	0.53	0.53	0.54

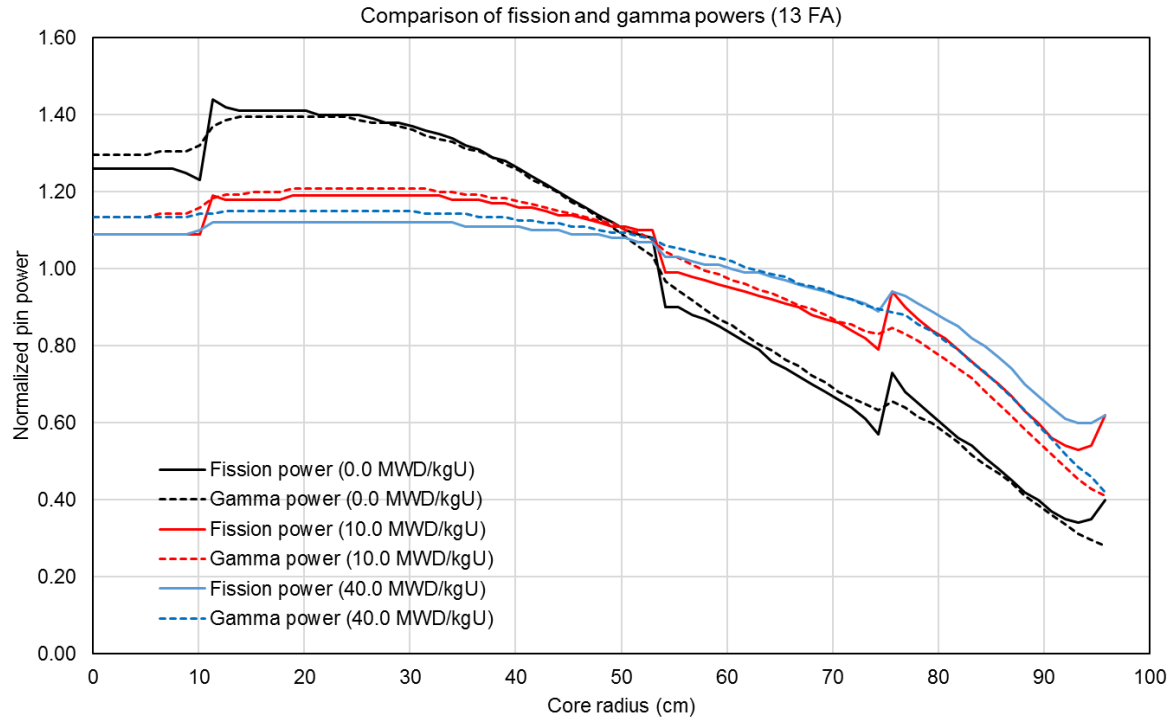


Figure 3.10. Comparison of the Fission and Gamma Power Distribution (Case 1D-a).

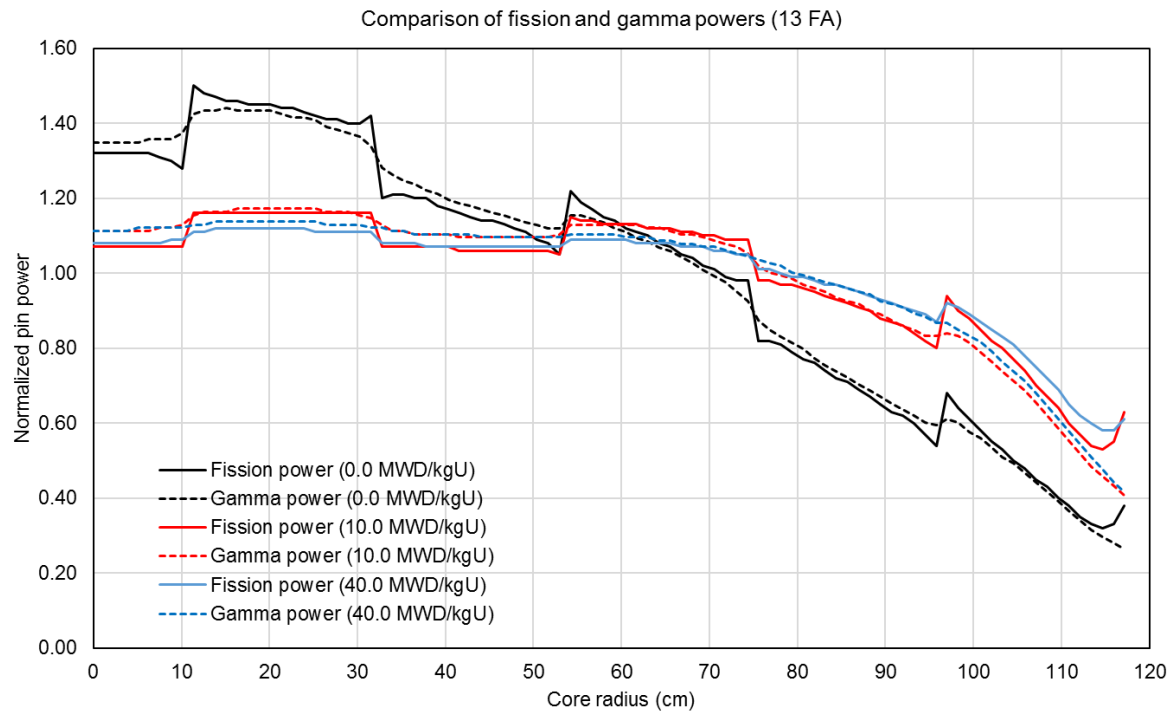
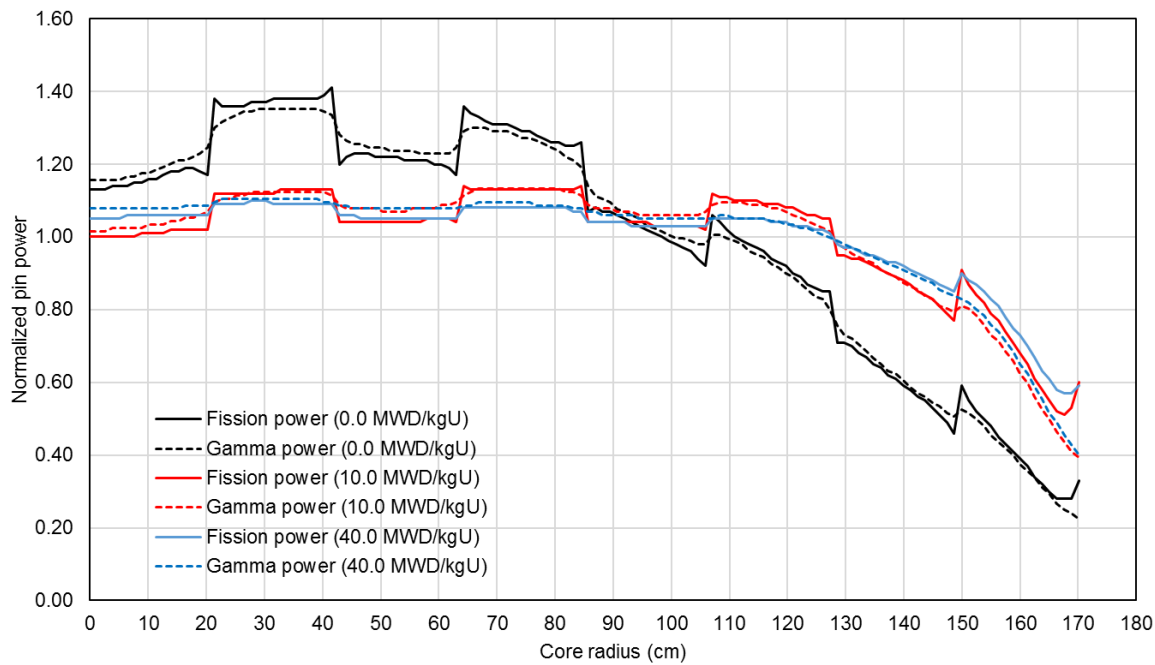
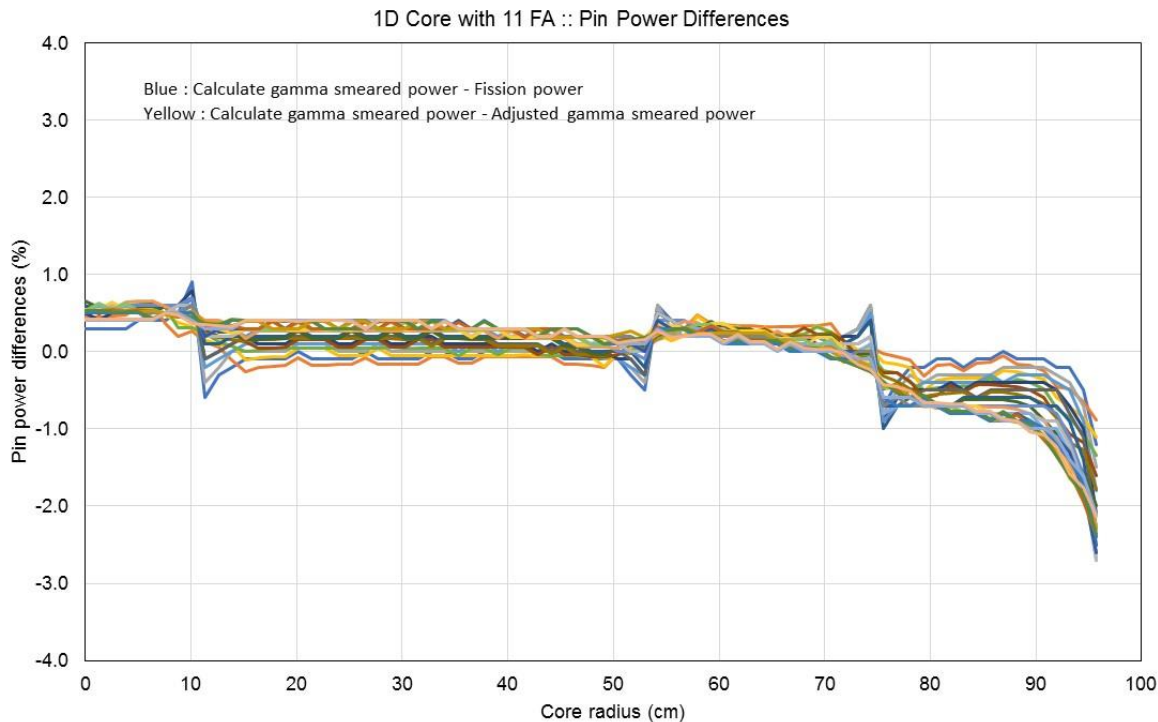


Figure 3.11. Comparison of the Fission and Gamma Power Distribution (Case 1D-b).

Comparison of fission and gamma powers (18 FA)

**Figure 3.12. Comparison of the Fission and Gamma Power Distribution (Case 1D-c).****Figure 3.13. Comparison of the Adjusted and Unadjusted Power Distribution (Case 1D-a).**

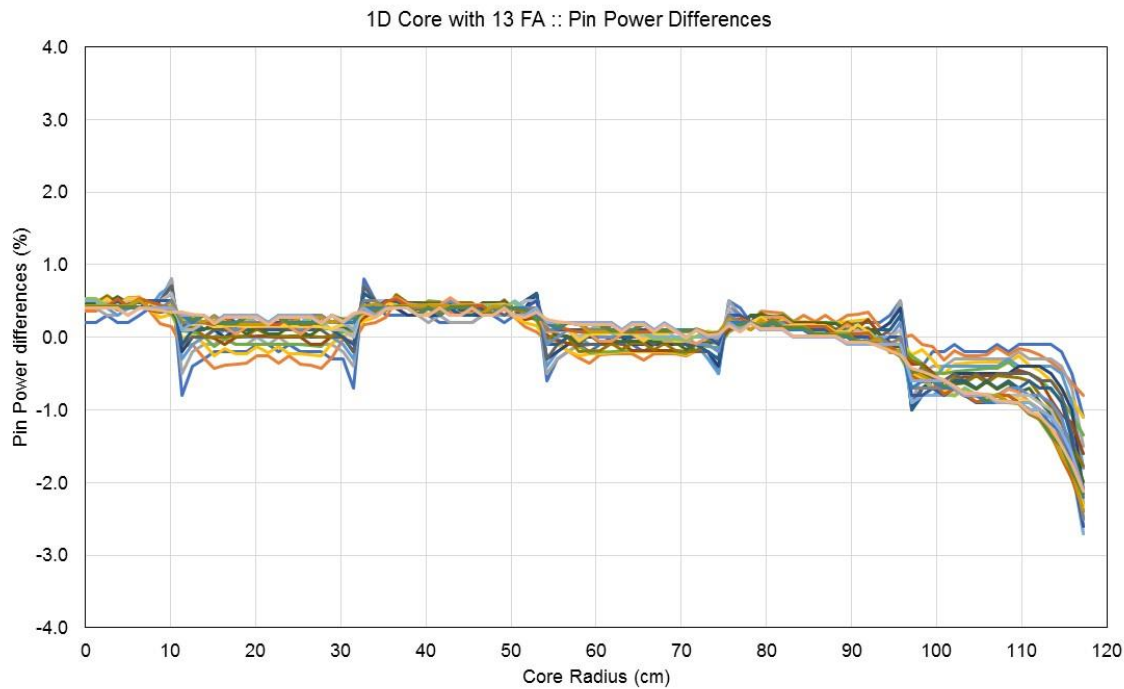


Figure 3.14. Comparison of the Adjusted and Unadjusted Power Distribution (Case 1D-b).

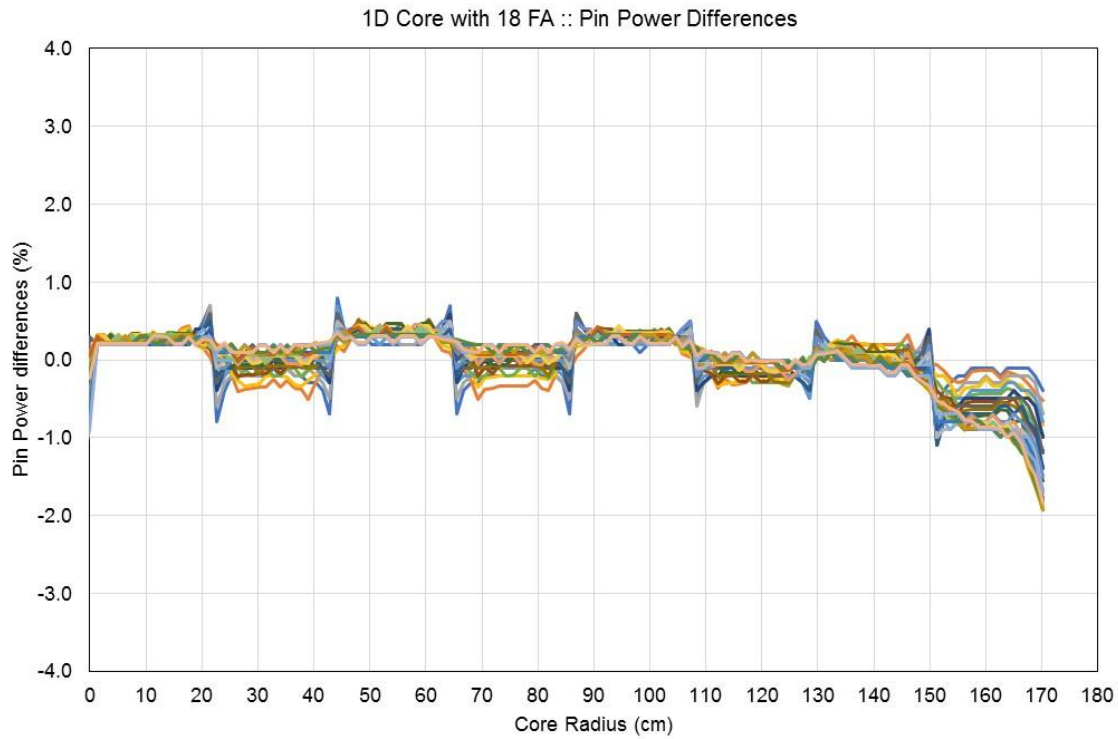


Figure 3.15. Comparison of the Adjusted and Unadjusted Power Distribution (Case 1D-c).



3.6 RESULTS FOR 2D CORE PROBLEMS

A new option for gamma-smeared power distribution has been implemented into MPACT and VERA-CS by using the following user option.

```
power_edit GAMMA-SMEARED
```

Gamma-smeared power distribution can be obtained by using Eq. (3.2). A 2D core benchmark calculation has been performed for the VERA progression problem 5B-2D, and pin power distributions have been obtained by using default power_edit with fission kappa and new gamma-smeared power options.

It was indicated in Section 3.5 that the approximate gamma smearing model could make a slight improvement for the whole core model. The MCNP calculations have been performed and the fission and actual gamma-smeared power distributions have been obtained by using the same method used in Reference [Wan17]. Table 3.12 provides various comparisons of power distribution. The RMS and maximum errors between the MCNP and MPACT fission powers are 0.78 % and 1.94 %, respectively, and Figure 3.16 shows a comparison of power distribution. The power differences between MPACT and MCNP are larger than the differences between KENO and MPACT which may be from less number of histories in MCNP. The differences between the fission and gamma-smeared powers for MCNP and MPACT are similar with each other as shown in Figure 3.17, which indicates that the approximate gamma smearing model is reasonable.

While the RMS and maximum errors between the MCNP gamma-smeared and the MPACT fission powers are 1.21 % and 3.51 %, respectively, the RMS and maximum errors between the MCNP and MPACT gamma-smeared powers are 1.09 % and 2.80 %. Figures 3.18 and 3.19 show the power differences for these two comparisons. It is noted that the approximate gamma smearing model improves the power distribution but the model still includes some approximation. Therefore, the approximate gamma smearing model can be partly a substitute for the gamma transport calculation.

Table 3.12. Comparison of power distributions (5B-2D)

Codes & power edit		Pin Power Error (%)		Δk_{eff} (pcm)
		RMS	Maximum	
MCNP fission	MPACT fission	0.78	1.94	70
MCNP fission	MCNP gamma-smeared	0.73	2.59	0
MPACT fission	MPACT gamma-smeared	0.50	2.48	0
MCNP gamma-smeared	MPACT fission	1.21	3.51	70
MCNP gamma-smeared	MPACT gamma-smeared	1.09	2.80	70

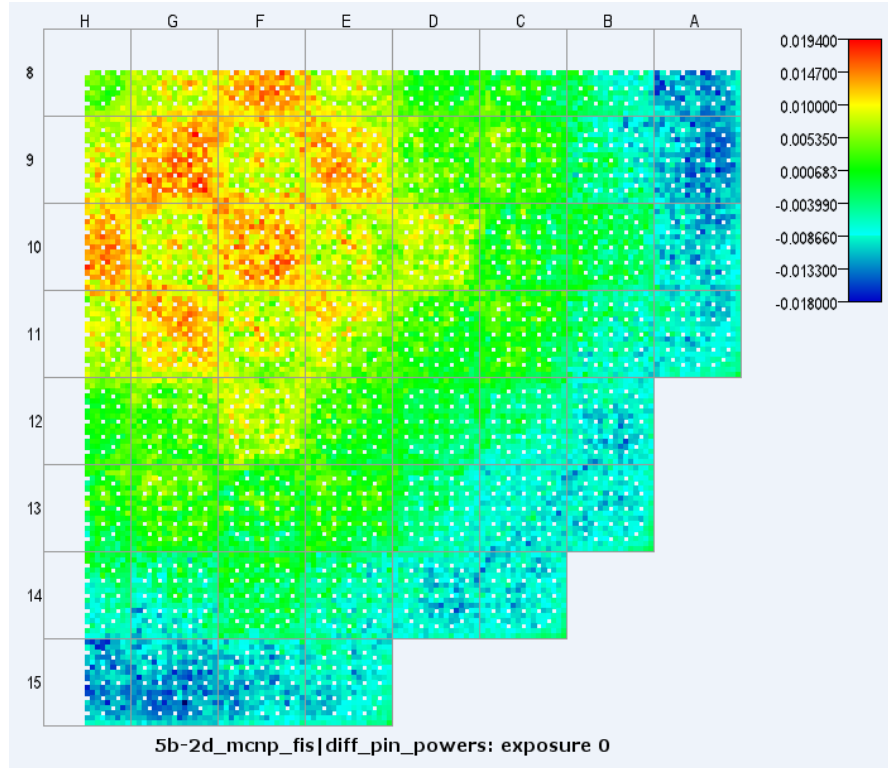


Figure 3.16. Comparison of the Fission Powers (MCNP vs. MPACT).

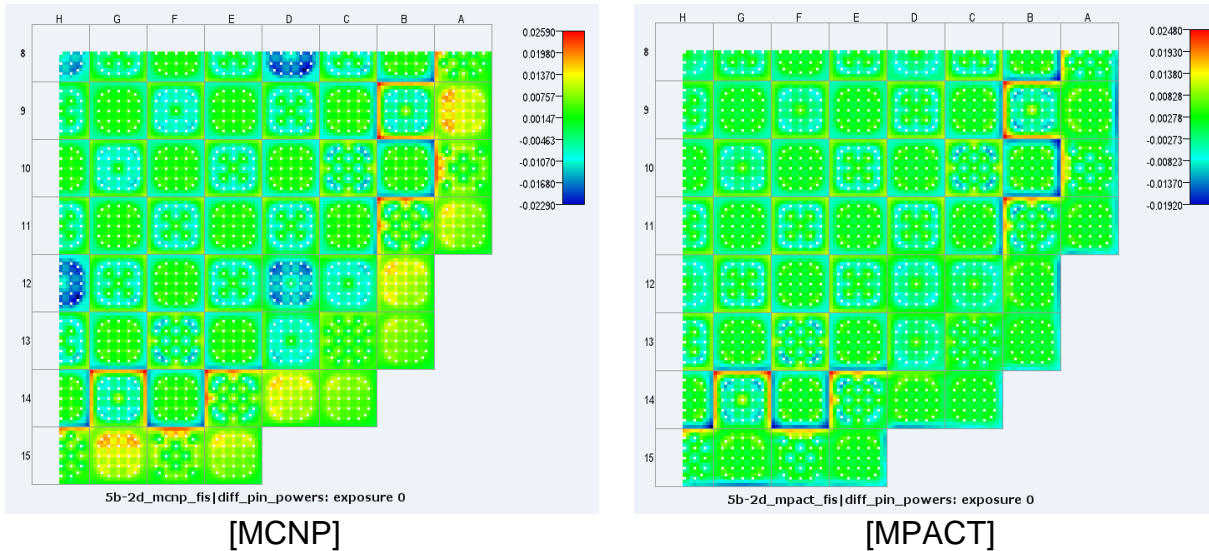


Figure 3.17. Comparison between Fission and Gamma Smeared Powers (MCNP & MPACT).

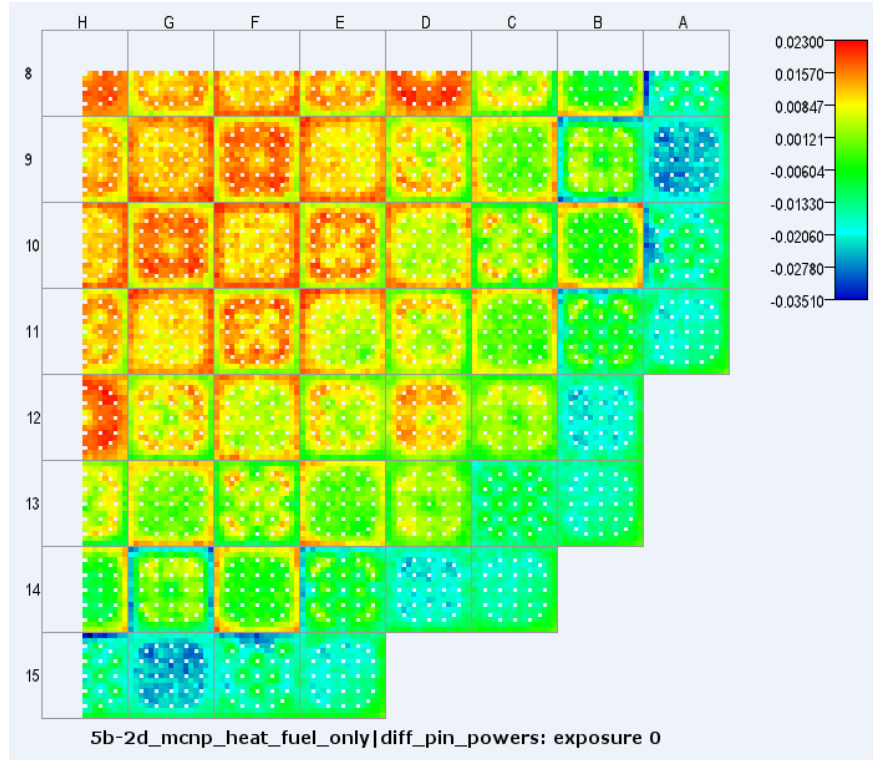


Figure 3.18. Comparison between the MCNP Gamma Smeared and MPACT Fission Powers.

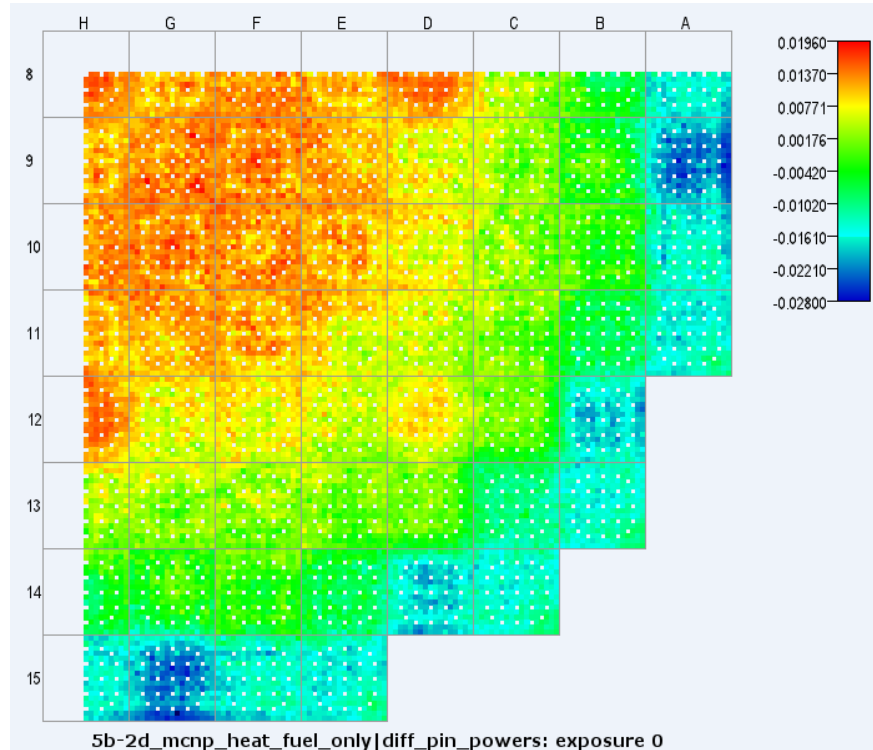


Figure 3.19. Comparison of the Gamma Smeared Powers (MCNP vs. MPACT).

4. MODEL EFFECT OF DELAYED ENERGY ON POWER NORMALIZATION IN DEPLETION CALCULATIONS

4.1 OVERVIEW

In a reactor depletion calculation, the neutron flux used for “burning” the fuel isotopes should be normalized to produce the heat that equals the specified reactor’s thermal power. An accurate flux normalization factor requires the energy-release-per-fission to be properly determined. The energy released by a fission event consists of various energy modes. Most energies are released instantaneously in the form of kinetic energy from fission products and fission neutrons, prompt gamma rays, or gamma rays from the capture of neutrons. An additional $\approx 7\%$ of energy is released at some point after the fission event as a result of the radioactive decay of fission products in the form of delayed beta and gamma rays.

The current energy deposition method in MPACT assumes that the release of delayed energy has reached equilibrium when performing the depletion calculation, so a time-independent value has been built into the total energy release per fission in the cross section library. A paper [Rat17] presented at the ANS Summer 2017 meeting accounts for the time-dependent delayed energy for flux normalization during the burnup calculation. In this study, a similar approach is taken to investigate this effect, using MPACT coupled with ORIGEN for a depletion calculation.

4.2 THEORY

The first step is to write the thermal power of a reactor into a prompt component and a delayed component,

$$P(t) = P_{pr}(t) + P_{de}(t). \quad (4.1)$$

As mentioned previously, the prompt power $P_{pr}(t)$ is contributed from the energy release of the prompt modes that directly relate to neutron fission and capture rates, i.e.,

$$P_{pr}(t) = f \sum_j V_j \left((1 - \gamma) \sum_{iso} \kappa_{f,iso} N_{iso,j} \sum_g \sigma_{f,g,iso,j} \phi_{g,j} + \sum_i \kappa_{c,iso} N_{iso,j} \sum_g \sigma_{c,g,iso,j} \phi_{g,j} \right), \quad (4.2)$$

where

f = Flux normalization factor

$\kappa_{f,iso}$ = Direct fission energy release for isotope iso (unit: J)

$\kappa_{c,iso}$ = Recoverable energy per neutron capture (unit: J)

γ = Fraction of the total direct fission energy that is delayed

V_j = Volume of material region j (unit: cm³)



$N_{iso,j}$ = Number density of isotope iso in material region j (unit: cm^{-3})

$\sigma_{f,g,iso,j}$ = Microscopic fission cross section (unit: cm^2)

$\sigma_{c,g,iso,j} = \sigma_{a,g,iso,j} - \sigma_{f,g,iso,j}$ Microscopic capture cross section (unit: cm^2)

$\phi_{g,j}$ = Neutron flux of energy group g in region j (unit: $\text{cm}^{-2}\text{s}^{-1}$).

Note that many of the terms (except V , κ and γ) are time dependent, but the argument of time is dropped for brevity. The flux normalization factor in Eq. (4.2) is determined so that summation of the prompt and delayed powers equals the thermal power $P(t)$.

To determine the delayed power $P_{de}(t)$, it is assumed that the numerous components of the delayed heat source can be lumped into a relatively small number of groups, similar to the approach taken with delayed neutrons. If $D_{m,j}$ is defined as the concentration of delayed heat group m at region j , then the balance equation that $D_{m,j}$ satisfies is given as

$$\frac{dD_{m,j}(t)}{dt} = \gamma_m f V_j \sum_{iso} \kappa_{f,iso} N_{iso,j} \sum_g \sigma_{f,g,iso,j} \phi_{g,j} - \lambda_m D_{m,j}(t), \quad (4.3)$$

where γ_m and λ_m are the yield and decay constant of delayed heat group m (see Table 4.1). By using $D_{m,j}$, the delayed power is written as

$$P_{de}(t) = \sum_j \sum_m \lambda_m D_{m,j}(t). \quad (4.4)$$

Equation (4.3) can be solved using the matrix exponential method in the depletion calculation [Rat17]. However, due to the large values of λ_m for short-lived precursors, a very fine time step is required to ensure the convergence of the Taylor series expansion of the matrix exponential. To use a standard depletion step for this calculation, we assume a constant value of the delayed heat source ($S_{m,j}$) over a standard burnup time step (or substep). Thus, Eq. (4.3) can be analytically solved within a time step of (t_1, t_2) ,

$$D_{m,j}(t) = D_{m,j}(t_1) e^{-\lambda_m(t-t_1)} + \frac{S_{m,j}}{\lambda_m} \left[1 - e^{-\lambda_m(t-t_1)} \right], \quad (4.5)$$

where

$$S_{m,j} = \gamma_m f V_j \sum_{iso} \kappa_{f,iso} N_{iso,j} \sum_g \sigma_{f,g,iso,j} \phi_{g,j}.$$

So the average $\bar{D}_{m,j}$ over a time step (or substep) that should be used for flux normalization is given as

$$\overline{D_{m,j}} = \frac{1}{\Delta t \lambda_m^2} \left([S_{m,j} - \lambda D_{m,j}(t_1)] e^{-\lambda_m \Delta t} + \lambda_m D_{m,j}(t_1) + \lambda_m S_{m,j} \Delta t - S_{m,j} \right). \quad (4.6)$$

Then the flux normalization factor is computed as

$$f = \frac{P - P_{de}}{P_{non}} = \frac{P - \sum_j \sum_m \lambda_m \overline{D_{m,j}}}{\sum_j V_j \left((1-\gamma) \sum_{iso} \kappa_{f,iso} N_{iso,j} \sum_g \sigma_{f,g,iso,j} \phi_{g,j} + \sum_i \kappa_{c,iso} N_{iso,j} \sum_g \sigma_{c,g,iso,j} \phi_{g,j} \right)}. \quad (4.7)$$

As seen in Eqs. (4.7) and (4.3), solutions for f and $D_{m,j}(t)$ are dependent on each other, so iterations are needed. The converged normalization factor f will be used for the regular depletion calculation in the current step (or substep).

The only approximation that is made here is to assume that the delayed energy source ($S_{m,j}$) is constant during the time step. This approximation holds well when the delayed power is a small portion of total power, so the prompt fission power is roughly time-independent within the time step. When the power is sharply reduced in a short time period, the delayed power dominates, so a finer time step may be required to model the variation of $S_{m,j}$. Although the finer time step could be an efficiency concern, as can be seen from the results, the delayed energy effect on flux normalization is marginal.

4.3 BENCHMARK RESULTS

The method described above has been implemented in MPACT. For a preliminary investigation, the group constants provided in RETRAN code [Epr98] and presented in Table 4.1 are used. These data are based on the fittings from a proposed 1973 ANS decay heat standard [Ans73].

Table 4.1. Data of delayed heat group

Delayed heat group	Yield	Decay constant (1/s)
1	2.990E-03	1.772E+00
2	8.250E-03	5.774E-01
3	1.550E-02	6.743E-02
4	1.935E-02	6.214E-03
5	1.165E-02	4.739E-04
6	6.450E-03	4.810E-05
7	2.310E-03	5.344E-06
8	1.640E-03	5.726E-07
9	8.500E-04	1.036E-07
10	4.300E-04	2.959E-08
11	5.700E-04	7.585E-10



First, a PWR pin cell problem is depleted for 10,000 hours (~417 days) at constant full power. In the first few hundred hours, a fine time step has been used to show the large variation in the flux normalization factor. In Figures 4.1 and 4.2, the energy release per fission is compared using equilibrium and time-dependent delayed energy models. The time-dependent model starts with an energy release that is ~7% smaller than the equilibrium, increases rapidly in the first few hours, and approaches the equilibrium value after a few thousand hours. The blue dots are the results of the time-dependent model with standard burnup time steps. They match the fine-step results very well.

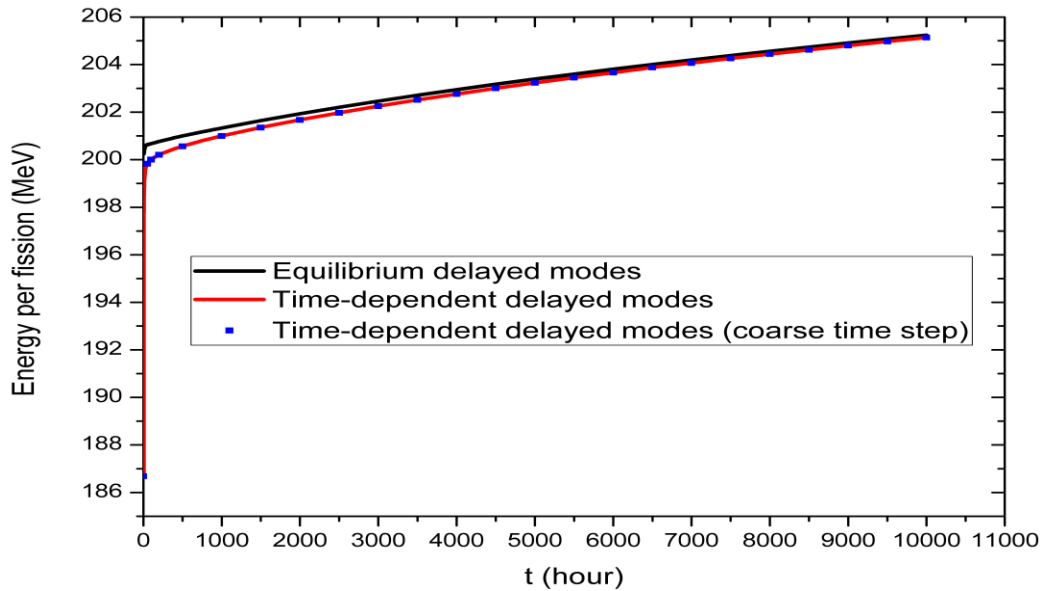


Figure 4.1. Energy per Fission of 10,000 h at Constant Full Power.

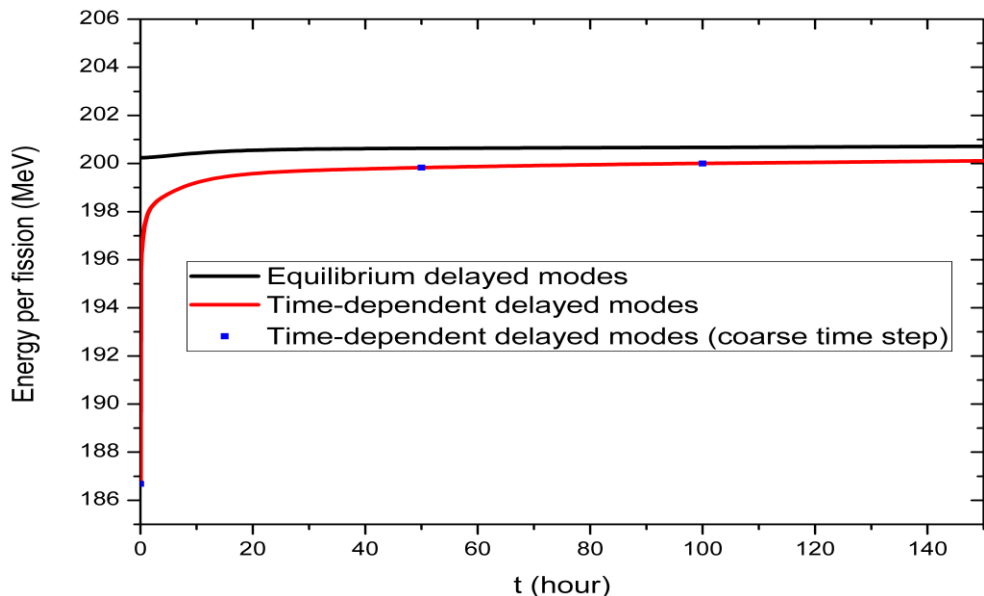


Figure 4.2. Energy per Fission in the First 150 h at Constant Full Power.

Next the normalized flux in Figure 4.3 is compared. The time-dependent model starts ~7% high consistent with the energy per fission and reduces to about 2% high in 10 minutes. Then the fluxes of both models increase due to xenon buildup. The difference between the two models becomes negligible over time. Although the normalized flux is larger in the first few hundreds of hours, the time-dependent delayed energy model does not result in a significant change in the isotopics. Basically, the difference of ^{235}U and ^{239}Pu contents at 10,000 hours are -0.06% and +0.05%, respectively, and the largest k_{eff} difference over the 10,000 hours is only 13 pcm.

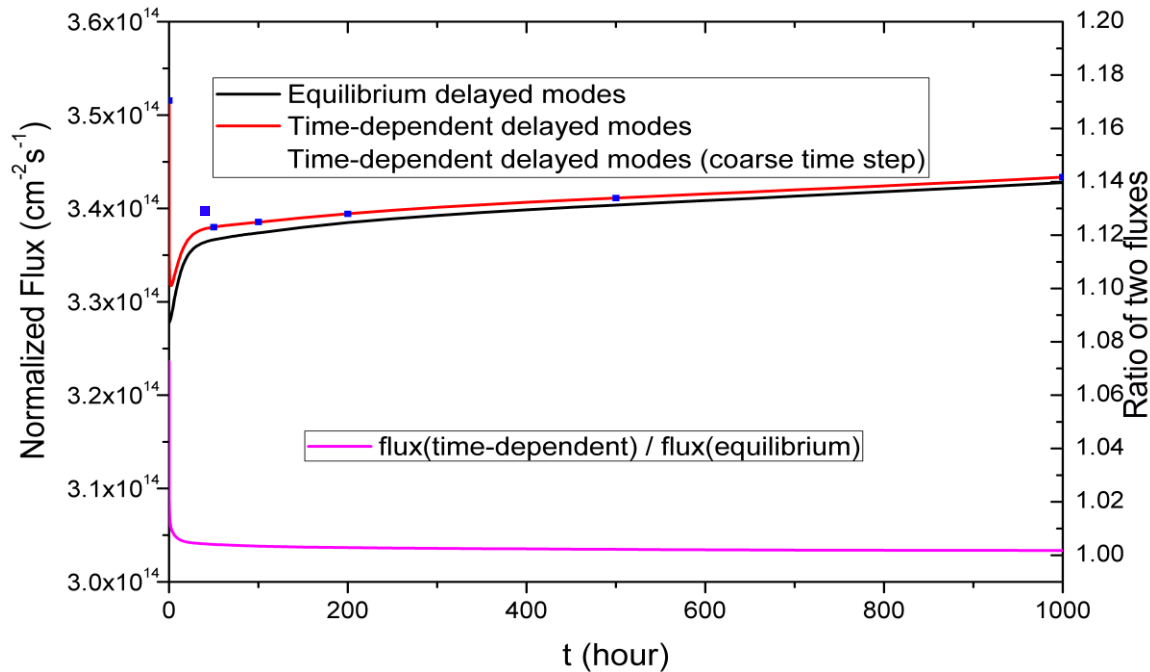


Figure 4.3. Normalized Flux in the First 1,000 h at Constant Full Power.

Since the constants of decay heat groups used here are based on the 1973 ANS standard, it is best to verify whether the latest 2005 ANS standard [Ans05] would have a significantly different result. It was found that the difference of energy release per fission between the two models tested in this case is essentially the same as the decay heat percentages after shutdown (following a long irradiation time) that can be obtained from the data in the 2005 ANS standard. To specify, the energy per fission for the equilibrium model and time-dependent model are defined as E_1 and E_2 . Appendix D shows that the relative difference between E_1 and E_2 , and the decay heat percentages H_{decay} calculated from ANS standard can be both written as

$$\frac{E_1(t) - E_2(t)}{E_1(t)} = \sum_m \gamma_m e^{-\lambda_m t} = H_{\text{decay}}(t). \quad (4.8)$$



Therefore, by comparing $\frac{E_1(t) - E_2(t)}{E_1(t)}$ of this case with the decay heat data of the 2005 ANS standard, the difference can be inferred for a case using the 2005 ANS standard for this calculation. The results shown in Table 4.2 indicate that the similar results could be obtained, even if the latest ANS standard had been used.

Table 4.2. Results verification with 2005 ANS standard

Time (h)	Diff. (%) of energy/fission	Decay heat power (%) for thermal fission of ^{235}U from 2005 ANS standard
0	6.77	-
0.1	2.32	2.40
1	1.29	1.33
10	0.63	0.66
100	0.34	0.36
1,000	0.17	0.18
10,000	0.07	0.08

Next a pin cell case with more complicated power history was run. Specifically, a series of full power in 1 h, 10 h, 100 h, 1,000 h and 5,000 h were applied. Between each of two adjacent full power ranges, a 1,000 h interval of 8% power was placed to let the decay heat go down. This case could be used to examine the integrated effects of the different time ranges of the delayed energy lag. Since the power was repeatedly reduced from 100% to 8%, a very fine time step was used in the first dozens of hours after the power change. Figure 4.4 shows the eigenvalue difference between the time-dependent and equilibrium-delayed energy. There were a few eigenvalue dips (~30pcm) during the changes of power due to xenon, but the effect on k_{eff} did not accumulate. The overall effect of time-dependent delayed energy gives a -13 pcm k_{eff} difference at 10,000 h. The differences of ^{235}U and ^{239}Pu contents at 10,000 hours are -0.06% and +0.06%, respectively. The maximum difference of ^{135}Xe during the excursion sometimes reached ~1% since it is sensitive to the flux normalization factor during power change, but it makes little difference to the overall depletion rate.

For the nominal reactor burnup calculation to compute the flux renormalization factor, it has been shown that the explicit delayed energy model does not result in significant difference with regard to the isotopics of depletion and k_{eff} as compared to the equilibrium-delayed energy. It can also be inferred that the conclusion is applicable to a core startup calculation since the effect is marginal even for the case with a severe power history. Future work will investigate the delayed energy effect on a fast transient such as RIA.

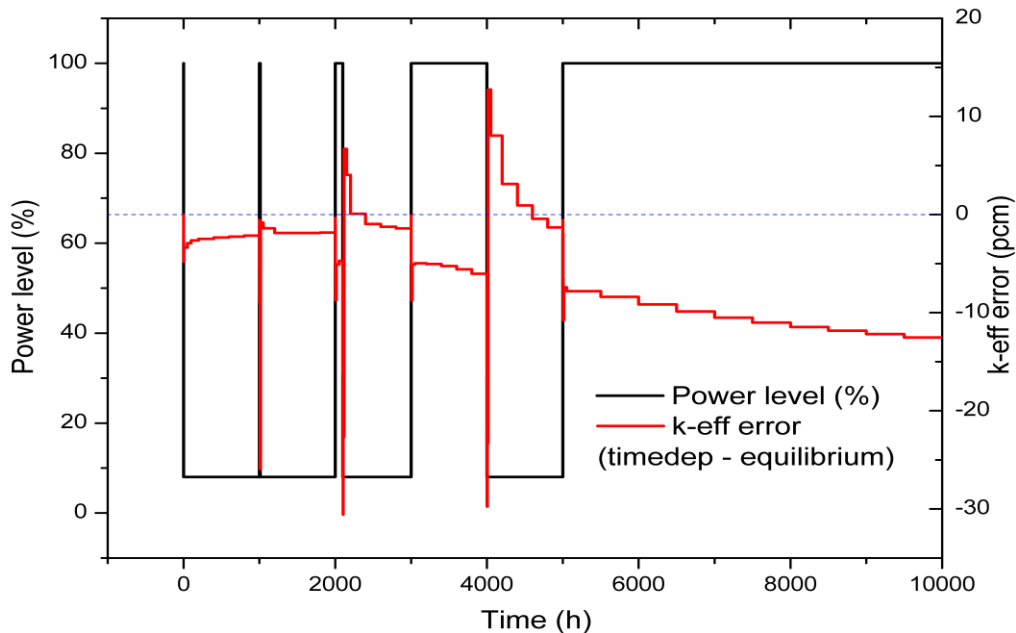


Figure 4.4. The Effect of Time-Dependent Delayed Energy on k_{eff} .



5. CONCLUSIONS AND FUTURE WORK

The overall neutron flux normalization procedure was reviewed in detail, and the best approach was determined for MPACT to include the neutron fission and capture recoverable energies to be used in on-the-fly neutron flux normalization. New ENDF/B-7.0 and 7.1 capture kappa values have been estimated for all ENDF/B nuclides by developing a program called *CapKappa*. These values have been incorporated into the ENDF/B-7.0 and 7.1 v5.1m0 Simplified AMPX 51-group libraries, and they also will be used in the AMPX and SCALE code packages. In addition, since the new approach includes an approximation in time-dependent delayed gamma source, the impact of the delayed gamma source on the multiplication factor has been investigated.

Since the CASL neutronics simulator MPACT does not include gamma transport capability, pin power distributions have been obtained by using kappa-fission or fission reaction rates. This approach includes non-negligible approximations that overestimate peaking powers. A simple approximate gamma smearing model has been investigated based on the facts that pin-wise gamma energy depositions are almost flat over a fuel assembly, and assembly-wise gamma energy deposition is proportional to kappa-fission energy deposition. The approximate gamma smearing model works well for single assembly cases, and can improve the gamma smeared power distribution for the whole core model as well. It can be said that the approximate gamma smearing model improves the power distribution but the model still includes some approximation.

Although the power distributions can be improved by the approximate gamma smearing model, still there is an issue to explicitly obtain local energy deposition. A new simple approach may need to be developed, or gamma transport (and/or coarse-mesh finite difference [CMFD]) capability may need to be incorporated into MPACT to estimate local energy deposition. This capability will enhance robust neutronics and thermal hydraulics coupled calculations for high-fidelity multi-physics simulations. Furthermore, time-dependent terms in neutron flux normalized must be explicitly considered by providing delayed heat source terms.

REFERENCES

- [Ans05] ANSI/ANS-5.1-2005, *Decay Heat Power in Light Water Reactors*, American Nuclear Society (2005).
- [Ans73] Proposed ANS Standard, *Decay Energy Release Rates Following Shutdown of Uranium-Fueled Thermal Reactors*, Approved by Subcommittee ANS-5, American Nuclear Society Standards Committee (Oct. 1971) (Revised Oct. 1973).
- [CAS15] Consortium for Advanced Simulation of Light Water Reactors (CASL). URL <http://www.casl.gov/> (2015).
- [Cha11] M. B. Chadwick et al., “ENDF/B-VII.1 Nuclear Data for Science and Technology: Cross Sections, Covariances, Fission Product Yields and Decay Data,” *Nuclear Data Sheets*, 112, Issue 12, 2887-2996 (2011).
- [Epr98] EPRI, *RETRAN-3D – A Program for Transient Thermal-Hydraulic Analysis of Complex Fluid Flow Systems, Volume 1: Theory and Numerics*, NP-7450, Volume 1, Rev. 3, Electric Power Research Institute (1998).
- [God14] Andrew T. Godfrey, *VERA Core Physics Benchmark Progression Problem Specifications*, CASL-U-2012-0131-004, Rev. 4 (8/29/2014).
- [Gol62] R. Goldstein and E. R. Cohen, “Theory of Resonance Absorption of Neutrons,” *Nucl. Sci. Eng.*, 13, 132 (1962).
- [Kim13] Kang Seog Kim and Ser Gi Hong, “Gamma Transport and Diffusion Calculation Capability Coupled with Neutron Transport Simulation in KARMA 1.2,” *Ann. Nucl. Energ.*, 57, 59–67 (2013).
- [Kim17] Kang Seog Kim, Kevin Clarno, Cole Gentry, Andrew Godfrey, Mark L. Williams, Dorothea Wiarda, Brendan Kochunas, and Yuxuan Liu, *Development of the V4.2m5 and V5.0m0 Multigroup Cross Section Libraries for MPACT for PWR and BWR*, CASL-U-2017-1280-000, ORNL/TM-2017/95 (2017).
- [Les07] F. Leszczynski et al., *WIMS-D Library Update*, IAEA (2007).
- [Mac94] R. E. MacFarlane, D. W. Muir, “The NJOY Nuclear Data Processing System Version 91,” *LA-12740-M Manual* (1994).
- [Mpa15] MPACT Team, *MPACT Theory Manual, Version 2.0.0*, CASL-U-2015-0078-000, Oak Ridge National Laboratory and University of Michigan (2015).
- [Rat17] M. A. Rathbun and D. P. Griesheimer, “Effect of Delayed Energy Release on Power Normalization in Reactor Depletion Calculations,” *ANS Summer 2017* (2017).
- [Rea16] B. T. Rearden and M. A. Jessee, *SCALE Code System*, ORNL/TM-2005/39, Version 6.2 (2016).
- [Rho08] Joel Rhodes, Kord Smith, and Zhiwen Xu, “CASMO-5 energy release per fission model,” *PHYSOR 2008*, Interlaken, Switzerland, (2008).
- [Sta98] R. J. J. Stamm’ler et al., *The HELIOS Methods*, Studsvik Scandpower (1998).
- [Trk12] A. Trkov, M. Herman, and D. A. Brown, *ENDF-6 Formats Manual, Data Formats and Procedures for the Evaluated Nuclear Data Files ENDF/B-VI and ENDF/B-VII*, CSEWG Document ENDF-102, BNL-90365-2009 Rev. 2 (2012).
- [Tur16] J. Turner et al., “The Virtual Environment for Reactor Applications (VERA): Design and architecture,” *Journal of Computational Physics*, 326, 544 (2016).



[Wan17] Xinyan Wang et al., “Energy Deposition Analysis of VERA Progression Problems Using MCNP6,” CASL-U-2017-1399-000 (2017).

APPENDIX A. PROGRAM SOURCE OF CAPKAPPA

```

program CapKappa
!-----+
! Program      : Calculate capture kappas for flux normalization
!                 Capture kappa = Q-capture (f1*(n,r)+f2*(n,a))
!                               + Decay Q-value of captured isotope
! Institute    : Oak Ridge National Laboratory
! Authors      : Kang Seog Kim
! Revision     : 05/05/2017 Initial version
!-----+
use param_M

! [Read input file]
call readin

! [Read ENDF decay data]
call rdendfdecay

! [Read ENDF xs data]
call rdendfxs

! [Write output file]
call writeout

! stop
end

module param_M
!-----+
! Function      : All the variables and parameters are defined in this module.
! Institute    : Oak Ridge National Laboratory
! Authors      : Kang-Seog Kim
! Revision     : 05/04/2017 Initial version
!-----+
implicit double precision (a-h,o-z)
implicit integer (i-n)

!-----+
! + Variables :: Common +
!-----+
!-----+
@ boltz_const          (r)    Boltzmann constant (0.861735e-4 eV/K)      +
@ pi                   (r)    Pi (3.141592654)                         +
@ amfactor             (r)    Atomic mass factor (1.00866491578)           +
@ ev_watt              (r)    Conversion factor eV<->watt (1.6021e-19)      +
!-----+
character(1) :: ss1,blank,bang
character(2) :: ss2
character(3) :: ss3
character(4) :: ss4
character(5) :: ss5
character(6) :: ss6
character(7) :: ss7
character(8) :: ss8
character(9) :: ss9
character(10) :: ss10
character(20) :: ss20
character(80) :: ss80
character(100) :: ss100
character(300) :: ss300
character(1000) :: ssw
logical :: kr,kr0,kr1,kr2,kr3,kr4,kr5,kr6,kr7,kr8,kr9
double precision :: zero,one,two,ev_watt
parameter(blank=' ',bang='!!')
parameter(boltz_const=0.861735e-4)
parameter(pi=3.141592654,amfactor=1.00866491578)
parameter(av0_n=0.6022045)

```



```

parameter(ev_watt=1.60219e-19)
parameter(zero=0.0d0,one=1.0d0,two=2.0d0)

!
+-----+
+ Variables :: Input +
+-----+

! @ endflib          (a100) ENDF neutron library file name      +
! @ decaylib         (a100) ENDF decay library file name      +
! @ numalpha          (i)    Number of nuclides to consider (n,a)   +
! @ nuclidalpha(i)   (i)    Nuclide ID for (n,a) (i=1,numalpha)   +
! @ weightalpha(i)   (r)    Weight for (n,a) (i=1,numalpha)      +
+-----+
parameter(indxa=97,indxz=122)
character(100) :: endflib,decaylib
integer :: numalpha
integer,allocatable :: nuclidalpha(:)
double precision,allocatable :: weightalpha(:)

!
+-----+
+ Variables :: ENDF data Library +
+-----+

! @ mxnuc            (i)    Maximum number of nuclides for endf/b xs file +
! @ mxdcy             (i)    Maximum number of nuclides for decay file      +
! @ numnuc            (i)    The number of nuclides in endf/b for the      +
!                           atomic mass & potential xs      +
! @ numdcy            (i)    The number of nuclides in endf/b decay library +
! @ endfdata(i)%      Type for atomic mass & potential xs
!                      (i=1,numnuc)      +
! @ %mat              (i)    ENDF/B MAT      +
! @ %nuclid           (i)    Numeric nuclide id. (ex: 922350)      +
! @ %amsss             (r)    Atomic mass      +
! @ %potxs             (r)    Potential xs      +
! @ %qmt102            (r)    q-value for mt=102 (n,r)      +
! @ %qmt107            (r)    q-value for mt=107 (n,a)      +
! @ %qcapiso           (r)    q-value of the (n,r) production nuclide +
! @ %halflife          (r)    Decay half-life (sec)      +
! @ %qcapiso2          (r)    q-value of the decayed nuclide      +
! @ %halflife2          (r)    Decay half-life (sec)      +
! @ %capkappa           (r)    Final capture kappa (eV)      +
! @ %nuclaid           (a10)  Alphanumeric nuclide id. (ex: 92-u -235) +
! @ %lcapisoxs          (l)    if product isotope includes XS or not +
! @ %lcapisoxs2          (l)    if 2nd product isotope includes XS or not +
! @ dcydata(i)%        [dcytype] Type for decay halflife (i=1,numdcy) +
! @ %mat                (i)    ENDF/B mat      +
! @ %nuclid             (i)    Numeric nuclide id. (ex: 922350)      +
! @ %halflife            (r)    Decay half-life (sec)      +
! @ %evnutrino           (r)    Nutrino energy (eV)      +
! @ %evqvalue            (r)    Q effective (eV)      +
! @ %nuclaid             (a10)  Alphanumeric nuclide id. (ex: 92-u -235) +
+-----+
parameter (mxnuc=800,mxdcy=4000)
integer :: numnuc,numdcy
type endftype
  integer :: mat,nuclid
  double precision :: amass,potxs,qmt102,qmt107,qcapiso,halflife,capkappa,
                     qcapiso2,halflife2
  character(10) :: nuclaid
  logical :: lcapisoxs,lcapisoxs2
endtype endftype
type(endftype),pointer :: endfdata(:)
type dcytype
  integer :: mat,nuclid
  double precision :: halflife,evnutrino,evqvalue
  character(10) :: nuclaid
endtype dcytype
type(dcytype),pointer :: dcydata(:)

!
end module param_M

```

```

subroutine rdendfdecay
!-----+
! Function   : Read decay constants & Q-values from the ENDF decay library
!-----+
use param_M
!
! [Open endf/b decay file]
open(62,file=decaylib,status='old')
!
! [Memory allocation & initialization]
!-----+
allocate(dcydata(mxdcy))
do i=1,mxdcy
    dcydata(i)%mat=0
    dcydata(i)%nuclid=0
    dcydata(i)%halflife=0.0
    dcydata(i)%evnutrino=0.0
    dcydata(i)%evqvalue=0.0
    dcydata(i)%nuclaid=' '
enddo
!
! [Read endf radioactive decay data]
!-----+
ix=0
kr=.false.
do i=1,1000000
    read(62,'(a80)',end=10) ss80
    if (ss80(72:75).eq."1451") then
        ix=ix+1
        read(ss80,'(2e11.6,44x,i4)' xval1,xval2,nid
        dcydata(ix)%mat=nid
        dcydata(ix)%nuclid=int(xval1)
        write(66,*) ix,dcydata(ix)%nuclid,nid
        read(62,*)
        read(62,*)
        read(62,*)
        read(62,'(x,a10)') dcydata(ix)%nuclaid
        do j=1,1000
            read(62,'(a80)',end=10) ss80
            if (ss80(1:21).eq.'Mean Neutrino Energy:') then
                read(ss80(22:32),*) xval1
                dcydata(ix)%evnutrino=xval1*1000.0
            elseif (ss80(1:12).eq.'Q effective:') then
                read(ss80(22:32),*) xval1
                dcydata(ix)%evqvalue=xval1*1000.0
            endif
            if (ss80(75:80).eq.'099999') exit
        enddo
        do j=1,10000
            read(62,'(a80)',end=10) ss80
            if (ss80(72:75).eq."8457") then
                read(62,'(a80)',end=10) ss80
                read(ss80(1:11),*) hltmp
                dcydata(ix)%halflife=hltmp
                exit
            endif
        enddo
    endif
enddo
10 continue
!
numdcy=ix
!
! Convert nuclide ID
!-----+
do i=1,numdcy
    nx=0
    if (dcydata(i)%nuclaid(10:10).eq.'m'.or.dcydata(i)%nuclaid(10:10).eq.'M') nx=1
    dcydata(i)%nuclid=dcydata(i)%nuclid*10+nx
enddo

```



```

!
  close(62)
!
  write(6,'(3x,"Successful reading decay data file.")')
!
  return
end

subroutine rdendfxs
use param_M
!
open(61,file=endflib,status='old')
!
[Memory allocation & initialization]
-----
allocate(endfdata(mxnucl))
do i=1,mxnucl
  endfdata(i)%mat=0
  endfdata(i)%nuclid=0
  endfdata(i)%amass=0.0
  endfdata(i)%potxs=0.0
  endfdata(i)%qmt102=0.0
  endfdata(i)%qmt107=0.0
  endfdata(i)%nuclaid=' '
  endfdata(i)%lcapisoxs=.false.
  endfdata(i)%qcapiso=0.0
  endfdata(i)%halflife=0.0
  endfdata(i)%lcapisoxs2=.false.
  endfdata(i)%qcapiso2=0.0
  endfdata(i)%halflife2=0.0
  endfdata(i)%capkappa=0.0
enddo
!
[Read the atomic mass and potential xs from endf/b file]
-----
ix=0
kr1=.false.
kr2=.false.
kr3=.false.
do i=1,1000000000
  read(61,'(a80)',end=20) ss80
  if (ss80(71:75).eq." 1451") then
    if (.not.kr1) then
      ix=ix+1
      read(ss80,'(2e11.6,44x,i4)' xval1,xval2,nid
      endfdata(ix)%mat=nid
      endfdata(ix)%nuclid=int(xval1)
      endfdata(ix)%amass=xval2*amfactor
      read(61,*,end=20)
      read(61,*,end=20)
      read(61,*,end=20)
      read(61,'(x,a10)',end=20) endfdata(ix)%nuclaid
      kr1=.true.
      write(6,*) ix,endfdata(ix)%nuclid
    endif
  elseif (ss80(71:75).eq." 3102") then
    if (.not.kr2) then
      read(61,'(e11.6)' endfdata(ix)%qmt102
      kr2=.true.
    endif
  elseif (ss80(71:75).eq." 3107") then
    if (.not.kr3) then
      read(61,'(e11.6)' endfdata(ix)%qmt107
      kr3=.true.
    endif
  elseif (ss80(67:80).eq."    0 0 0      0") then
    kr1=.false.
    kr2=.false.
    kr3=.false.
  endif
end

```

```

      enddo
20 continue
      ntot=ix
      numnuc=ntot
      write(6,*) numnuc
!
! Convert nuclide ID
! -----
do i=1,numnuc
      nx=0
      if (endfdata(i)%nuclaid(10:10).eq.'m'.or.endfdata(i)%nuclaid(10:10).eq.'M') nx=1
      endfdata(i)%nuclid=endfdata(i)%nuclid*10+nx
enddo
!
close(61)
!
write(6,'(3x,"Successful reading atomic mass & potentail xs.")')
!
return
end

subroutine readin
! -----
! Subroutine : Read input file 'CapKappa.in'
! Institute  : Oak Ridge National Laboratory
! Authors    : Kang Seog Kim
! Revision   : 05/05/2017 Initial version
! -----
use param_M
!
! [Read input file]
open(1,file='CapKappa.in',status='old')
read(1,*) ss2,endflib
read(1,*) ss5,decaylib
ix=0
do i=1,1000
      read(1,*,<end=10>) ss5
      if (ss5.eq.'ALPHA') ix=ix+1
      if (ss5.eq.'%END') exit
enddo
10 numalpha=ix
allocate(nuclidalpha(numalpha),weightalpha(numalpha))
rewind(1)
ix=0
do i=1,1000
      read(1,'(a100)',<end=20>) ss100; read(ss100,*) ss5
      if (ss5.eq.'ALPHA') then
          ix=ix+1
          read(ss100,*) ss5,nuclidalpha(ix),weightalpha(ix)
      elseif (ss5.eq.'%END') then
          exit
      endif
enddo
20 continue
!
close(1)
!
return
end

subroutine writeout
! -----
! Subroutine : Write output file 'CapKappa.out'
! Institute  : Oak Ridge National Laboratory
! Authors    : Kang Seog Kim
! Revision   : 05/05/2017 Initial version
! -----
use param_M
!
open(11,file='CapKappa.out',status='unknown')

```



```

open(12,file='CapKappa.dat',status='unknown')
!
! [Check if a captured nuclide includes XS or not.]
! -----
do i=1,numnuc
  nid2=endfdata(i)%nuclid+10
  nid3=nid2+10000
  do j=1,numnuc
    if (nid2.eq.endfdata(j)%nuclid) then
      !endfdata(i)%lcapisoxs=.true.
      exit
    endif
  enddo
  do k=1,numdcy
    if (nid2.eq.dcydata(k)%nuclid) then
      endfdata(i)%qcapiso=dcydata(k)%evqvalue-dcydata(k)%evnutrino
      endfdata(i)%halflife=dcydata(k)%halflife
      if (dcydata(k)%halflife.gt.5.0E+5.or.dcydata(k)%halflife.le.0.0) then
        endfdata(i)%lcapisoxs=.true.
      endif
      exit
    endif
  enddo
  do k=1,numdcy
    if (nid3.eq.dcydata(k)%nuclid) then
      endfdata(i)%qcapiso2=dcydata(k)%evqvalue-dcydata(k)%evnutrino
      endfdata(i)%halflife2=dcydata(k)%halflife
      if (dcydata(k)%halflife.gt.5.0E+5.or.dcydata(k)%halflife.le.0.0) then
        endfdata(i)%lcapisoxs2=.true.
      endif
      exit
    endif
  enddo
enddo
!
! [Print out atomic mass and potential xs from endf/b file]
! -----
write(11,'(@Summary of endf/b information")')
write(11,'(-----")')
write(11,'("The number of nuclides =",i5)' numnuc
write(11,'("TCriteria for T-half = 5.0E+5 sec")')
write(11,*)
do i=1,numnuc
  factor1=1.0; factor2=0.0
  do j=1,numalpha
    if (endfdata(i)%nuclid.eq.nuclidalpha(j)) then
      factor2=weightalpha(j)/100.0
      factor1=1.0-factor2
      exit
    endif
  enddo
  if (endfdata(i)%qmt107.gt.0.0) then
    endfdata(i)%capkappa=endfdata(i)%qmt102*factor1+endfdata(i)%qmt107*factor2
  else
    endfdata(i)%capkappa=endfdata(i)%qmt102*factor1
  endif
  endfdata(i)%capkappa0=endfdata(i)%capkappa
  if (.not.endfdata(i)%lcapisoxs) then
    endfdata(i)%capkappa=endfdata(i)%capkappa+endfdata(i)%qcapiso*factor1
    if (.not.endfdata(i)%lcapisoxs2) then
      endfdata(i)%capkappa=endfdata(i)%capkappa+endfdata(i)%qcapiso2*factor1
    endif
  endif
!
  write(11,*)
  write(11,'(".....")')
  write(11,'("No =",i5,2x,i6,2x,i8,2x,a10)')
  i,endfdata(i)%mat,endfdata(i)%nuclid,endfdata(i)%nuclaid
  write(11,'(".....")')
  write(11,'(3x,"C-kappa =",1pe13.5," eV")') endfdata(i)%capkappa
  write(11,'(3x,"C-kappa0 =",1pe13.5," eV")') endfdata(i)%capkappa0

```

```

        write(11,'(3x,"C-kappa1  =",1pe13.5," eV")') endfdata(i)%capkappa-endfdata(i)%capkappa0
        write(11,*)
        write(11,'(3x,"MT102      =",1pe13.5," eV",0pf9.2," %")') endfdata(i)%qmt102,factor1*100.0
        write(11,'(3x,"MT107      =",1pe13.5," eV",0pf9.2," %")') endfdata(i)%qmt107,factor2*100.0
        write(11,'(3x,"1ST DECAY =",13,1pe13.5," sec",1pe13.5," eV")')
endfdata(i)%lcapisoxs,endfdata(i)%halflife,endfdata(i)%qcapiso
        write(11,'(3x,"2nd DECAY =",13,1pe13.5," sec",1pe13.5," eV")')
endfdata(i)%lcapisoxs2,endfdata(i)%halflife2,endfdata(i)%qcapiso2
!
enddo
!
! [Print out atomic mass and decay constant]
-----
write(11,*)
write(11,*)
write(11,'(@Summary of endf/b decay data")')
write(11,'(-----")')
write(11,*)
write(11,'(3x,"The number of nuclides =",i5)') numdcy
write(11,*)
write(11,'(8x,"no",7x,"mat",8x,"id",7x,"nuclide",8x,"half life",9x,"Q-
value",9x,"Nutrino")')
write(11,'(5x,95("."))')
do i=1,numdcy
    write(11,'(3i10,5x,a10,1p3e16.5)') i,dcydata(i)%mat,dcydata(i)%nuclid, &
                                         dcydata(i)%nuclaid,dcydata(i)%halflife,           &
                                         dcydata(i)%evqvalue,dcydata(i)%evnutrino
enddo
!
close(11)
!
Write 'CapKappa.dat'
write(12,'(I5)') numnuc
do i=1,numnuc
    write(12,'(i5,i8,i10,5x,a10,1p2e14.5)') i,endfdata(i)%mat,endfdata(i)%nuclid, &
                                                 endfdata(i)%nuclaid,endfdata(i)%capkappa0,endfdata(i)%capkappa-endfdata(i)%capkappa0
enddo
write(12,'("%END")')
close(12)
!
return
end

```



APPENDIX B. RESULT OF CAPKAPPA WITH ENDF/B-7.0

393						
1	125	10010	1-H - 1	2.22463E+06	0.00000E+00	
2	128	10020	1-H - 2	6.25740E+06	0.00000E+00	
3	131	10030	1-H - 3	0.00000E+00	0.00000E+00	
4	225	20030	2-He- 3	2.05778E+07	0.00000E+00	
5	228	20040	2-He- 4	0.00000E+00	0.00000E+00	
6	325	30060	3-Li- 6	7.25060E+06	0.00000E+00	
7	328	30070	3-Li- 7	2.03280E+06	0.00000E+00	
8	419	40070	4-Be- 7	0.00000E+00	0.00000E+00	
9	425	40090	4-Be- 9	4.35992E+05	0.00000E+00	
10	525	50100	5-B - 10	2.78952E+06	0.00000E+00	
11	528	50110	5-B - 11	3.25192E+06	6.29767E+06	
12	600	60000	6-C - 0	2.26078E+06	0.00000E+00	
13	725	70140	7-N - 14	2.03668E+06	0.00000E+00	
14	728	70150	7-N - 15	8.83950E+05	2.57151E+06	
15	825	80160	8-O - 16	2.48605E+04	0.00000E+00	
16	828	80170	8-O - 17	1.86299E+06	0.00000E+00	
17	925	90190	9-F - 19	1.59091E+06	9.91790E+05	
18	1122	110220	11-Na- 22	1.24200E+07	0.00000E+00	
19	1125	110230	11-Na- 23	6.95949E+06	4.67727E+06	
20	1225	120240	12-Mg- 24	5.46226E+06	0.00000E+00	
21	1228	120250	12-Mg- 25	8.65232E+06	0.00000E+00	
22	1231	120260	12-Mg- 26	6.33474E+06	1.56759E+06	
23	1325	130270	13-Al- 27	7.64022E+06	2.99298E+06	
24	1425	140280	14-Si- 28	7.94852E+06	0.00000E+00	
25	1428	140290	14-Si- 29	9.11399E+06	0.00000E+00	
26	1431	140300	14-Si- 30	6.59200E+06	5.96118E+05	
27	1525	150310	15-P - 31	7.68417E+06	0.00000E+00	
28	1625	160320	16-S - 32	5.83168E+06	0.00000E+00	
29	1628	160330	16-S - 33	4.60946E+06	0.00000E+00	
30	1631	160340	16-S - 34	6.63065E+06	0.00000E+00	
31	1637	160360	16-S - 36	4.31399E+06	3.73234E+06	
32	1725	170350	17-Cl- 35	8.57977E+06	0.00000E+00	
33	1731	170370	17-Cl- 37	6.10783E+06	2.99354E+06	
34	1825	180360	18-Ar- 36	8.26951E+06	0.00000E+00	
35	1831	180380	18-Ar- 38	6.42151E+06	0.00000E+00	
36	1837	180400	18-Ar- 40	6.09939E+06	1.74774E+06	
37	1925	190390	19-K - 39	7.38254E+06	0.00000E+00	
38	1928	190400	19-K - 40	9.84713E+06	0.00000E+00	
39	1931	190410	19-K - 41	7.53499E+06	1.70935E+06	
40	2025	200400	20-Ca- 40	6.70249E+06	0.00000E+00	
41	2031	200420	20-Ca- 42	7.84190E+06	0.00000E+00	
42	2034	200430	20-Ca- 43	1.11320E+07	0.00000E+00	
43	2037	200440	20-Ca- 44	7.41477E+06	0.00000E+00	
44	2043	200460	20-Ca- 46	7.27610E+06	1.67300E+06	
45	2049	200480	20-Ca- 48	5.14663E+06	4.85273E+06	
46	2125	210450	21-Sc- 45	8.76069E+06	0.00000E+00	
47	2225	220460	22-Ti- 46	8.83301E+06	0.00000E+00	
48	2228	220470	22-Ti- 47	1.15707E+07	0.00000E+00	
49	2231	220480	22-Ti- 48	8.14240E+06	0.00000E+00	
50	2234	220490	22-Ti- 49	1.09394E+07	0.00000E+00	
51	2237	220500	22-Ti- 50	6.37239E+06	1.23697E+06	
52	2300	230000	23-V - 0	7.31130E+06	0.00000E+00	
53	2425	240500	24-Cr- 50	9.26170E+06	0.00000E+00	
54	2431	240520	24-Cr- 52	7.93923E+06	0.00000E+00	
55	2434	240530	24-Cr- 53	9.71909E+06	0.00000E+00	
56	2437	240540	24-Cr- 54	6.24635E+06	1.10167E+06	
57	2525	250550	25-Mn- 55	7.27055E+06	2.52023E+06	
58	2625	260540	26-Fe- 54	9.29800E+06	0.00000E+00	
59	2631	260560	26-Fe- 56	7.64609E+06	0.00000E+00	
60	2634	260570	26-Fe- 57	1.00445E+07	0.00000E+00	
61	2637	260580	26-Fe- 58	6.58096E+06	0.00000E+00	
62	2722	270580	27-Co- 58	1.04500E+07	0.00000E+00	
63	2723	270581	27-Co- 58M	1.04500E+07	0.00000E+00	
64	2725	270590	27-Co- 59	7.49000E+06	0.00000E+00	
65	2825	280580	28-Ni- 58	8.95682E+06	0.00000E+00	
66	2828	280590	28-Ni- 59	1.03302E+07	0.00000E+00	

67	2831	280600	28-Ni-	60	7.82005E+06	0.00000E+00
68	2834	280610	28-Ni-	61	1.05973E+07	0.00000E+00
69	2837	280620	28-Ni-	62	6.83791E+06	0.00000E+00
70	2843	280640	28-Ni-	64	6.09806E+06	1.18577E+06
71	2925	290630	29-Cu-	63	7.91602E+06	3.10165E+05
72	2931	290650	29-Cu-	65	7.06599E+06	1.16438E+06
73	3000	300000	30-Zn-	0	1.01981E+07	0.00000E+00
74	3125	310690	31-Ga-	69	7.65439E+06	6.51674E+05
75	3131	310710	31-Ga-	71	6.52120E+06	3.20491E+06
76	3225	320700	32-Ge-	70	7.41589E+06	0.00000E+00
77	3231	320720	32-Ge-	72	6.78289E+06	0.00000E+00
78	3234	320730	32-Ge-	73	1.01962E+07	0.00000E+00
79	3237	320740	32-Ge-	74	6.50522E+06	4.55472E+05
80	3243	320760	32-Ge-	76	6.07257E+06	1.95455E+06
81	3322	330740	33-As-	74	1.02430E+07	0.00000E+00
82	3325	330750	33-As-	75	7.32900E+06	1.48748E+06
83	3425	340740	34-Se-	74	8.02769E+06	0.00000E+00
84	3431	340760	34-Se-	76	7.41839E+06	0.00000E+00
85	3434	340770	34-Se-	77	1.04970E+07	0.00000E+00
86	3437	340780	34-Se-	78	6.96059E+06	0.00000E+00
87	3440	340790	34-Se-	79	9.91209E+06	0.00000E+00
88	3443	340800	34-Se-	80	6.70109E+06	6.19062E+05
89	3449	340820	34-Se-	82	5.89539E+06	3.33030E+05
90	3525	350790	35-Br-	79	7.89239E+06	8.00984E+05
91	3531	350810	35-Br-	81	7.59342E+06	2.77642E+06
92	3625	360780	36-Kr-	78	8.36039E+06	2.45386E+06
93	3631	360800	36-Kr-	80	7.88139E+06	0.00000E+00
94	3637	360820	36-Kr-	82	7.46509E+06	0.00000E+00
95	3640	360830	36-Kr-	83	1.05200E+07	0.00000E+00
96	3643	360840	36-Kr-	84	7.11139E+06	0.00000E+00
97	3646	360850	36-Kr-	85	9.85600E+06	0.00000E+00
98	3649	360860	36-Kr-	86	5.51539E+06	2.10399E+06
99	3725	370850	37-Rb-	85	8.65029E+06	0.00000E+00
100	3728	370860	37-Rb-	86	9.91900E+06	0.00000E+00
101	3731	370870	37-Rb-	87	6.07769E+06	2.72843E+06
102	3825	380840	38-Sr-	84	8.53000E+06	0.00000E+00
103	3831	380860	38-Sr-	86	8.42819E+06	0.00000E+00
104	3834	380870	38-Sr-	87	1.11130E+07	0.00000E+00
105	3837	380880	38-Sr-	88	6.36700E+06	0.00000E+00
106	3840	380890	38-Sr-	89	7.80240E+06	0.00000E+00
107	3843	380900	38-Sr-	90	5.80269E+06	1.38962E+06
108	3925	390890	39-Y-	89	6.85700E+06	9.33817E+05
109	3928	390900	39-Y-	90	7.92900E+06	0.00000E+00
110	3931	390910	39-Y-	91	6.54389E+06	1.70020E+06
111	4025	400900	40-Zr-	90	7.19400E+06	0.00000E+00
112	4028	400910	40-Zr-	91	8.63509E+06	0.00000E+00
113	4031	400920	40-Zr-	92	6.73199E+06	0.00000E+00
114	4034	400930	40-Zr-	93	8.21859E+06	0.00000E+00
115	4037	400940	40-Zr-	94	6.47089E+06	0.00000E+00
116	4040	400950	40-Zr-	95	7.85269E+06	0.00000E+00
117	4043	400960	40-Zr-	96	5.58089E+06	1.13274E+06
118	4125	410930	41-Nb-	93	7.21400E+06	0.00000E+00
119	4128	410940	41-Nb-	94	8.49079E+06	0.00000E+00
120	4131	410950	41-Nb-	95	6.89289E+06	2.69141E+06
121	4225	420920	42-Mo-	92	8.06739E+06	0.00000E+00
122	4231	420940	42-Mo-	94	7.37119E+06	0.00000E+00
123	4234	420950	42-Mo-	95	9.15400E+06	0.00000E+00
124	4237	420960	42-Mo-	96	6.82109E+06	0.00000E+00
125	4240	420970	42-Mo-	97	8.64229E+06	0.00000E+00
126	4243	420980	42-Mo-	98	5.92559E+06	5.38967E+05
127	4246	420990	42-Mo-	99	8.29089E+06	0.00000E+00
128	4249	421000	42-Mo-100		5.39820E+06	2.78410E+06
129	4325	430990	43-Tc-	99	6.76400E+06	1.39662E+06
130	4425	440960	44-Ru-	96	8.05123E+06	2.10831E+06
131	4431	440980	44-Ru-	98	7.46519E+06	0.00000E+00
132	4434	440990	44-Ru-	99	9.67320E+06	0.00000E+00
133	4437	441000	44-Ru-100		6.80139E+06	0.00000E+00
134	4440	441010	44-Ru-101		9.21900E+06	0.00000E+00
135	4443	441020	44-Ru-102		6.23240E+06	0.00000E+00
136	4446	441030	44-Ru-103		8.90390E+06	0.00000E+00
137	4449	441040	44-Ru-104		5.91010E+06	1.38404E+06



138	4452	441050	44-Ru-105	8.46520E+06	0.00000E+00
139	4455	441060	44-Ru-106	5.44839E+06	2.18731E+06
140	4525	451030	45-Rh-103	6.99900E+06	9.97235E+05
141	4531	451050	45-Rh-105	6.58730E+06	1.61922E+06
142	4625	461020	46-Pd-102	7.62438E+06	0.00000E+00
143	4631	461040	46-Pd-104	7.09438E+06	0.00000E+00
144	4634	461050	46-Pd-105	9.56200E+06	0.00000E+00
145	4637	461060	46-Pd-106	6.53838E+06	0.00000E+00
146	4640	461070	46-Pd-107	9.22339E+06	0.00000E+00
147	4643	461080	46-Pd-108	6.15338E+06	3.61416E+05
148	4649	461100	46-Pd-110	5.75638E+06	8.80416E+05
149	4725	471070	47-Ag-107	7.26969E+06	6.25281E+05
150	4731	471090	47-Ag-109	6.80900E+06	1.21704E+06
151	4735	471101	47-Ag-110M	8.84139E+06	3.96220E+05
152	4737	471110	47-Ag-111	6.47900E+06	1.99630E+06
153	4825	481060	48-Cd-106	7.92739E+06	1.91404E+06
154	4831	481080	48-Cd-108	7.33000E+06	0.00000E+00
155	4837	481100	48-Cd-110	6.97680E+06	0.00000E+00
156	4840	481110	48-Cd-111	9.39529E+06	0.00000E+00
157	4843	481120	48-Cd-112	6.53980E+06	0.00000E+00
158	4846	481130	48-Cd-113	9.04270E+06	0.00000E+00
159	4849	481140	48-Cd-114	6.14800E+06	5.11244E+05
160	4853	481151	48-Cd-115M	8.88100E+06	2.81336E+06
161	4855	481160	48-Cd-116	5.76500E+06	2.52190E+06
162	4925	491130	49-In-113	7.27539E+06	7.76363E+05
163	4931	491150	49-In-115	6.78339E+06	1.38473E+06
164	5025	501120	50-Sn-112	7.74539E+06	0.00000E+00
165	5028	501130	50-Sn-113	1.02990E+07	0.00000E+00
166	5031	501140	50-Sn-114	7.54659E+06	0.00000E+00
167	5034	501150	50-Sn-115	9.56239E+06	0.00000E+00
168	5037	501160	50-Sn-116	6.94419E+06	0.00000E+00
169	5040	501170	50-Sn-117	9.32619E+06	0.00000E+00
170	5043	501180	50-Sn-118	6.48449E+06	0.00000E+00
171	5046	501190	50-Sn-119	9.10659E+06	0.00000E+00
172	5049	501200	50-Sn-120	6.17139E+06	1.15600E+05
173	5055	501220	50-Sn-122	5.94639E+06	0.00000E+00
174	5058	501230	50-Sn-123	8.49039E+06	0.00000E+00
175	5061	501240	50-Sn-124	5.73339E+06	0.00000E+00
176	5064	501250	50-Sn-125	8.19300E+06	0.00000E+00
177	5067	501260	50-Sn-126	5.64739E+06	9.82723E+05
178	5125	511210	51-Sb-121	6.80710E+06	1.00655E+06
179	5131	511230	51-Sb-123	6.46720E+06	0.00000E+00
180	5134	511240	51-Sb-124	8.71009E+06	0.00000E+00
181	5137	511250	51-Sb-125	6.22139E+06	0.00000E+00
182	5140	511260	51-Sb-126	8.38200E+06	1.21215E+06
183	5225	521200	52-Te-120	7.17539E+06	0.00000E+00
184	5231	521220	52-Te-122	6.93343E+06	0.00000E+00
185	5234	521230	52-Te-123	9.42542E+06	0.00000E+00
186	5237	521240	52-Te-124	6.57143E+06	0.00000E+00
187	5240	521250	52-Te-125	9.11839E+06	0.00000E+00
188	5243	521260	52-Te-126	6.29039E+06	2.29428E+05
189	5247	521271	52-Te-127M	8.86699E+06	0.00000E+00
190	5249	521280	52-Te-128	6.08609E+06	6.03236E+05
191	5253	521291	52-Te-129M	8.51789E+06	0.00000E+00
192	5255	521300	52-Te-130	5.92970E+06	1.13027E+06
193	5261	521320	52-Te-132	5.82100E+06	2.89196E+06
194	5325	531270	53-I -127	6.82540E+06	8.14748E+05
195	5331	531290	53-I -129	6.46339E+06	2.41478E+06
196	5334	531300	53-I -130	8.58300E+06	0.00000E+00
197	5337	531310	53-I -131	6.32639E+06	2.74450E+06
198	5349	531350	53-I -135	3.80030E+06	4.32002E+06
199	5422	541230	54-Xe-123	1.04720E+07	0.00000E+00
200	5425	541240	54-Xe-124	7.60360E+06	1.32379E+06
201	5431	541260	54-Xe-126	7.22539E+06	0.00000E+00
202	5437	541280	54-Xe-128	6.90769E+06	0.00000E+00
203	5440	541290	54-Xe-129	9.25509E+06	0.00000E+00
204	5443	541300	54-Xe-130	6.60560E+06	0.00000E+00
205	5446	541310	54-Xe-131	8.93500E+06	0.00000E+00
206	5449	541320	54-Xe-132	6.43830E+06	1.82401E+05
207	5452	541330	54-Xe-133	8.53439E+06	0.00000E+00
208	5455	541340	54-Xe-134	6.45230E+06	5.63861E+05

209	5458	541350	54-Xe-135	7.99039E+06	0.00000E+00
210	5461	541360	54-Xe-136	4.02480E+06	1.88373E+06
211	5525	551330	55-Cs-133	6.89100E+06	0.00000E+00
212	5528	551340	55-Cs-134	8.82739E+06	0.00000E+00
213	5531	551350	55-Cs-135	6.76439E+06	0.00000E+00
214	5534	551360	55-Cs-136	8.27339E+06	0.00000E+00
215	5537	551370	55-Cs-137	4.28139E+06	3.60061E+06
216	5625	561300	56-Ba-130	7.49439E+06	0.00000E+00
217	5631	561320	56-Ba-132	7.18739E+06	0.00000E+00
218	5634	561330	56-Ba-133	9.46800E+06	0.00000E+00
219	5637	561340	56-Ba-134	6.97339E+06	0.00000E+00
220	5640	561350	56-Ba-135	9.10739E+06	0.00000E+00
221	5643	561360	56-Ba-136	6.89839E+06	0.00000E+00
222	5646	561370	56-Ba-137	8.61139E+06	0.00000E+00
223	5649	561380	56-Ba-138	4.72340E+06	9.46645E+05
224	5655	561400	56-Ba-140	4.82520E+06	2.81535E+06
225	5725	571380	57-La-138	8.77839E+06	0.00000E+00
226	5728	571390	57-La-139	5.16030E+06	2.87722E+06
227	5731	571400	57-La-140	6.68800E+06	9.88859E+05
228	5825	581360	58-Ce-136	7.48100E+06	6.16157E+05
229	5831	581380	58-Ce-138	7.45500E+06	0.00000E+00
230	5834	581390	58-Ce-139	9.20100E+06	0.00000E+00
231	5837	581400	58-Ce-140	5.42840E+06	0.00000E+00
232	5840	581410	58-Ce-141	7.16860E+06	0.00000E+00
233	5843	581420	58-Ce-142	5.14443E+06	7.23480E+05
234	5846	581430	58-Ce-143	6.89600E+06	0.00000E+00
235	5849	581440	58-Ce-144	4.76039E+06	7.23827E+05
236	5925	591410	59-Pr-141	5.84200E+06	8.67174E+05
237	5928	591420	59-Pr-142	7.35200E+06	0.00000E+00
238	5931	591430	59-Pr-143	5.75639E+06	1.23888E+06
239	6025	601420	60-Nd-142	6.12300E+06	0.00000E+00
240	6028	601430	60-Nd-143	7.81600E+06	0.00000E+00
241	6031	601440	60-Nd-144	5.75600E+06	0.00000E+00
242	6034	601450	60-Nd-145	7.56500E+06	0.00000E+00
243	6037	601460	60-Nd-146	5.29100E+06	0.00000E+00
244	6040	601470	60-Nd-147	7.33300E+06	0.00000E+00
245	6043	601480	60-Nd-148	5.03800E+06	0.00000E+00
246	6049	601500	60-Nd-150	5.33400E+06	6.26725E+05
247	6149	611470	61-Pm-147	5.90139E+06	1.30180E+06
248	6152	611480	61-Pm-148	7.26439E+06	0.00000E+00
249	6153	611481	61-Pm-148M	7.40800E+06	0.00000E+00
250	6155	611490	61-Pm-149	5.55839E+06	2.18716E+06
251	6161	611510	61-Pm-151	5.94000E+06	0.00000E+00
252	6225	621440	62-Sm-144	6.75700E+06	0.00000E+00
253	6234	621470	62-Sm-147	8.14200E+06	0.00000E+00
254	6237	621480	62-Sm-148	5.87100E+06	0.00000E+00
255	6240	621490	62-Sm-149	7.98500E+06	0.00000E+00
256	6243	621500	62-Sm-150	5.59600E+06	0.00000E+00
257	6246	621510	62-Sm-151	8.25800E+06	0.00000E+00
258	6249	621520	62-Sm-152	5.86700E+06	3.31489E+05
259	6252	621530	62-Sm-153	7.96700E+06	0.00000E+00
260	6255	621540	62-Sm-154	5.80700E+06	6.66972E+05
261	6325	631510	63-Eu-151	6.30790E+06	0.00000E+00
262	6328	631520	63-Eu-152	8.55039E+06	0.00000E+00
263	6331	631530	63-Eu-153	6.44220E+06	0.00000E+00
264	6334	631540	63-Eu-154	8.15220E+06	0.00000E+00
265	6337	631550	63-Eu-155	6.33860E+06	0.00000E+00
266	6340	631560	63-Eu-156	7.45339E+06	6.57397E+05
267	6343	631570	63-Eu-157	5.81500E+06	0.00000E+00
268	6425	641520	64-Gd-152	6.24700E+06	0.00000E+00
269	6428	641530	64-Gd-153	8.89400E+06	0.00000E+00
270	6431	641540	64-Gd-154	6.43500E+06	0.00000E+00
271	6434	641550	64-Gd-155	8.53600E+06	0.00000E+00
272	6437	641560	64-Gd-156	6.36000E+06	0.00000E+00
273	6440	641570	64-Gd-157	7.93700E+06	0.00000E+00
274	6443	641580	64-Gd-158	5.94300E+06	3.65779E+05
275	6449	641600	64-Gd-160	5.63500E+06	9.81466E+05
276	6525	651590	65-Tb-159	6.37539E+06	0.00000E+00
277	6528	651600	65-Tb-160	7.69700E+06	0.00000E+00
278	6625	661560	66-Dy-156	6.96900E+06	3.65435E+05
279	6631	661580	66-Dy-158	6.83100E+06	0.00000E+00



280	6637	661600	66-Dy-160	6.45400E+06	0.00000E+00
281	6640	661610	66-Dy-161	8.19600E+06	0.00000E+00
282	6643	661620	66-Dy-162	6.27100E+06	0.00000E+00
283	6646	661630	66-Dy-163	7.65800E+06	0.00000E+00
284	6649	661640	66-Dy-164	5.71500E+06	4.73591E+05
285	6725	671650	67-Ho-165	6.24240E+06	7.23995E+05
286	6729	671661	67-Ho-166M	7.28999E+06	2.07801E+05
287	6825	681620	68-Er-162	6.90470E+06	4.84080E+04
288	6831	681640	68-Er-164	6.64970E+06	6.48362E+05
289	6837	681660	68-Er-166	6.43670E+06	0.00000E+00
290	6840	681670	68-Er-167	7.77070E+06	0.00000E+00
291	6843	681680	68-Er-168	6.00370E+06	0.00000E+00
292	6849	681700	68-Er-170	5.68170E+06	7.91883E+05
293	7125	711750	71-Lu-175	6.19140E+06	0.00000E+00
294	7128	711760	71-Lu-176	7.07200E+06	0.00000E+00
295	7225	721740	72-Hf-174	6.82420E+06	0.00000E+00
296	7231	721760	72-Hf-176	6.40455E+06	0.00000E+00
297	7234	721770	72-Hf-177	7.66986E+06	0.00000E+00
298	7237	721780	72-Hf-178	6.11573E+06	0.00000E+00
299	7240	721790	72-Hf-179	7.18000E+06	0.00000E+00
300	7243	721800	72-Hf-180	5.65402E+06	0.00000E+00
301	7328	731810	73-Ta-181	6.07000E+06	0.00000E+00
302	7331	731820	73-Ta-182	6.93000E+06	6.32749E+05
303	7431	741820	74-W -182	6.19074E+06	0.00000E+00
304	7434	741830	74-W -183	7.41180E+06	0.00000E+00
305	7437	741840	74-W -184	5.75378E+06	0.00000E+00
306	7443	741860	74-W -186	5.46675E+06	7.55940E+05
307	7525	751850	75-Re-185	6.17800E+06	3.56694E+05
308	7531	751870	75-Re-187	5.87300E+06	8.42549E+05
309	7725	771910	77-Ir-191	6.19800E+06	0.00000E+00
310	7731	771930	77-Ir-193	6.06700E+06	9.01302E+05
311	7925	791970	79-Au-197	6.51238E+06	7.30748E+05
312	8025	801960	80-Hg-196	6.98100E+06	4.81649E+05
313	8031	801980	80-Hg-198	6.64900E+06	0.00000E+00
314	8034	801990	80-Hg-199	8.02900E+06	0.00000E+00
315	8037	802000	80-Hg-200	6.22500E+06	0.00000E+00
316	8040	802010	80-Hg-201	7.75600E+06	0.00000E+00
317	8043	802020	80-Hg-202	5.99300E+06	0.00000E+00
318	8049	802040	80-Hg-204	5.66800E+06	5.43349E+05
319	8225	822040	82-Pb-204	6.73151E+06	0.00000E+00
320	8231	822060	82-Pb-206	6.73779E+06	0.00000E+00
321	8234	822070	82-Pb-207	7.36782E+06	0.00000E+00
322	8237	822080	82-Pb-208	3.93738E+06	1.97500E+05
323	8325	832090	83-Bi-209	4.60000E+06	3.89006E+05
324	8825	882230	88-Ra-223	6.50069E+06	6.63185E+06
325	8828	882240	88-Ra-224	4.88869E+06	0.00000E+00
326	8831	882250	88-Ra-225	6.38869E+06	0.00000E+00
327	8834	882260	88-Ra-226	4.56469E+06	5.24788E+05
328	8925	892250	89-Ac-225	5.38369E+06	6.45150E+06
329	8928	892260	89-Ac-226	6.52769E+06	0.00000E+00
330	8931	892270	89-Ac-227	5.03569E+06	0.00000E+00
331	9025	902270	90-Th-227	7.12869E+06	0.00000E+00
332	9028	902280	90-Th-228	5.24879E+06	0.00000E+00
333	9031	902290	90-Th-229	6.78969E+06	0.00000E+00
334	9034	902300	90-Th-230	5.12050E+06	0.00000E+00
335	9040	902320	90-Th-232	4.78600E+06	4.26372E+05
336	9043	902330	90-Th-233	6.19199E+06	0.00000E+00
337	9046	902340	90-Th-234	4.53369E+06	4.89034E+05
338	9131	912310	91-Pa-231	5.55300E+06	1.09520E+06
339	9134	912320	91-Pa-232	6.51669E+06	0.00000E+00
340	9137	912330	91-Pa-233	5.21900E+06	0.00000E+00
341	9219	922320	92-U -232	5.74340E+06	0.00000E+00
342	9222	922330	92-U -233	6.84420E+06	0.00000E+00
343	9225	922340	92-U -234	5.29780E+06	0.00000E+00
344	9228	922350	92-U -235	6.54520E+06	0.00000E+00
345	9231	922360	92-U -236	5.12590E+06	0.00000E+00
346	9234	922370	92-U -237	6.15380E+06	0.00000E+00
347	9237	922380	92-U -238	4.80650E+06	9.02490E+05
348	9240	922390	92-U -239	5.93080E+06	9.08942E+04
349	9243	922400	92-U -240	4.58410E+06	4.44994E+05
350	9246	922410	92-U -241	5.68340E+06	1.14805E+06

351	9340	932350	93-Np-235	5.73943E+06	0.00000E+00
352	9343	932360	93-Np-236	6.57335E+06	0.00000E+00
353	9346	932370	93-Np-237	5.48200E+06	8.39466E+05
354	9349	932380	93-Np-238	6.21636E+06	4.43291E+05
355	9352	932390	93-Np-239	5.16810E+06	0.00000E+00
356	9428	942360	94-Pu-236	5.87702E+06	0.00000E+00
357	9431	942370	94-Pu-237	6.99800E+06	0.00000E+00
358	9434	942380	94-Pu-238	4.80600E+06	0.00000E+00
359	9437	942390	94-Pu-239	6.53370E+06	0.00000E+00
360	9440	942400	94-Pu-240	5.24100E+06	0.00000E+00
361	9443	942410	94-Pu-241	6.30080E+06	0.00000E+00
362	9446	942420	94-Pu-242	5.07100E+06	1.93152E+05
363	9449	942430	94-Pu-243	6.02000E+06	0.00000E+00
364	9452	942440	94-Pu-244	4.72000E+06	1.05539E+06
365	9458	942460	94-Pu-246	5.96964E+06	7.11590E+05
366	9543	952410	95-Am-241	5.53910E+06	0.00000E+00
367	9546	952420	95-Am-242	6.36710E+06	0.00000E+00
368	9547	952421	95-Am-242M	6.37000E+06	0.00000E+00
369	9549	952430	95-Am-243	5.36290E+06	1.14999E+06
370	9552	952440	95-Am-244	6.05299E+06	3.23778E+05
371	9553	952441	95-Am-244M	6.14099E+06	0.00000E+00
372	9628	962410	96-Cm-241	6.96800E+06	0.00000E+00
373	9631	962420	96-Cm-242	5.70300E+06	0.00000E+00
374	9634	962430	96-Cm-243	6.79950E+06	0.00000E+00
375	9637	962440	96-Cm-244	5.52243E+06	0.00000E+00
376	9640	962450	96-Cm-245	6.45000E+06	0.00000E+00
377	9643	962460	96-Cm-246	5.16000E+06	0.00000E+00
378	9646	962470	96-Cm-247	6.21143E+06	0.00000E+00
379	9649	962480	96-Cm-248	4.71300E+06	3.00579E+05
380	9652	962490	96-Cm-249	5.83243E+06	0.00000E+00
381	9655	962500	96-Cm-250	4.40643E+06	5.63250E+05
382	9752	972490	97-Bk-249	4.97000E+06	1.19525E+06
383	9755	972500	97-Bk-250	8.64999E+05	0.00000E+00
384	9852	982490	98-Cf-249	6.62300E+06	0.00000E+00
385	9855	982500	98-Cf-250	5.11000E+06	0.00000E+00
386	9858	982510	98-Cf-251	6.17000E+06	0.00000E+00
387	9861	982520	98-Cf-252	4.79000E+06	0.00000E+00
388	9864	982530	98-Cf-253	5.98000E+06	0.00000E+00
389	9867	982540	98-Cf-254	4.44999E+06	0.00000E+00
390	9913	992530	99-Es-253	5.09200E+06	0.00000E+00
391	9914	992540	99-Es-254	5.98269E+06	0.00000E+00
392	9915	992550	99-Es-255	4.90169E+06	0.00000E+00
393	9936	1002550	00-Fm-255	6.38669E+06	0.00000E+00

%END



APPENDIX C. RESULT OF CAPKAPPA WITH ENDF/B-7.1

423					
1	125	10010	1-H - 1	2.22463E+06	0.00000E+00
2	128	10020	1-H - 2	6.25740E+06	0.00000E+00
3	131	10030	1-H - 3	0.00000E+00	0.00000E+00
4	225	20030	2-He- 3	2.05778E+07	0.00000E+00
5	228	20040	2-He- 4	0.00000E+00	0.00000E+00
6	325	30060	3-Li- 6	7.25060E+06	0.00000E+00
7	328	30070	3-Li- 7	2.03280E+06	0.00000E+00
8	419	40070	4-Be- 7	0.00000E+00	0.00000E+00
9	425	40090	4-Be- 9	4.35992E+05	0.00000E+00
10	525	50100	5-B - 10	2.78952E+06	0.00000E+00
11	528	50110	5-B - 11	3.25192E+06	6.29855E+06
12	600	60000	6-C - 0	2.26050E+06	0.00000E+00
13	725	70140	7-N - 14	2.03668E+06	0.00000E+00
14	728	70150	7-N - 15	8.83950E+05	2.57198E+06
15	825	80160	8-O - 16	2.48675E+04	0.00000E+00
16	828	80170	8-O - 17	1.86299E+06	0.00000E+00
17	925	90190	9-F - 19	1.59091E+06	9.91956E+05
18	1122	110220	11-Na- 22	1.24200E+07	0.00000E+00
19	1125	110230	11-Na- 23	6.95949E+06	4.67700E+06
20	1225	120240	12-Mg- 24	5.46226E+06	0.00000E+00
21	1228	120250	12-Mg- 25	8.65232E+06	0.00000E+00
22	1231	120260	12-Mg- 26	6.33474E+06	1.56788E+06
23	1325	130270	13-Al- 27	7.64022E+06	2.98777E+06
24	1425	140280	14-Si- 28	7.94852E+06	0.00000E+00
25	1428	140290	14-Si- 29	9.11399E+06	0.00000E+00
26	1431	140300	14-Si- 30	6.59200E+06	5.96900E+05
27	1525	150310	15-P - 31	7.68417E+06	0.00000E+00
28	1625	160320	16-S - 32	5.83168E+06	0.00000E+00
29	1628	160330	16-S - 33	4.60946E+06	0.00000E+00
30	1631	160340	16-S - 34	6.63065E+06	0.00000E+00
31	1637	160360	16-S - 36	4.31399E+06	3.73200E+06
32	1725	170350	17-Cl- 35	8.57977E+06	0.00000E+00
33	1731	170370	17-Cl- 37	6.10783E+06	3.02600E+06
34	1825	180360	18-Ar- 36	8.26951E+06	0.00000E+00
35	1831	180380	18-Ar- 38	6.42151E+06	0.00000E+00
36	1837	180400	18-Ar- 40	6.09939E+06	1.74810E+06
37	1925	190390	19-K - 39	7.38254E+06	0.00000E+00
38	1928	190400	19-K - 40	9.84713E+06	0.00000E+00
39	1931	190410	19-K - 41	7.53499E+06	1.70900E+06
40	2025	200400	20-Ca- 40	6.70249E+06	0.00000E+00
41	2031	200420	20-Ca- 42	7.84190E+06	0.00000E+00
42	2034	200430	20-Ca- 43	1.11320E+07	0.00000E+00
43	2037	200440	20-Ca- 44	7.41477E+06	0.00000E+00
44	2043	200460	20-Ca- 46	7.27610E+06	1.61550E+06
45	2049	200480	20-Ca- 48	5.14663E+06	4.86600E+06
46	2125	210450	21-Sc- 45	8.76069E+06	0.00000E+00
47	2225	220460	22-Ti- 46	8.83301E+06	0.00000E+00
48	2228	220470	22-Ti- 47	1.15707E+07	0.00000E+00
49	2231	220480	22-Ti- 48	8.14240E+06	0.00000E+00
50	2234	220490	22-Ti- 49	1.09394E+07	0.00000E+00
51	2237	220500	22-Ti- 50	6.37239E+06	1.23900E+06
52	2325	230500	23-V - 50	1.10512E+07	0.00000E+00
53	2328	230510	23-V - 51	7.31134E+06	2.51400E+06
54	2425	240500	24-Cr- 50	9.26170E+06	0.00000E+00
55	2431	240520	24-Cr- 52	7.93923E+06	0.00000E+00
56	2434	240530	24-Cr- 53	9.71909E+06	0.00000E+00
57	2437	240540	24-Cr- 54	6.24635E+06	1.10200E+06
58	2525	250550	25-Mn- 55	7.27100E+06	2.52100E+06
59	2625	260540	26-Fe- 54	9.29800E+06	0.00000E+00
60	2631	260560	26-Fe- 56	7.64609E+06	0.00000E+00
61	2634	260570	26-Fe- 57	1.00445E+07	0.00000E+00
62	2637	260580	26-Fe- 58	6.58096E+06	0.00000E+00
63	2722	270580	27-Co- 58	1.04540E+07	0.00000E+00
64	2723	270581	27-Co- 58M	1.04500E+07	0.00000E+00
65	2725	270590	27-Co- 59	7.49000E+06	0.00000E+00
66	2825	280580	28-Ni- 58	8.95682E+06	0.00000E+00

67	2828	280590	28-Ni-	59	1.03302E+07	0.00000E+00
68	2831	280600	28-Ni-	60	7.82005E+06	0.00000E+00
69	2834	280610	28-Ni-	61	1.05973E+07	0.00000E+00
70	2837	280620	28-Ni-	62	6.83791E+06	0.00000E+00
71	2843	280640	28-Ni-	64	6.09806E+06	1.18590E+06
72	2925	290630	29-Cu-	63	7.91602E+06	3.13313E+05
73	2931	290650	29-Cu-	65	7.06599E+06	1.16400E+06
74	3025	300640	30-Zn-	64	7.97932E+06	0.00000E+00
75	3028	300650	30-Zn-	65	1.10592E+07	0.00000E+00
76	3031	300660	30-Zn-	66	7.05233E+06	0.00000E+00
77	3034	300670	30-Zn-	67	1.01981E+07	0.00000E+00
78	3037	300680	30-Zn-	68	6.48207E+06	3.21600E+05
79	3043	300700	30-Zn-	70	5.83357E+06	1.35700E+06
80	3125	310690	31-Ga-	69	7.65439E+06	6.51674E+05
81	3131	310710	31-Ga-	71	6.52120E+06	3.23890E+06
82	3225	320700	32-Ge-	70	7.41589E+06	0.00000E+00
83	3231	320720	32-Ge-	72	6.78289E+06	0.00000E+00
84	3234	320730	32-Ge-	73	1.01962E+07	0.00000E+00
85	3237	320740	32-Ge-	74	6.50522E+06	4.55200E+05
86	3243	320760	32-Ge-	76	6.07257E+06	1.95420E+06
87	3322	330740	33-As-	74	1.02430E+07	0.00000E+00
88	3325	330750	33-As-	75	7.32960E+06	1.48800E+06
89	3425	340740	34-Se-	74	8.02769E+06	0.00000E+00
90	3431	340760	34-Se-	76	7.41839E+06	0.00000E+00
91	3434	340770	34-Se-	77	1.04970E+07	0.00000E+00
92	3437	340780	34-Se-	78	6.96059E+06	0.00000E+00
93	3440	340790	34-Se-	79	9.91209E+06	0.00000E+00
94	3443	340800	34-Se-	80	6.70109E+06	6.18900E+05
95	3449	340820	34-Se-	82	5.89539E+06	3.23470E+06
96	3525	350790	35-Br-	79	7.89239E+06	8.00982E+05
97	3531	350810	35-Br-	81	7.59342E+06	2.77680E+06
98	3625	360780	36-Kr-	78	8.33433E+06	2.50100E+06
99	3631	360800	36-Kr-	80	7.88139E+06	0.00000E+00
100	3637	360820	36-Kr-	82	7.46509E+06	0.00000E+00
101	3640	360830	36-Kr-	83	1.05200E+07	0.00000E+00
102	3643	360840	36-Kr-	84	7.11139E+06	0.00000E+00
103	3646	360850	36-Kr-	85	9.85600E+06	0.00000E+00
104	3649	360860	36-Kr-	86	5.51539E+06	2.10400E+06
105	3725	370850	37-Rb-	85	8.65029E+06	0.00000E+00
106	3728	370860	37-Rb-	86	9.91900E+06	0.00000E+00
107	3731	370870	37-Rb-	87	6.07769E+06	2.72900E+06
108	3825	380840	38-Sr-	84	8.53000E+06	0.00000E+00
109	3831	380860	38-Sr-	86	8.42819E+06	0.00000E+00
110	3834	380870	38-Sr-	87	1.11130E+07	0.00000E+00
111	3837	380880	38-Sr-	88	6.36700E+06	0.00000E+00
112	3840	380890	38-Sr-	89	7.80240E+06	0.00000E+00
113	3843	380900	38-Sr-	90	5.80269E+06	1.37430E+06
114	3925	390890	39-Y -	89	6.85700E+06	9.33000E+05
115	3928	390900	39-Y -	90	7.92900E+06	0.00000E+00
116	3931	390910	39-Y -	91	6.54389E+06	1.70200E+06
117	4025	400900	40-Zr-	90	7.19400E+06	0.00000E+00
118	4028	400910	40-Zr-	91	8.63500E+06	0.00000E+00
119	4031	400920	40-Zr-	92	6.73300E+06	0.00000E+00
120	4034	400930	40-Zr-	93	8.22000E+06	0.00000E+00
121	4037	400940	40-Zr-	94	6.46300E+06	0.00000E+00
122	4040	400950	40-Zr-	95	7.85400E+06	0.00000E+00
123	4043	400960	40-Zr-	96	5.57900E+06	1.99530E+06
124	4125	410930	41-Nb-	93	7.21400E+06	0.00000E+00
125	4128	410940	41-Nb-	94	8.49079E+06	0.00000E+00
126	4131	410950	41-Nb-	95	6.89289E+06	2.69140E+06
127	4225	420920	42-Mo-	92	8.06739E+06	0.00000E+00
128	4231	420940	42-Mo-	94	7.37119E+06	0.00000E+00
129	4234	420950	42-Mo-	95	9.15400E+06	0.00000E+00
130	4237	420960	42-Mo-	96	6.82109E+06	0.00000E+00
131	4240	420970	42-Mo-	97	8.64229E+06	0.00000E+00
132	4243	420980	42-Mo-	98	5.92559E+06	5.40900E+05
133	4246	420990	42-Mo-	99	8.29089E+06	0.00000E+00
134	4249	421000	42-Mo-	100	5.39820E+06	2.78410E+06
135	4325	430990	43-Tc-	99	6.76400E+06	1.39400E+06
136	4425	440960	44-Ru-	96	8.05123E+06	2.12183E+06
137	4431	440980	44-Ru-	98	7.46519E+06	0.00000E+00



138	4434	440990	44-Ru- 99	9.67320E+06	0.00000E+00
139	4437	441000	44-Ru-100	6.80139E+06	0.00000E+00
140	4440	441010	44-Ru-101	9.21900E+06	0.00000E+00
141	4443	441020	44-Ru-102	6.23240E+06	0.00000E+00
142	4446	441030	44-Ru-103	8.90390E+06	0.00000E+00
143	4449	441040	44-Ru-104	5.91010E+06	1.38390E+06
144	4452	441050	44-Ru-105	8.46520E+06	0.00000E+00
145	4455	441060	44-Ru-106	5.44839E+06	2.16940E+06
146	4525	451030	45-Rh-103	6.99900E+06	9.97234E+05
147	4531	451050	45-Rh-105	6.58730E+06	1.62200E+06
148	4625	461020	46-Pd-102	7.62438E+06	0.00000E+00
149	4631	461040	46-Pd-104	7.09438E+06	0.00000E+00
150	4634	461050	46-Pd-105	9.56200E+06	0.00000E+00
151	4637	461060	46-Pd-106	6.53838E+06	0.00000E+00
152	4640	461070	46-Pd-107	9.22339E+06	0.00000E+00
153	4643	461080	46-Pd-108	6.15338E+06	3.61500E+05
154	4649	461100	46-Pd-110	5.75638E+06	8.80000E+05
155	4725	471070	47-Ag-107	7.26969E+06	6.25283E+05
156	4731	471090	47-Ag-109	6.80900E+06	1.21704E+06
157	4735	471101	47-Ag-110M	8.84139E+06	4.60228E+05
158	4737	471110	47-Ag-111	6.47900E+06	1.99600E+06
159	4825	481060	48-Cd-106	7.92739E+06	1.90300E+06
160	4831	481080	48-Cd-108	7.33000E+06	0.00000E+00
161	4837	481100	48-Cd-110	6.97680E+06	0.00000E+00
162	4840	481110	48-Cd-111	9.39529E+06	0.00000E+00
163	4843	481120	48-Cd-112	6.53980E+06	0.00000E+00
164	4846	481130	48-Cd-113	9.04270E+06	0.00000E+00
165	4849	481140	48-Cd-114	6.14800E+06	5.09700E+05
166	4853	481151	48-Cd-115M	8.88100E+06	2.80890E+06
167	4855	481160	48-Cd-116	5.76500E+06	2.47540E+06
168	4925	491130	49-In-113	7.27539E+06	7.76363E+05
169	4931	491150	49-In-115	6.78339E+06	1.38700E+06
170	5025	501120	50-Sn-112	7.74539E+06	0.00000E+00
171	5028	501130	50-Sn-113	1.02990E+07	0.00000E+00
172	5031	501140	50-Sn-114	7.54659E+06	0.00000E+00
173	5034	501150	50-Sn-115	9.56239E+06	0.00000E+00
174	5037	501160	50-Sn-116	6.94419E+06	0.00000E+00
175	5040	501170	50-Sn-117	9.32619E+06	0.00000E+00
176	5043	501180	50-Sn-118	6.48449E+06	0.00000E+00
177	5046	501190	50-Sn-119	9.10659E+06	0.00000E+00
178	5049	501200	50-Sn-120	6.17139E+06	1.15800E+05
179	5055	501220	50-Sn-122	5.94639E+06	0.00000E+00
180	5058	501230	50-Sn-123	8.49039E+06	0.00000E+00
181	5061	501240	50-Sn-124	5.73339E+06	0.00000E+00
182	5064	501250	50-Sn-125	8.19300E+06	0.00000E+00
183	5067	501260	50-Sn-126	5.64739E+06	3.27430E+06
184	5125	511210	51-Sb-121	6.80710E+06	1.00886E+06
185	5131	511230	51-Sb-123	6.46720E+06	0.00000E+00
186	5134	511240	51-Sb-124	8.71009E+06	0.00000E+00
187	5137	511250	51-Sb-125	6.22139E+06	0.00000E+00
188	5140	511260	51-Sb-126	8.38200E+06	1.20190E+06
189	5225	521200	52-Te-120	7.17539E+06	0.00000E+00
190	5231	521220	52-Te-122	6.93343E+06	0.00000E+00
191	5234	521230	52-Te-123	9.42542E+06	0.00000E+00
192	5237	521240	52-Te-124	6.57143E+06	0.00000E+00
193	5240	521250	52-Te-125	9.11839E+06	0.00000E+00
194	5243	521260	52-Te-126	6.29039E+06	2.29400E+05
195	5247	521271	52-Te-127M	8.86699E+06	0.00000E+00
196	5249	521280	52-Te-128	6.08609E+06	6.05400E+05
197	5253	521291	52-Te-129M	8.51789E+06	2.89000E+05
198	5255	521300	52-Te-130	5.92970E+06	1.13100E+06
199	5261	521320	52-Te-132	5.82100E+06	2.87290E+06
200	5325	531270	53-I -127	6.82540E+06	8.14748E+05
201	5331	531290	53-I -129	6.46339E+06	2.41480E+06
202	5334	531300	53-I -130	8.58300E+06	0.00000E+00
203	5337	531310	53-I -131	6.32639E+06	2.74450E+06
204	5349	531350	53-I -135	3.80030E+06	4.28600E+06
205	5422	541230	54-Xe-123	1.04829E+07	0.00000E+00
206	5425	541240	54-Xe-124	7.60328E+06	1.34200E+06
207	5431	541260	54-Xe-126	7.22539E+06	0.00000E+00
208	5437	541280	54-Xe-128	6.90769E+06	0.00000E+00

209	5440	541290	54-Xe-129	9.25509E+06	0.00000E+00
210	5443	541300	54-Xe-130	6.60560E+06	0.00000E+00
211	5446	541310	54-Xe-131	8.93500E+06	0.00000E+00
212	5449	541320	54-Xe-132	6.43830E+06	1.82400E+05
213	5452	541330	54-Xe-133	8.53439E+06	0.00000E+00
214	5455	541340	54-Xe-134	6.45230E+06	5.69100E+05
215	5458	541350	54-Xe-135	7.99039E+06	0.00000E+00
216	5461	541360	54-Xe-136	4.02480E+06	1.86600E+06
217	5525	551330	55-Cs-133	6.89100E+06	0.00000E+00
218	5528	551340	55-Cs-134	8.82739E+06	0.00000E+00
219	5531	551350	55-Cs-135	6.76439E+06	0.00000E+00
220	5534	551360	55-Cs-136	8.27339E+06	0.00000E+00
221	5537	551370	55-Cs-137	4.28139E+06	3.60100E+06
222	5625	561300	56-Ba-130	7.49439E+06	0.00000E+00
223	5631	561320	56-Ba-132	7.18739E+06	0.00000E+00
224	5634	561330	56-Ba-133	9.46800E+06	0.00000E+00
225	5637	561340	56-Ba-134	6.97339E+06	0.00000E+00
226	5640	561350	56-Ba-135	9.10739E+06	0.00000E+00
227	5643	561360	56-Ba-136	6.89839E+06	0.00000E+00
228	5646	561370	56-Ba-137	8.61139E+06	0.00000E+00
229	5649	561380	56-Ba-138	4.72340E+06	9.47000E+05
230	5655	561400	56-Ba-140	4.82520E+06	2.80700E+06
231	5725	571380	57-La-138	8.77839E+06	0.00000E+00
232	5728	571390	57-La-139	5.16030E+06	2.85270E+06
233	5731	571400	57-La-140	6.68800E+06	9.89000E+05
234	5825	581360	58-Ce-136	7.48100E+06	6.05000E+05
235	5831	581380	58-Ce-138	7.45500E+06	0.00000E+00
236	5834	581390	58-Ce-139	9.20100E+06	0.00000E+00
237	5837	581400	58-Ce-140	5.42840E+06	0.00000E+00
238	5840	581410	58-Ce-141	7.16860E+06	0.00000E+00
239	5843	581420	58-Ce-142	5.14443E+06	7.24000E+05
240	5846	581430	58-Ce-143	6.89600E+06	0.00000E+00
241	5849	581440	58-Ce-144	4.76039E+06	2.23300E+06
242	5925	591410	59-Pr-141	5.84200E+06	8.67174E+05
243	5928	591420	59-Pr-142	7.35200E+06	0.00000E+00
244	5931	591430	59-Pr-143	5.75639E+06	1.23900E+06
245	6025	601420	60-Nd-142	6.12300E+06	0.00000E+00
246	6028	601430	60-Nd-143	7.81600E+06	0.00000E+00
247	6031	601440	60-Nd-144	5.75600E+06	0.00000E+00
248	6034	601450	60-Nd-145	7.56500E+06	0.00000E+00
249	6037	601460	60-Nd-146	5.29100E+06	0.00000E+00
250	6040	601470	60-Nd-147	7.33300E+06	0.00000E+00
251	6043	601480	60-Nd-148	5.03800E+06	1.20780E+06
252	6049	601500	60-Nd-150	5.33400E+06	2.08650E+06
253	6149	611470	61-Pm-147	5.90139E+06	1.30300E+06
254	6152	611480	61-Pm-148	7.26439E+06	3.79500E+05
255	6153	611481	61-Pm-148M	7.40800E+06	0.00000E+00
256	6155	611490	61-Pm-149	5.55839E+06	2.23000E+06
257	6161	611510	61-Pm-151	5.94000E+06	1.62300E+06
258	6225	621440	62-Sm-144	6.75700E+06	0.00000E+00
259	6234	621470	62-Sm-147	8.14200E+06	0.00000E+00
260	6237	621480	62-Sm-148	5.87100E+06	0.00000E+00
261	6240	621490	62-Sm-149	7.98500E+06	0.00000E+00
262	6243	621500	62-Sm-150	5.59600E+06	0.00000E+00
263	6246	621510	62-Sm-151	8.25800E+06	0.00000E+00
264	6249	621520	62-Sm-152	5.86700E+06	3.31200E+05
265	6252	621530	62-Sm-153	7.96700E+06	0.00000E+00
266	6255	621540	62-Sm-154	5.80700E+06	6.67100E+05
267	6325	631510	63-Eu-151	6.30790E+06	0.00000E+00
268	6328	631520	63-Eu-152	8.55039E+06	0.00000E+00
269	6331	631530	63-Eu-153	6.44220E+06	0.00000E+00
270	6334	631540	63-Eu-154	8.15220E+06	0.00000E+00
271	6337	631550	63-Eu-155	6.33860E+06	0.00000E+00
272	6340	631560	63-Eu-156	7.45339E+06	6.57400E+05
273	6343	631570	63-Eu-157	5.81500E+06	2.16000E+06
274	6425	641520	64-Gd-152	6.24700E+06	0.00000E+00
275	6428	641530	64-Gd-153	8.89400E+06	0.00000E+00
276	6431	641540	64-Gd-154	6.43500E+06	0.00000E+00
277	6434	641550	64-Gd-155	8.53600E+06	0.00000E+00
278	6437	641560	64-Gd-156	6.36000E+06	0.00000E+00
279	6440	641570	64-Gd-157	7.93700E+06	0.00000E+00



280	6443	641580	64-Gd-158	5.94300E+06	3.65700E+05
281	6449	641600	64-Gd-160	5.63500E+06	9.82300E+05
282	6525	651590	65-Tb-159	6.37539E+06	0.00000E+00
283	6528	651600	65-Tb-160	7.69700E+06	0.00000E+00
284	6625	661560	66-Dy-156	6.96900E+06	1.06140E+06
285	6631	661580	66-Dy-158	6.83100E+06	0.00000E+00
286	6637	661600	66-Dy-160	6.45400E+06	0.00000E+00
287	6640	661610	66-Dy-161	8.19600E+06	0.00000E+00
288	6643	661620	66-Dy-162	6.27100E+06	0.00000E+00
289	6646	661630	66-Dy-163	7.65800E+06	0.00000E+00
290	6649	661640	66-Dy-164	5.71500E+06	4.73900E+05
291	6725	671650	67-Ho-165	6.24240E+06	7.25000E+05
292	6729	671661	67-Ho-166M	7.28999E+06	2.07800E+05
293	6825	681620	68-Er-162	6.90470E+06	1.45700E+06
294	6831	681640	68-Er-164	6.64970E+06	1.28780E+06
295	6837	681660	68-Er-166	6.43670E+06	0.00000E+00
296	6840	681670	68-Er-167	7.77070E+06	0.00000E+00
297	6843	681680	68-Er-168	6.00370E+06	0.00000E+00
298	6849	681700	68-Er-170	5.68170E+06	7.92200E+05
299	6922	691680	69-Tm-168	8.03240E+06	0.00000E+00
300	6925	691690	69-Tm-169	6.59300E+06	0.00000E+00
301	6928	691700	69-Tm-170	7.48600E+06	0.00000E+00
302	7125	711750	71-Lu-175	6.19140E+06	0.00000E+00
303	7128	711760	71-Lu-176	7.07200E+06	0.00000E+00
304	7225	721740	72-Hf-174	6.78969E+06	0.00000E+00
305	7231	721760	72-Hf-176	6.38369E+06	0.00000E+00
306	7234	721770	72-Hf-177	7.62669E+06	0.00000E+00
307	7237	721780	72-Hf-178	6.09969E+06	0.00000E+00
308	7240	721790	72-Hf-179	7.38869E+06	0.00000E+00
309	7243	721800	72-Hf-180	5.69569E+06	0.00000E+00
310	7325	731800	73-Ta-180	7.57676E+06	0.00000E+00
311	7328	731810	73-Ta-181	6.06294E+06	0.00000E+00
312	7331	731820	73-Ta-182	6.93000E+06	6.32500E+05
313	7425	741800	74-W -180	6.68100E+06	0.00000E+00
314	7431	741820	74-W -182	6.19100E+06	0.00000E+00
315	7434	741830	74-W -183	7.41100E+06	0.00000E+00
316	7437	741840	74-W -184	5.75300E+06	0.00000E+00
317	7443	741860	74-W -186	5.46700E+06	7.94000E+05
318	7525	751850	75-Re-185	6.17936E+06	3.56600E+05
319	7531	751870	75-Re-187	5.87175E+06	8.42000E+05
320	7725	771910	77-Ir-191	6.19800E+06	0.00000E+00
321	7731	771930	77-Ir-193	6.06700E+06	8.94000E+05
322	7925	791970	79-Au-197	6.51238E+06	7.30300E+05
323	8025	801960	80-Hg-196	6.98100E+06	6.24700E+05
324	8031	801980	80-Hg-198	6.64900E+06	0.00000E+00
325	8034	801990	80-Hg-199	8.02900E+06	0.00000E+00
326	8037	802000	80-Hg-200	6.22500E+06	0.00000E+00
327	8040	802010	80-Hg-201	7.75600E+06	0.00000E+00
328	8043	802020	80-Hg-202	5.99300E+06	0.00000E+00
329	8049	802040	80-Hg-204	5.66800E+06	5.44500E+05
330	8125	812030	81-Tl-203	6.65600E+06	0.00000E+00
331	8131	812050	81-Tl-205	6.50300E+06	5.39400E+05
332	8225	822040	82-Pb-204	6.73151E+06	0.00000E+00
333	8231	822060	82-Pb-206	6.73779E+06	0.00000E+00
334	8234	822070	82-Pb-207	7.36782E+06	0.00000E+00
335	8237	822080	82-Pb-208	3.93738E+06	1.97400E+05
336	8325	832090	83-Bi-209	4.60000E+06	3.89100E+05
337	8825	882230	88-Ra-223	6.50069E+06	6.63200E+06
338	8828	882240	88-Ra-224	4.88869E+06	0.00000E+00
339	8831	882250	88-Ra-225	6.38869E+06	0.00000E+00
340	8834	882260	88-Ra-226	4.56469E+06	5.26200E+05
341	8925	892250	89-Ac-225	5.39932E+06	6.87430E+06
342	8928	892260	89-Ac-226	6.53059E+06	0.00000E+00
343	8931	892270	89-Ac-227	5.02628E+06	1.41190E+06
344	9025	902270	90-Th-227	7.10530E+06	0.00000E+00
345	9028	902280	90-Th-228	5.25699E+06	0.00000E+00
346	9031	902290	90-Th-229	6.79386E+06	0.00000E+00
347	9034	902300	90-Th-230	5.11802E+06	1.83400E+05
348	9037	902310	90-Th-231	6.44029E+06	0.00000E+00
349	9040	902320	90-Th-232	4.78600E+06	4.26100E+05
350	9043	902330	90-Th-233	6.19027E+06	0.00000E+00

351	9046	902340	90-Th-234	4.43025E+06	7.09000E+05
352	9125	912290	91-Pa-229	5.79478E+06	0.00000E+00
353	9128	912300	91-Pa-230	6.82010E+06	0.00000E+00
354	9131	912310	91-Pa-231	5.55300E+06	1.09370E+06
355	9134	912320	91-Pa-232	6.52906E+06	0.00000E+00
356	9137	912330	91-Pa-233	5.21900E+06	1.68540E+06
357	9213	922300	92-U -230	5.87866E+06	1.67100E+05
358	9216	922310	92-U -231	7.26795E+06	0.00000E+00
359	9219	922320	92-U -232	5.76209E+06	0.00000E+00
360	9222	922330	92-U -233	6.84420E+06	0.00000E+00
361	9225	922340	92-U -234	5.29780E+06	0.00000E+00
362	9228	922350	92-U -235	6.54520E+06	0.00000E+00
363	9231	922360	92-U -236	5.12590E+06	0.00000E+00
364	9234	922370	92-U -237	6.15380E+06	0.00000E+00
365	9237	922380	92-U -238	4.80650E+06	9.09600E+05
366	9240	922390	92-U -239	5.93080E+06	1.64080E+06
367	9243	922400	92-U -240	4.58410E+06	4.48800E+05
368	9246	922410	92-U -241	5.68340E+06	1.56160E+06
369	9337	932340	93-Np-234	6.98312E+06	0.00000E+00
370	9340	932350	93-Np-235	5.73668E+06	0.00000E+00
371	9343	932360	93-Np-236	6.57735E+06	0.00000E+00
372	9346	932370	93-Np-237	5.48200E+06	8.39500E+05
373	9349	932380	93-Np-238	6.21520E+06	4.49900E+05
374	9352	932390	93-Np-239	5.06897E+06	1.53090E+06
375	9428	942360	94-Pu-236	5.88073E+06	0.00000E+00
376	9431	942370	94-Pu-237	6.99988E+06	0.00000E+00
377	9434	942380	94-Pu-238	5.64660E+06	0.00000E+00
378	9437	942390	94-Pu-239	6.53370E+06	0.00000E+00
379	9440	942400	94-Pu-240	5.24152E+06	0.00000E+00
380	9443	942410	94-Pu-241	6.30080E+06	0.00000E+00
381	9446	942420	94-Pu-242	5.03420E+06	1.98800E+05
382	9449	942430	94-Pu-243	6.02000E+06	0.00000E+00
383	9452	942440	94-Pu-244	4.77080E+06	1.06420E+06
384	9458	942460	94-Pu-246	4.47051E+06	7.11800E+05
385	9540	952400	95-Am-240	6.64709E+06	0.00000E+00
386	9543	952410	95-Am-241	5.53910E+06	1.99100E+05
387	9546	952420	95-Am-242	6.36710E+06	0.00000E+00
388	9547	952421	95-Am-242M	6.37000E+06	0.00000E+00
389	9549	952430	95-Am-243	5.36290E+06	1.14950E+06
390	9552	952440	95-Am-244	6.05299E+06	3.18200E+05
391	9553	952441	95-Am-244M	6.14099E+06	0.00000E+00
392	9625	962400	96-Cm-240	6.09333E+06	0.00000E+00
393	9628	962410	96-Cm-241	6.96952E+06	0.00000E+00
394	9631	962420	96-Cm-242	5.69294E+06	0.00000E+00
395	9634	962430	96-Cm-243	6.80126E+06	0.00000E+00
396	9637	962440	96-Cm-244	5.52026E+06	0.00000E+00
397	9640	962450	96-Cm-245	6.45758E+06	0.00000E+00
398	9643	962460	96-Cm-246	5.15586E+06	0.00000E+00
399	9646	962470	96-Cm-247	6.21302E+06	0.00000E+00
400	9649	962480	96-Cm-248	4.71337E+06	3.00300E+05
401	9652	962490	96-Cm-249	5.83243E+06	0.00000E+00
402	9655	962500	96-Cm-250	4.41274E+06	1.02280E+06
403	9740	972450	97-Bk-245	5.91833E+06	7.72900E+06
404	9743	972460	97-Bk-246	6.54913E+06	0.00000E+00
405	9746	972470	97-Bk-247	5.48194E+06	0.00000E+00
406	9749	972480	97-Bk-248	6.30170E+06	0.00000E+00
407	9752	972490	97-Bk-249	4.96957E+06	1.19520E+06
408	9755	972500	97-Bk-250	5.79507E+06	4.59800E+05
409	9843	982460	98-Cf-246	6.02643E+06	1.59200E+05
410	9849	982480	98-Cf-248	5.58546E+06	0.00000E+00
411	9852	982490	98-Cf-249	6.62515E+06	0.00000E+00
412	9855	982500	98-Cf-250	5.10849E+06	0.00000E+00
413	9858	982510	98-Cf-251	6.17195E+06	0.00000E+00
414	9861	982520	98-Cf-252	4.80429E+06	0.00000E+00
415	9864	982530	98-Cf-253	6.03156E+06	0.00000E+00
416	9867	982540	98-Cf-254	4.60308E+06	0.00000E+00
417	9911	992510	99-Es-251	5.28953E+06	0.00000E+00
418	9912	992520	99-Es-252	6.35161E+06	0.00000E+00
419	9913	992530	99-Es-253	5.09303E+06	0.00000E+00
420	9914	992540	99-Es-254	5.97443E+06	0.00000E+00
421	9915	992541	99-Es-254M	6.05863E+06	0.00000E+00



```
422    9916    992550    99-Es-255    4.97419E+06    0.00000E+00
423    9936    1002550    00-Fm-255    6.38446E+06    0.00000E+00
%END
```

APPENDIX D. PROOF OF EQUATION (4.8)

First the equality of the left side in Eq. (4.8) is proved. By definition,

$$\begin{aligned} E_1 &= \frac{P(t)}{f_1 R_f} \quad \text{and} \quad E_2 = \frac{P(t)}{f_2 R_f}, \\ R_f &= \sum_j V_j \sum_{iso} N_{iso,j} \sum_g \sigma_{f,g,iso,j} \phi_{g,j} \end{aligned} \quad (\text{D.1})$$

where R_f is the non-normalized total fission rate. This shows the marginal effect of time-dependent delayed energy model on isotopes and k_{eff} , so the non-normalized fission rate is assumed to be essentially the same between the two models. Then, the difference between E_1 and E_2 is simply

$$\frac{E_1 - E_2}{E_1} = 1 - \frac{f_1}{f_2}. \quad (\text{D.2})$$

Next, f_1 and f_2 are written explicitly:

$$f_1 = \frac{P(t)}{R_f} \quad \text{and} \quad f_2 = \frac{P(t) - P_{de}(t)}{R_f(1-\gamma)}. \quad (\text{D.3})$$

Replacing f_1 and f_2 in Eq. (D.2) by Eq. (D.3) gives

$$\frac{E_1 - E_2}{E_1} = \frac{\gamma P(t) - P_{de}(t)}{P(t) - P_{de}(t)}. \quad (\text{D.4})$$

If $P(t)$ is written by its prompt and delayed components, and if $P_{pr}(t)$ is expressed by using the previous definition of $S_{m,j}$, then Eq. (D.4) can be written as

$$\frac{E_1 - E_2}{E_1} = \frac{\gamma P_{pr}(t) + \gamma P_{de}(t) - P_{de}(t)}{P_{pr}(t)} = \frac{(1-\gamma) \sum_j \sum_m S_{m,j} - (1-\gamma) P_{de}(t)}{\sum_j \sum_m S_{m,j}} = \frac{\gamma \left(\sum_j \sum_m S_{m,j} - P_{de}(t) \right)}{\gamma \sum_j \sum_m S_{m,j}}. \quad (\text{D.5})$$

For $P_{pr}(t)$, the energy release from neutron capture is intentionally neglected to be consistent with the 2005 ANS standard. Now, $P_{de}(t)$ is written out using Eqs. (4.4) and (4.5),



$$P_{de}(t) = \sum_j \sum_m \lambda_m \left(D_{m,j}(0) e^{-\lambda_m(t)} + \frac{S_{m,j}}{\lambda_m} [1 - e^{-\lambda_m(t)}] \right). \quad (\text{D.6})$$

Although Eq. (4.5) was derived within a time step, use of Eq. (4.5) can be extended to the entire calculation time since a constant full power is applied in this case. The initial condition of Eq. (D.6) is $D_{m,j}(0) = 0$, and then we obtain

$$P_{de}(t) = \sum_j \sum_m S_{m,j} [1 - e^{-\lambda_m(t)}]. \quad (\text{D.7})$$

Replacing $P_{de}(t)$ in Eq. (D.5) by Eq. (D.7), the equality of left side in Eq. (4.8) is proved.

The proof of right side in Eq. (4.8) is straightforward. By definition,

$$H_{decay}(t) = \frac{P_{de}(t)}{P}. \quad (\text{D.8})$$

Here, P is the reactor power before shutdown, and $P_{de}(t)$ is the decay heat power after shutdown. The same heat group approach can be used to formulate $P_{de}(t)$. The equilibrium delayed energy after a long time operation can be solved from Eq. (4.3) by setting $\frac{dD_{m,j}(t)}{dt} = 0$, which is the initial condition at shutdown ($t=0$),

$$\lambda_m D_{m,j}(0) = \gamma_m f V_j \sum_{iso} \kappa_{f,iso} N_{iso,j} \sum_g \sigma_{f,g,iso,j} \phi_{g,j} = S_{m,j}. \quad (\text{D.9})$$

Since the decay heat source term is zero after shutdown, by replacing $\lambda_m D_{m,j}(0)$ in Eq. (D.6),

$$P_{de}(t) = \sum_j \sum_m S_{m,j} e^{-\lambda_m(t)}. \quad (\text{D.10})$$

Therefore, the percentage of decay heat in Eq. (D.8) is written as

$$H_{decay}(t) = \frac{\sum_j \sum_m S_{m,j} e^{-\lambda_m(t)}}{\frac{1}{\gamma} \sum_j \sum_m S_{m,j}} = \sum_m \gamma_m e^{-\lambda_m(t)}. \quad (\text{D.11})$$